ANALYSIS AND INTEGRATION OF OMICS DATA: APPLICATIONS IN DRUG PHARMACOGENOMICS AND ENDOGENOUS CIRCADIAN BEHAVIOR

By

ALISON ACEVEDO

A dissertation submitted to the:

School of Graduate Studies

Rutgers, The State University of New Jersey

In partial fulfillment of the requirements

For the degree of

Doctor of Philosophy

Graduate Program in Biomedical Engineering

Written under the direction of

Ioannis P. Androulakis

And approved by:

_____

_____

_____

_____

New Brunswick, New Jersey

October, 2019

ABSTRACT OF THE DISSERTATION

ANALYSIS AND INTEGRATION OF OMICS DATA: APPLICATIONS IN DRUG PHARMACOGENOMICS AND ENDOGENOUS CIRCADIAN BEHAVIOR

by ALISON ACEVEDO

Dissertation Director:

Ioannis P. Androulakis

The integration of data across omics levels is necessary to accurately reflect physiology, whose behavior is not limited to one molecular component level. Further, integration of information across experimental platforms, time scales, dosing regiments, tissues, and organisms is necessary for the extraction of all possible meaning from the wealth of existing data stored across databases globally and for the development of research that is translatable between organisms. In the enclosed dissertation, we present a pathway-based meta-analysis approach integrated with multivariate decomposition techniques for processing temporal expression data. This framework is designed for application to expression data from any omics level, incorporates information from multiple databases, and is modular in that it can interrogate expression data with pathways extracted from multiple databases. This framework is applied to investigate the dosing- and tissue-dependent effects of the corticosteroid methylprednisolone, as well as the endogenous expression of model organisms critical to pre-clinical studies, rat and mouse. Such analyses both characterize systems not yet completely understood and exemplify the strength of a systems pharmacology understanding applied within translational research.

Acknowledgements

As will be presented in the following dissertation, everything exists as part of a functional network and I would be nothing without the support of everyone around me. I would like to specifically thank the following people who are integral to the success that I am lucky enough to enjoy.

My advisor, Dr. Ioannis Androulakis

My committee, Dr. Gyan Bhanot, Dr. Li Cai, Dr. Charles Roth

My husband, Silvio Dantas, a rare and cherished partner

My immediate family, who are very patient with me

Anne Coogan, Joseph Acevedo, Gary Meisch, Anne Marie Flynn, Dian Butler

Kelsey Meisch, Sean Meisch, Elizabeth Flynn, Sara Braunstein

My past and current lab mates, who helped me to treasure this experience

Stanley Ko, Rohit Rao, Seul-A Bae, Kamau Pierre, Clara Hartmanshenn, Megerle Scherholz, Matthew Putnins, Mohit Kumar

The Biotechnology Training Program and GAANN Fellowship, notably Dr. Martin Yarmush, Dr. Ann Stock, and Mary Ellen Presa

The lab of Dr. William Jusko at SUNY Buffalo

The Biomedical Engineering Administrative Office: Lawrence Stromberg, Robin Yarborough, Stratos Loukidis, and Linda Johnson

Thank you for answering all of my questions and guiding me through.

Table of Contents

List of Tables

List of Illustrations

Chapter 1: From Gene-Phenotype Associations to Therapy Development

1.1 Contemporary Data Wealth Capturing Complex Diseases and Drug Effects

Genetic analyses investigating drug effects and disease development seek to identify association between variation in the expression of a biomarker and a physiological phenotype (Wilke, Mareedu et al. 2008, Jin, Zuo et al. 2014). These investigations can be hypothesis-driven (focus on a small number of candidate genes) or exploratory (a hypothesis-generating screen for the identification of multiple candidate genes) (Wilke, Mareedu et al. 2008). Complex diseases including autoimmune diseases such as osteoporosis, rheumatoid arthritis, metabolic syndrome, various cancers, and other chronic inflammatory conditions, rely on both investigation approaches because they are multifactorial, i.e. they manifest as the result of gene locus heterogeneity, gene-gene interactions (also gene-protein, protein-protein, etc.), and environmental factors (Macfarlane, Forbes et al. 2008, Moore and Williams 2009, Wong, Chin et al. 2016, Sulli, Manoogian et al. 2018). The combination of demands for investigation into these complex diseases and the continuous improvement of omics screening technology has led to growth in the amount of available data capturing all manner of gene-phenotype associations (Caporaso, Kuczynski et al. 2010). Given this wealth of data, our scientific community is motivated to glean physiological meaning with analytical methods that reflect the multifactorial complexity of disease- and drug-induced phenotypes, notably with the ultimate aims of health and therapy development (Ginsburg and Phillips 2018, Krzyszczyk, Acevedo et al. 2018).

1.2 High-throughput Omics Data Techniques Motivate Pathway-based Investigations

Garcia et al. aptly reports that “most basic high-throughput data analysis [results] exist first as overwhelmingly large lists of isolated genes detached of biological context (García-Campos,

Espinal-Enríquez et al.)" and that the first step in approaching analysis of such data is with a functional enrichment step. These initial analyses are designed to contextualize genes with recognizable physiological features, such as a signaling, metabolic, or disease pathways (Jin, Zuo et al. 2014, García-Campos, Espinal-Enríquez et al. 2015). Because physiological functions manifest in the context of a network of molecular components (genes, transcripts, proteins, metabolites, etc.) not truly composed of independent components, it is difficult to isolate any module or set of genomic/transcriptomic/proteomic (or other *-omic* levels) components and affiliate this set with a single function. We are aware that cellular functions "are caused by the combined action of different genes that, in turn, are highly pleiotropic and often participate in more than one cell activity (Amadoz, Hidalgo et al. 2018)." However, the hypothesis of a biochemical pathway is a useful tool, with which molecular component activity is contextualized in a physiologically meaningful way (Jin, Zuo et al. 2014, García-Campos, Espinal-Enríquez et al. 2015). We therefore rely on pathway-based analyses to discern meaning from our own multivariate data. We take the conventional definition of a pathway as functional group of genomic components that accomplish a specific physiological function (Jin, Zuo et al. , García-Campos, Espinal-Enríquez et al. , Amadoz, Hidalgo et al.), and used functional enrichment and feature-based selection techniques to identify these pathway associations, analyze their dynamics, and thus discern physiological meaning from our data, processes essential to the fields of systems biology and systems pharmacology (Androulakis 2016).

Generally, pathway-based analyses of high-throughput data can be defined as genome-wide association studies (GWAS) that identify variations in gene expression associated with a functional group manifesting a phenotype such as metabolic or signaling action or disease development (Jin, Zuo et al. 2014). For example, genome-wide association studies are used in the context of analyzing circadian regulation in multiple organisms (Almon, Yang et al. 2008,

Almon, Yang et al. 2008, Ovacik, Sukumaran et al. 2010, Sukumaran, Xue et al. 2010, Mavroudis, DuBois et al. 2018), the development of chronic diseases, as well as to investigate drug consequences across various tissues and omics levels such as the investigation of corticosteroids within liver, muscle, and kidney (Sun, DuBois et al. 1998, Almon, DuBois et al. 2002, Ramakrishnan, DuBois et al. 2002, Ramakrishnan, DuBois et al. 2002, Almon, DuBois et al. 2004, Almon, Dubois et al. 2005, Almon, DuBois et al. 2007, Almon, DuBois et al. 2007, Hazra, Pyszczynski et al. 2007, Hazra, DuBois et al. 2008, Yao, Hoffman et al. 2008, Fang, Sukumaran et al. 2013, Nouri-Nigjeh, Sukumaran et al. 2014, Kamisoglu, Sukumaran et al. 2015, Acevedo, Berthel et al. 2019). These studies functionally enrich their data in the context of metabolic and signaling pathways collected from various databases detailed below. GWAS studies fall into a few categories: (1) over-representation analysis (ORA) which identifies over-represented pathways within data and associates a significance statistic commonly using Fisher's Exact Test; (2) gene set-based scoring, an extension of ORA which, unlike ORA, does not assume all genes have equivalent importance and calculates a pathway's enrichment score (ES) incorporating this assumption; (3) multivariate techniques which addresses the interdependence of expression data (collinearity) issues in high-throughput data by using decomposition techniques including principal component analysis and singular value decomposition); and (4) topological-based analyses which are extensions of the aforementioned approaches in that both individual genes (nodes) and their relationships (branches) are considered in the calculation of pathway significance (Jin, Zuo et al. , García-Campos, Espinal-Enríquez et al. , Amadoz, Hidalgo et al. 2018). The analyses presented in this thesis employ over-representation analysis and multivariate decomposition techniques primarily, while also acknowledging topological information in pathways notably within the ongoing analysis in endogenous circadian expression in rat and mouse (Chapter 4).

1.3 Supporting Databases for Pathway-based Analysis

Pathway-based analysis relies upon artificially defined pathways or predefined pathways from pathway databases. Adopted from Garcia et al., a comprehensive list of widely used pathway databases are presented in Table 1 (Jin, Zuo et al. , García-Campos, Espinal-Enríquez et al.). A more exhaustive list of the increasing number of pathway databases available are presented in **pathguide.org** which, as of the publication date of this document, hosts 702 databases, reporting for each of these, various details not limited to database accessibility (free/subscription-based), organisms included, and pathway types (metabolic, signaling, protein-protein interactions, genetic interaction networks, etc.) (Bader, Cary et al. 2006).

Table 1 Short list of popular pathway databases adopted from Garcia et al. (García-Campos, Espinal-Enríquez et al.) (PPI, protein-protein interactions; PCI, protein-compound interactions; M, metabolic; S, signaling; GR, gene regulation; D, diagrams; PS, protein sequence).

Pathway Database Name	**Pathway Focus**	**Website**	**Year of Release**
BioCyc (EcoCyc, MetaCyc, HumanCyc, etc.)	M,S	biocyc.org	1995
KEGG	M,S,D	kegg.jp	1996
RegulonDB	GR	regulondb.ccg.unam.mx	1997
STRINGDB	PPI	string-db.org	2000
PANTHER	S,D,PS	pantherdb.org	2004
Gene Ontology	PPI,M,S	geneontology.org	2000
Reactome	M,S,D	reactome.org	2005
MSigDb	M,S,GR	broadinstitute.org/gsea/msigdb	2005
Ingenuity Knowledge Base	PPI, PCI, M, S, GR, D	ingenuity.com	2005
NCI PID	S,D	pid.nci.nih.gov	2006
WikiPathways	M,S,D	wikipathways.org	2008
Small Molecule Pathway DB	M,S	smpdb.ca	2009

ConsensusPathDB	PPI, PCI, M, S, GR	consensuspathdb.org	2009
Pathway Commons	PPI, PCI, M, S	pathwaycommons.org	2010

For our analyses, we rely on one of the most popular and freely available pathway databases, Kyoto Encyclopedia of Genes and Genomes (KEGG) (Kanehisa and Goto , Aoki and Kanehisa , Bader, Cary et al. 2006, Amadoz, Hidalgo et al. , Kanehisa, Sato et al. , Acevedo, Berthel et al.). Our decision to rely on this database as our primary pathway source for the investigations described herein was motivated by: the comprehensive nature of the KEGG database with respect to its available signaling, metabolic, tissue-specific, organism-specific pathways; it's public availability; it's ubiquity of use in research; and the highly curated nature of its content (Bader, Cary et al. 2006, Acevedo, Berthel et al.). Other databases, such as Reactome (Fabregat, Jupe et al. 2018), are comparably useful and it will be shown how these databases were considered in our research and how our pathway-based analysis (Chapter 2) is modular and thus designed for use of pathways from any database.

It is important to reflect on the limitations of pathway databases when using them in research. Pathway databases are nonuniform in their content, define pathways based on analysis of available literature and other databases, are curated by independent research groups, and update their information at different time intervals (Kanehisa and Goto , Aoki and Kanehisa , Bader, Cary et al. , García-Campos, Espinal-Enríquez et al. , Amadoz, Hidalgo et al. , Fabregat, Jupe et al. 2018, Kanehisa, Sato et al.). Designing a pathway-based analysis with sufficient flexibility to cater to the mutable nature of pathway databases enables a more robust analysis, such as in the development of our modular framework (Acevedo, Berthel et al.).

1.4 Development of Feature-based Analyses for High-throughput Omics Data

Toward the analysis of high-throughput omics data for investigation into drug effects, disease development, and characterization of endogenous expression, we continue to develop feature-based techniques foundational to the investigations presented in this dissertation. These techniques take the assumption essential to pathway-based analyses: that genes relevant to the underlying dynamics of the system exist as part of a concerted mechanism (Jin, Zuo et al. 2014, García-Campos, Espinal-Enríquez et al. 2015, Amadoz, Hidalgo et al. 2018) (and thus exhibit temporal consistency) and that "informative genes…contribute to global deviations away from the baseline (Yang, Almon et al.)."

Clustering algorithms are an essential tool for biological pattern discovery (Eisen, Spellman et al. 1998, Androulakis, Yang et al. 2007). Not without its issues, when applying clustering techniques: (1) it is not immediately obvious what the optimal number of clusters is; (2) every clustering method relies on the definition of an appropriate metric; (3) all metrics have their own bias and assumptions; and (4) there exists the issue of genes that have some probability of existing in more than one cluster (Nguyen, Nowakowski et al. 2009). To address these concerns, we have previously developed an algorithm that tested data using multiple clustering methods using multiple metrics and built an agreement matrix with this information (Nguyen, Nowakowski et al. 2009). This matrix identified gene groups reporting coexpression and non-coexpression and isolated the subset of genes that were consistently clusterable. Genes that were inconsistent in their cluster assignments were considered inconsistent and eliminated. Thus, this investigation enabled rapid and robust selection of meaningful genes in a data set without the risk of bias inherent to manually selecting one method of unsupervised clustering (Nguyen, Nowakowski et al.).

In the context of gene expression analysis, clustering techniques are useful for identifying consistent features of expression between genes (Jin, Almon et al. , Androulakis, Yang et al. 2007, Nguyen, Nowakowski et al. 2009). However, factors inherent to the data effect the quality of results. Transcriptomic data from microarray platforms is noisy and exhibits uncertainty in measurements of mRNA, issues which reduce the quality of information processed with clustering techniques (Yang, Almon et al. 2008). Yang et al. was motivated to design a feature-based technique which could extract intrinsic dynamics within microarray expression data that endeavored to overcome the issues of noise and uncertainty in microarray data (Yang, Almon et al.). This investigation proposed an algorithm that uses signal discretization and symbolic representation of these discrete features to identify groups of genes that have similar response profiles. With this, they were thus able to capture essential dynamics of cellular response in liver to corticosteroid administration while minimizing for common sources of data-dependent error (Yang, Almon et al.).

In order to reflect system complexity appropriately within the context of a network and analyze dynamics of these complex systems, we began to apply feature identification techniques within pathway-based analyses (Ovacik, Sukumaran et al. , Kamisoglu, Sukumaran et al. , Acevedo, Berthel et al.). In an analysis of endogenous circadian expression in liver, a pathway-based analysis was integrated with the multivariate decomposition technique, singular value decomposition (SVD) (Ovacik, Sukumaran et al.). Multivariate decomposition techniques are unsupervised identification algorithms useful for feature identification and noise reduction (Alter, Brown et al. 2000, Ding and He 2004, Tomfohr, Lu et al. , Ovacik, Sukumaran et al.). Such techniques are useful especially for identifying trends within gene sets that do not meet arbitrary thresholds of differential expression significance but which contain meaningful biological phenomena (Ovacik, Sukumaran et al.).

Similarly, pathway-based analysis integrated with a singular value decomposition technique was used to investigate gene expression changes in testes development in response to Dibutyl Phthalate exposure (Euling, White et al. 2011, Euling, Thompson et al. 2013, Euling, White et al. 2013, Makris, Euling et al. 2013, Ovacik, Sen et al. 2013), a plasticizer with toxic effect in testes development during gestation and commonly found in flexible plastics and personal care products including perfumes and nail polish (Euling, White et al. 2011, Euling, Thompson et al. 2013, Euling, White et al. 2013, Makris, Euling et al. 2013, Ovacik, Sen et al. 2013). This investigation was a case study supported by the US EPA in their effort to incorporate toxicogenomic analyses into risk assessments. Further, this pathway-based analysis integrated with multivariate techniques facilitated investigation into anticipated damage to testes development as well as screened for additional affected pathways that would inform possible modes of action of DBP (Euling, White et al. 2011, Euling, Thompson et al. 2013, Euling, White et al. 2013, Makris, Euling et al. 2013, Ovacik, Sen et al. 2013). Thus, pathway-based analyses enabled characterization response of complex data in the context of a system and used multivariate techniques which enabled assessment of coherent and subtle trends in expression and noise reduction in data, echoing the goals of previous investigations (Nguyen, Nowakowski et al.) and the investigations described in the following chapters.

1.5 Pathway-based Analyses and the Integration of Omics Data

Pathway-based analysis also enables the development of personalized and precision medicine by its rapid and large-scale identification of potential drug targets and disease biomarkers (Kamisoglu, Calvano et al. 2014, Kamisoglu, Sukumaran et al. 2015, Kamisoglu, Acevedo et al. 2017, Krzyszczyk, Acevedo et al. 2018). Such investigations enable the identification of relationships between molecular targets, diseases, and drug effects. This further facilitates the development of accurate drug action models, an enhancement of classic

pharmacokinetics/pharmacodynamics modeling toward the systems perspective of quantitative systems pharmacology (Iyengar, Zhao et al. 2012, Jusko 2013, Androulakis 2016, Kamisoglu, Acevedo et al. 2017).

For example, toward the development of regulatory models that capture corticosteroid action in liver, Kamisoglu et al. describes the application of pathway-based analysis and consensus clustering toward the identification of significant genes functionally relevant to corticosteroids, at the transcriptomic and proteomic level (Kamisoglu, Sukumaran et al. 2015, Kamisoglu, Acevedo et al. 2017). Clustering techniques were used to identify co-regulatory relationships within genes common to both transcriptomic and proteomic data capturing liver response to an acute bolus dose of the corticosteroid methylprednisolone (Kamisoglu, Sukumaran et al. 2015). This analysis revealed coregulatory relationships between the omics levels in genes representing heat shock protein regulation, oxidative stress, lipid metabolism, and bile acid biosynthesis, all functions associated with corticosteroid action (Kamisoglu, Sukumaran et al. 2015). This study enabled the development of a preliminary regulatory model whose nodes (six protein, six mRNA) connected by mRNA-protein regulatory relationships established from literature (Kamisoglu, Acevedo et al. 2017). Similarly, a pathway-based analysis integrating transcriptomic and metabolomic data investigated the human leukocyte response to bacterial endotoxin (lipopolysaccharide; LPS) (Kamisoglu, Calvano et al. 2014). Endotoxemia response is associated with metabolic fluctuations, so metabolic pathways were focused on within this analysis and the integration of multiple omics levels allowed for investigation into both the transcriptional regulation of leukocyte metabolic processes and how regulatory patterns might have been affected by concurrent fluctuations of metabolites (Kamisoglu, Calvano et al. 2014, Kamisoglu, Acevedo et al. 2017).

1.6 Summary of Thesis

The integration of data across omics levels is necessary to accurately reflect physiology, whose behavior is not limited to one molecular component level. Further, integration of information across experimental platforms, time scales, dosing regiments, tissues, and organisms is necessary for the extraction of all possible meaning from the wealth of existing data stored across databases globally and for the development of research that is translatable between organisms (Kamisoglu, Calvano et al. , Kamisoglu, Sukumaran et al. , Kamisoglu, Acevedo et al. , Ginsburg and Phillips 2018, Krzyszczyk, Acevedo et al. 2018).

Therefore, in the following chapters we present a pathway-based meta-analysis approach integrated with multivariate decomposition techniques (Chapter 2) which processes temporal expression data. This framework is designed for application to expression data from any omics level, incorporates information from multiple databases, and is modular in that it can interrogate expression data with pathways extracted from multiple databases. Subsequent chapters use this framework to investigate the dosing- and tissue-dependent effects of the corticosteroid methylprednisolone (Chapters 3 and 4), as well as the endogenous expression of model organisms critical to pre-clinical studies, rat and mouse (Chapter 5). In the final chapter, we further detail the application of this work in pre-clinical pharmacology research and how this research will continue in this perspective.

Chapter 2: Development of a Pathway-based Analysis Framework for Decomposition of High-Throughput Omics Data

2.1 Introduction

Described in greater depth in Chapter 1, pathway-based analysis techniques were designed for, and enabled characterization of, high-throughput omics data. Pharmacological time-series high-throughput data obtained from different (transcriptomic or other) platforms and time-scales, including multiple dosing regimens (Jin, Almon et al. 2003, Almon, DuBois et al.), are complicated to analyze. Approaches to analyzing and comparing such data generally classify into two main categories: (1) integrate profiles from different studies into one dataset so that available analysis tools can be directly applied to the concatenated data set, or (2) analyze and interpret each data set separately and subsequently compare the analysis (meta-analysis) (Jiang, Deng et al. 2004, Mecham, Klus et al. 2004, Carter, Eklund et al. 2005, Morris, Wu et al. 2006, Park, Yi et al. 2006, Kim, Ki et al. 2007, Lu, Lee et al. 2007, Shabalin, Tjelmeland et al. 2008). Since combining data across different platforms remains a serious challenge, meta-analysis approaches are gaining popularity (Ghosh, Barette et al. 2003, Ramasamy, Mondry et al. 2008) given the underlying hypothesis is that even though raw data may not be comparable, the results of the individual analyses are.

As an alternative to the meta-analysis approach, we recently proposed the mapping of transcriptomic data onto signaling and metabolic pathways which are scored based on the emerging activity of the pathway, as manifested via the obtained transcriptional data (Ovacik, Sukumaran et al. 2010, Euling, Thompson et al. 2013, Euling, White et al. 2013, Ovacik, Sen et al. 2013). The pathway scoring expresses the overall, intrinsic dynamic of the pathway and its

score does not rely on measuring a consistent set of transcriptional profiles across the various conditions – provided the score can be robustly determined (see Results section herein).

In the present investigation, we extend and expand our earlier framework and present an integrated approach for decomposing high throughput omics-based pathway activities enabling the characterization of the emerging expression dynamics within this data. This framework is applied to multiple case studies in subsequent chapters including analysis of drug response in various tissues and across multiple dosing regiments, as well as of endogenous activity of drug-free tissues across multiple organisms.

2.2 Development of Pathway-based Framework

2.2.1 Animals Model and Experimental Data

This framework was designed for processing and comparing high-throughput omics expression data (temporal or across conditions). We have applied the framework to multiple case studies discussed in depth in subsequent chapters. Tables reporting each data set analyzed over the course of this thesis are included within the Appendix (ST 1).

2.2.2 Microarray Data Preprocessing

Only probes that registered as present or marginal within each microarray were retained within for analysis. Data preprocessing steps include using row-average data imputation to supplement missing values in incomplete expression profiles. Active genes are then identified using differential expression analysis with the software Extraction and Analysis of Gene Expression (EDGE) (Leek, Monsen et al. 2006). Differentially expressed genes are identified by p-value. Differentially expressed profiles are then z-scored with respect to the individual profile mean and standard deviation. Replicate profiles are then averaged together, yielding averaged z-scored profiles.

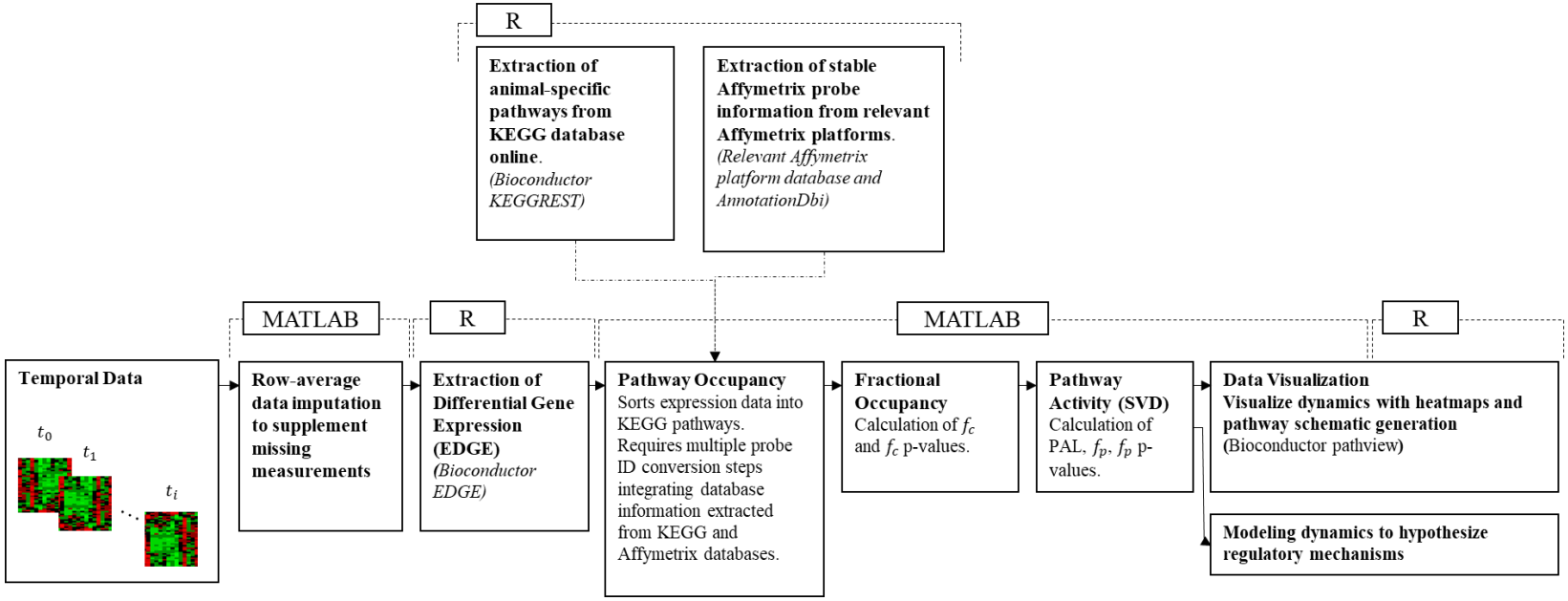

Figure 1 Pathway activity analysis framework which processes temporal expression data, curates differentially expressed genes into pathway gene sets, and assesses their fractional occupancy and pathway activity, and applies a model fitting technique. For this analysis KEGG pathways were used though other databases are applicable (Acevedo, Berthel et al.).

2.2.3 Mapping Transcriptomic Data onto Pathways

A pathway can be defined as a network of molecular interactions and reactions designed to link genes in the genome to gene products. Pathways express layered and complementary activities, meaning pathways are groups of genes linked mechanistically that effect a biochemical action. Numerous databases exist describing pathway definition. The Kyoto Encyclopedia of Genes and Genomes (KEGG) pathways is used as the functional grouping instrument. KEGG is one of the most comprehensive and readily used by genomics researchers (Kanehisa and Goto 2000, Kanehisa, Furumichi et al. 2016, Kanehisa, Sato et al. 2018). Approximately 300 of the available KEGG pathways are relevant to Rattus norvegicus (relevant to analysis of liver and muscle data in Chapter 3, and endogenous rat expression in muscle tissues in Chapter 4) and to Mus musculus (relevant to analysis endogenous mouse expression across multiple tissues in Chapter 4). Pathways unrelated to a specific tissue or organism are irrelevant to their respective study and the categories of pathways eliminated for each of our analyses in rat and mouse are detailed in the Approach section of each chapter. For example, within the study of MPL influence within the liver, pathways unrelated to the liver (ex. Cardiac muscle contraction, Complement and coagulation cascades, Platelet activation), describing neurological diseases (ex. Non-alcoholic fatty liver disease, Alzheimer's disease, Parkinson's disease, Huntington's disease), irrelevant to the liver (Olfactory transduction), or redundant for all other metabolic pathways (KEGG's pathway entitled Metabolic pathways rno:01100 is the set of all other metabolism related pathways) are removed from consideration in the analysis.

In order to begin characterizing the responses captured in our various data sets, the microarray data is contextualized by identifying which of the tissue- and organism-relevant pathways are populated by the data sets. Fractional coverage (f_c) is calculated for each pathway, a fraction that

communicates the number of unique genes (rno) identified within the microarray data relative to the number of genes within the KEGG pathway (Equation 1). The metric quantifies the extent to which a pathway is represented in the dataset and is reported in the genome-wide transcriptomic studies. In the early stages of the framework, multiple databases were used for convert Affymetrix probe names to recognizable genes names and KEGG gene identifiers (Acevedo, Berthel et al.). However, the most recent version of the framework (Acevedo, DuBois et al. 2019 (submitted)), uses an improved approach. For the gene-to-pathway mapping, Affymetrix probe identifiers within the microarray template and are converted into KEGG IDs in order to be sorted into rat-relevant pathways from KEGG. Affymetrix probe identifiers are translated into their NCBI Entrez IDs and Gene Symbols using the Bioconductor packages for each Affymetrix Platform. For example, within the analysis of the muscle data, processing of the chronic MPL muscle data is facilitated by package rae230a.db which contains the annotation data for Affymetrix Rat Expression Set 230A used to capture the chronic MPL muscle data and package rgu34a.db contains the annotation data for Affymetrix Rat Genome U34 Array used to capture the acute MPL muscle data.

$$f_c = \frac{rno\ in\ dataset}{rno\ in\ KEGG\ pathway} \qquad 1$$

In order to assess the confidence in the fractional coverage, an associated p-value (f_c p-value) is calculated. Confidence in f_c is important for two reasons: 1) to quantify the extent to which the fractional coverage of a pathway based on the specific experiment could have be obtained by a random collection of genes; and 2) more importantly, since different experiments may not be quantifying the same subsets of pathway-specific genes we need to establish significant coverage based on different subsets. The significance of the f_c is determined using the 1-tail Fisher's Exact

test such that the total rat genome is the set of unique rat genes in all of KEGG's rat-relevant pathways.

Following the gene-to-pathway assignment, the coverage of the KEGG pathways is assessed by evaluating the fractional coverage (f_c) of each pathway (Acevedo, Berthel et al. , Acevedo, DuBois et al. 2019 (submitted)). This statistic is the fraction of genes within a pathway for which gene profiles are available. To assess the confidence in the fractional coverage, an associated p-value (f_c p-value) is determined using the 1-tail Fisher's Exact test such that the total rat genome is the set of unique rat genes in all KEGG's rat-relevant pathways (Acevedo, Berthel et al.). Some pathways with low fractional occupancy yield inconclusive p-values as an artifact of the Fisher's Exact Test and were eliminated from analysis, discussed further in ST 2.

A pathway may yield a high f_c value but contain a small population of actual genes. The selection of the list of significant pathways that make up the pathway solution set is presented in the Results section. In the process of determining this list of significant pathways, the actual gene population for each pathway is necessary to consider. Additionally, determining whether a set of pathways is significant involves consideration of the average actual gene count for the set. An average rno (rno_{avg}) is calculated for a pathway solution set. The significance of this statistic is reported as a p-value (rno_{avg} p-value) calculated using a bootstrapping technique (Equation 2). Given a pathway set containing P pathways, N random pathway sets of length P are selected and rno_{avg}' is calculated for each. The distribution of rno_{avg}' is compared against the rno_{avg} from the original set of P pathways yielding n pathways with rno_{avg}' greater than rno_{avg}.

$$rno_{avg}\ \ p-value = \frac{n_{(rno_{avg}' > rno_{avg})}}{N} \qquad 2$$

2.2.4 Pathway Activity Analysis

MPL administration, environmental cues, and endogenous clock mechanism are the drivers for genomic activity, directly and indirectly, within the datasets considered in the investigations of this thesis. Pathways determined to have significant fractional coverage are analyzed with pathway activity analysis (Figure 1)[1]. This component of the analysis determines whether a pathway is active without eliminating individual genes; no gene expression profiles are eliminated using conventional differential expression analysis and user-defined threshold cutoff (Subramanian, Tamayo et al. 2005). Instead, singular value decomposition (SVD) is used to identify global and subtle expression trends within the pathway gene sets.

Pathway analysis assumes that pathways exhibits layered behaviors of subgroups of genes. Singular value decomposition is used as a dimension reduction technique, reducing temporal gene expression datasets into sets of singular vectors and singular values that communicate global trends and relative trend dominance (Ovacik, Sukumaran et al. 2010, Euling, White et al. 2011, Euling, White et al. 2013, Ovacik, Sen et al. 2013). (As a preprocessing step before application of SVD pathway activity analysis, gene expression profiles are z-scored.) This technique is previously applied within investigations assessing for subtle circadian rhythmicity in genes that otherwise are not recognized as differentially expressed (Ovacik, Sukumaran et al. 2010) and for identifying the effects of dibutyl phthalate in male reproductive organ development (Euling, White et al. 2011, Euling, White et al. 2013, Ovacik, Sen et al. 2013). Within this investigation, complex tissue-specific behavior is revealed by the SVD decomposition of pathway gene sets.

[1] The version of the framework used in the liver analysis did not include an EDGE step.

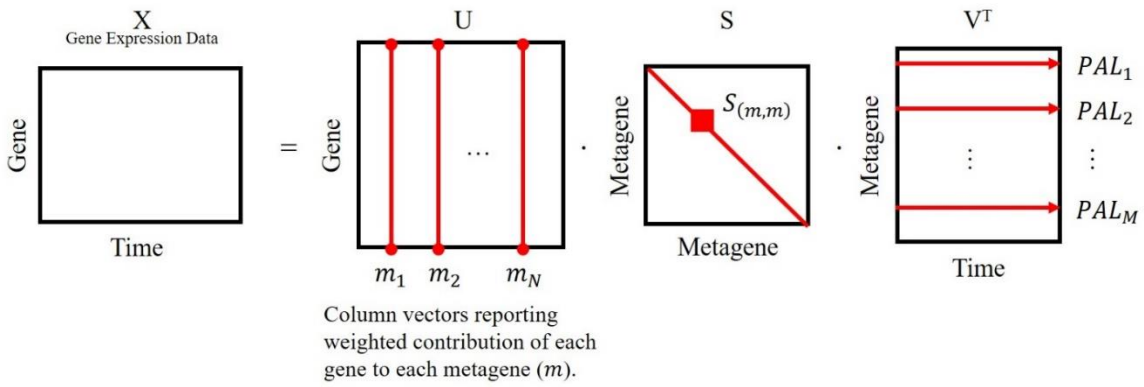

Figure 2 Singular value decomposition (SVD) of a pathway gene set. A pathway matrix (X) designed such that each row is a unique gene and columns are samples at each timepoint from 0 to 72 hours. SVD yields: (1) matrices U (translational matrix) in which the rows are individual genes and columns indicate a gene's match to a metagene (G genes make up a gene set and M metagenes results from SVD where the number of metagenes is equal to the number of sample times.); (2) matrix S, a diagonal singular value matrix reporting the dominance of each metagene; (3) and matrix V, the transform denoted V^T, an additional translational matrix in which the rows of V^T indicate each metagene and the columns indicate time. PAL profiles are taken as metagene expression over time - the rows of V^T.

Application of SVD to a pathway gene set yields two translational matrices (U and V) and a singular value matrix (S) (Figure 2). The subtle global trends within the pathways are the activities of metagenes, an abstract object that captures dominant characteristics common to many gene expression profiles within the dataset. The "expression" or activity of a metagene over time is defined as the pathway activity level (PAL) profile. PAL profiles are found within the row vectors of the transpose of the translational matrix V (i.e. PAL profiles are the row vectors of V^T) denoted in Equation 3.

The dominance of each metagene's activity is preserved in the order in which the PAL profiles appear descending in V^T as well as in the diagonal of the singular value matrix (S); the most dominant metagene appears first. To quantify this dominance, the singular values within the diagonal of matrix S are normalized by the sum of the diagonal (Equation 4) to yield the fraction

of pathway activity of a PAL defined as the f_p statistic (Ovacik, Sukumaran et al. 2010). Each PAL describes a pathway activity profile and corresponds to a unique f_p value which reports the percent of total pathway activity represented by that PAL.

The number of PAL profiles reported by V^T is equal to the number of samples (time points). However, not all patterns are significant. To determine PAL significance, a bootstrapping calculation is used to generate a p-value associated with f_p statistic. The original gene set is bootstrapped ($\mathrm{N} = 1000$). Bootstrapped gene sets are constructed by scrambling the pathway gene set N times (Kallio, Vuokko et al. 2011). Each bootstrapped pathway gene set is decomposed with SVD, yielding N sets of PAL' profiles and associated $f_p{}'$ values for each PAL' profile. For each PAL, the distribution of $\mathrm{f_p'}$ values which results from the bootstrapped pathway gene sets are compared to the original f_p values. The number of $\mathrm{f_p'}$ greater than an $\mathrm{f_p}$ is divided by N to determine whether each $\mathrm{f_p}$ (and by association the PAL) is likely to emerge from a randomized gene set (Equation 5).

This investigation seeks to characterize the consequences of MPL within the liver from a pathway perspective. However, the correlation of each metagene to each gene is important to our understanding of the consequences of MPL and is identified within the translational matrix U. Rows of U correspond to genes and columns to metagenes. The correlation of each gene (g) to each metagene (m) is defined as $W_{g,m}$ (Equation 6). The correlation of each gene to each metagene ($W_{g,m}$) is the correlation of each gene expression profile to each PAL profile.

Thus, global trends (PAL) in a gene set each have an associated fraction of the pathway activity (f_p) that they capture. Multiple significant PAL may emerge for each gene set and each gene's

correlation to each PAL is given by its weight. PAL are also symmetric, thus two PAL profiles, of opposite sign but equal magnitude, indicate the same expression activity events.

The list of pathways with significant fractional coverage (f_c p-value $\leq 10^{-3}$) is further reduced to the list of pathways that also yield significant pathway activity. Pathways capable of generating at least one significant PAL profile are considered significant and a PAL profile is significant if its corresponding f_p p-value $\leq 10^{-3}$.

$$PAL_m = V^T(m, \vec{t}) \quad (3)$$

$$f_p = \frac{S(m,m)^2}{\sum_{m=1}^{M} S(m,m)^2} \quad (4)$$

$$f_p\ p - value = \frac{n_{(f'_p > f_p)}}{N} \quad (5)$$

$$W_{g,m} = U(g, m) \quad (6)$$

2.2.5 Prediction of Pathway Activity with Bootstrapping

Variability exists in expression data capturing the influence of MPL within the muscle and liver and endogenous expression in rat and mouse tissues, indicating non-uniformity that must be accounted for in our analysis in order to be scientifically rigorous. To account for the variability, a bootstrapping approach is used to generate pathway gene sets likely to exist given additional MPL dosing studies which are then assessed for pathway activity. In this component of the investigation, the range of activity capable of emerging from the system is investigated.

Bootstrapped gene sets are constructed from bootstrapped gene expression profiles, where each profile is projected within a normal distribution about the gene's average expression. In short, each gene expression profile is bootstrapped within a normal distribution about the gene

expression profile's mean. The bootstrapped genes are assembled into appropriate pathway gene sets, ultimately yielding N bootstrapped pathway gene sets for each pathway ($N = 1000$ bootstrapped gene sets per pathway). Each of these bootstrapped pathway gene sets is decomposed with SVD. Significant PAL profiles identified from these bootstrapped gene and their corresponding f_p and f_p p-value statistics, are retained for each significant pathway. All PAL profiles extracted from these bootstrapped gene sets are assumed likely system behavior that would emerge if the rat experiments were repeated.

For each pathway, the significant bootstrapped PAL are clustered such that common activity patterns group together. the MATLAB ® function *evalclusters.m* is applied to assess optimal cluster number using the gap statistic and applying kmeans clustering (MATLAB 2016b). Thus, a finite set of PAL centroids are identified, indicating a finite list of activity patterns are induced by MPL to emerge from each pathway.

2.2.6 Evaluating Pathway Dynamics

The pathway activity analysis decomposes a pathway's intrinsic dynamics into its leading, independent constitutive elements. To compare activities based on non-overlapping gene sets, across dosing regimens of different time horizons, we introduce a novel model-based approach, where the dynamics of each dominant PAL is approximated using PKPD-driven models exploring alternative hypotheses for the mechanisms of regulation of a pathway. For analyses in liver and muscle, the influence of MPL is studied so the PKPD-drive model approach is designed in the established PKPD of MPL with adaptation of previously established regulatory models (Ramakrishnan, DuBois et al. 2002, Hazra, DuBois et al. 2008, Acevedo, Berthel et al.) (Ramakrishnan, DuBois et al. 2002, Hazra, DuBois et al. 2008) (Jin, Almon et al. , Hazra, DuBois et al. 2008, Yao, Hoffman et al. 2008).

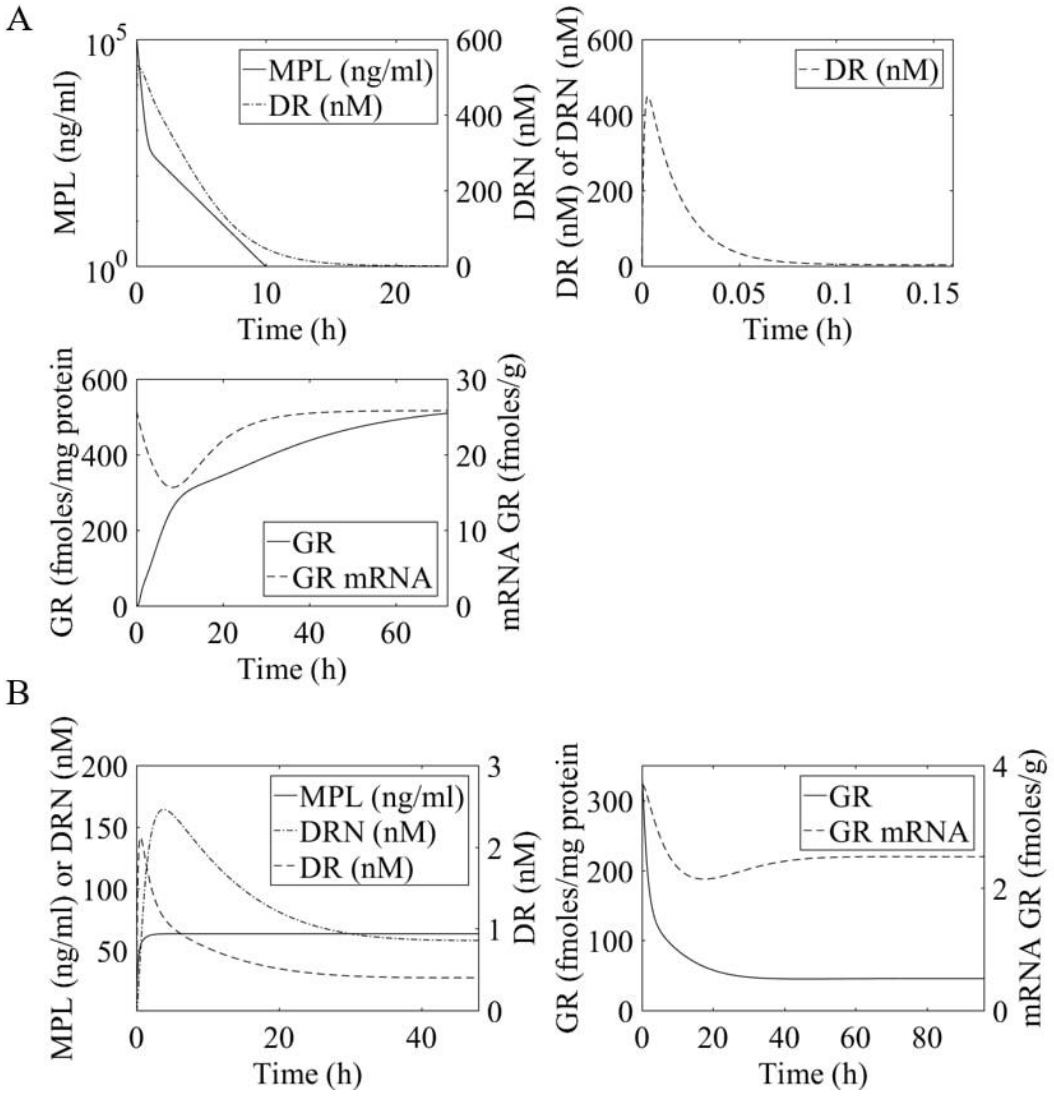

Figure 3 Time profiles of MPL pharmacokinetics and receptor dynamics for (A) acute 50 mg/ml bolus MPL dose and (B) chronic infusion of 0.3 mg/(kg·h) MPL. MPL influence over transcription within the liver is dosing-dependent and receptor mediated. (Sun, DuBois et al. , Ramakrishnan, DuBois et al. , Ramakrishnan, DuBois et al. , Jin, Almon et al. , Hazra, Pyszczynski et al. , Hazra, DuBois et al.)

Pharmacokinetics: The PK of MPL in both regimens was shown to be appropriately described by a two-compartment model (Figure 3, Equations 7 and 8) (Ramakrishnan, DuBois et al. 2002, Hazra, DuBois et al. 2008). A_p and A_t denote drug in the plasma and tissue compartments respectively. Term k_0 is the zero-order rate constant for drug input into the plasma, CL indicates

clearance, V_p indicates plasma volume of distribution, and k_{12} and k_{21} are the intercompartmental distribution rate constants. In the case of acute MPL administration, $k_0 = 0$ indicating a bolus injection. Parameter values are adopted from Ramakrishnan et al. and presented in Table 2 (Ramakrishnan, DuBois et al. 2002, Hazra, DuBois et al. 2008).

$$\frac{dA_p}{dt} = k_0 + k_{21} \cdot A_t - \left(k_{12} + \frac{CL}{V_p} \right) \cdot A_p \qquad 7$$

$$\frac{dA_t}{dt} = k_{12} \cdot A_p - k_{21} \cdot A_t \qquad 8$$

Table 2 Pharmacokinetics parameters for acute and chronic MPL administration (Ramakrishnan, DuBois et al. 2002).

Parameter	Definition	Acute	Chronic
$k_0 \left(\frac{1}{h}\right)$	Rate of drug concentration into central plasma compartment	0	220
CL $\left(\frac{l}{h \cdot kg}\right)$	Clearance	3.48	5.61
$V_p \left(\frac{l}{kg}\right)$	Central volume of drug distribution	0.73	0.82
$k_{12} \left(\frac{1}{h}\right)$	Drug distribution rate constant	0.98	0.32
$k_{21} \left(\frac{1}{h}\right)$	Drug distribution rate constant	1.78	0.68

Table 3 Parameters for receptor-mediated effects of acute and chronic MPL administration (Hazra, DuBois et al. 2008).

Parameter	Definition	Acute	Chronic
$k_{sRm} \left(\frac{fmol}{g \cdot h}\right)$	Receptor mRNA synthesis rate constant	3.15	0.45

$k_{dRm}\left(\frac{1}{h}\right)$	Receptor mRNA degradation rate constant	0.122	
$IC_{50Rm}\left(\frac{nmol}{L \cdot mg_{protein}}\right)$	DRN required for 50% inhibition of the synthesis rate of Rm	123.7	
$k_{sR}\left(\frac{nmol}{L \cdot mg_{protein} \cdot fmol_{Rm} \cdot g \cdot h}\right)$	Receptor synthesis rate	0.84	3.63
$k_{re}\left(\frac{1}{h}\right)$	Loss rate for drug receptor in the nucleus	0.402	
$k_{on}\left(\frac{l}{nmol \cdot h}\right)$	Association rate for receptor-drug binding	0.019	
$k_{dR}\left(\frac{1}{h}\right)$	Receptor loss/degradation rate	0.0403	
$k_T\left(\frac{1}{h}\right)$	Translocation of receptor into the nucleus	58.1	
R_f	Receptor recycling factor from nucleus to cytosol	0.69	

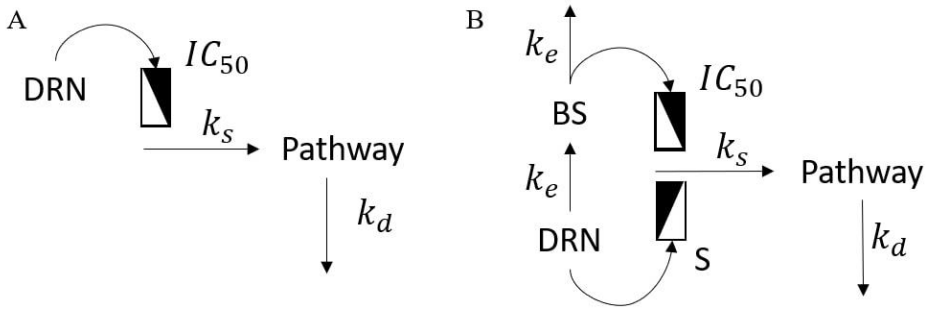

Figure 4 Regulatory mechanism schematics for the (A) monophasic activity model and (B) biphasic activity model adapted from Hazra et al (Hazra, DuBois et al. 2008). (A) MPL regulates transcription via binding to glucocorticoid receptors within the cytosol, transporting into the nucleus, and binding to a GRE element thus initiating targeted transcription, as captured by the monophasic model. (B) The biphasic model describes this GRE-binding activity in combination with an additional mechanism of MPL regulation, that of binding to an intermediate biosignal (BS) which influences targeted transcription rate. (Sun, DuBois et al. , Ramakrishnan, DuBois et al. , Ramakrishnan, DuBois et al. , Jin, Almon et al. , Hazra, Pyszczynski et al. , Hazra, DuBois et al.)

Receptor dynamics: MPL action is receptor-mediated (Figure 4, Equations 9 through 12) (Sun, DuBois et al. 1998, Ramakrishnan, DuBois et al. 2002, Hazra, DuBois et al. 2008). Parameter values are adopted from Hazra et al. and presented in Table 3 (Hazra, DuBois et al. 2008). R_m indicates mRNA of the free cytosolic receptor, R indicates the free cytosolic receptor, DR indicates the cytosolic drug-receptor complex, and DRN indicates the drug-receptor complex in the nucleus (Ramakrishnan, DuBois et al. 2002). The concentration at which the synthesis rate of receptor mRNA drops to 50% of its baseline value is indicated by IC_{50Rm}, parameter. Parameter k_{on} indicates a second-order rate constant for drug-receptor binding. Parameters k_T and k_{re} are first-order rates of receptor translocation between the nucleus and the cytosol (k_{re}: to the nucleus; k_{re}: recycling back to the nucleus) (Ramakrishnan, DuBois et al. 2002). The fraction of receptor recycled is indicated by parameter R_f. C_{MPL} corresponds to the concentration of free receptor in the cytosol and is determined by the equation $C_{MPL} = 0.43\frac{\mathrm{A_p}}{\mathrm{V_p}}$ where 0.43 is the fraction of unbound MPL within the cytosol (Ramakrishnan, DuBois et al. 2002, Hazra, DuBois et al. 2008).

$$\frac{dRm}{dt} = k_{sRm} \cdot \left(1 - \frac{DRN}{IC_{50Rm} + DRN}\right) - k_{dRm} \cdot Rm \qquad 9$$

$$\frac{dR}{dt} = k_{sR} \cdot Rm + R_f \cdot k_{re} \cdot DRN - k_{on} \cdot C_{MPL} \cdot R - k_{dR} \cdot R \qquad 10$$

$$\frac{dDR}{dt} = k_{on} \cdot C_{MPL} \cdot R - k_T \cdot DR \qquad 11$$

$$\frac{dDRN}{dt} = k_T \cdot DR - k_{re} \cdot DRN \qquad 12$$

Pathway pharmacodynamics: Once a pathway's activity has been decomposed to its constitutive intrinsic components, we characterize its dynamics in a model-based manner by assuming that each PAL is approximated by an appropriate dynamic model. Comparisons across dosing regimens are then performed in the space of models as opposed to the space of transcriptional data. We hypothesized (based on the results to be discussed shortly) that the dynamic decomposition of the pathway activity indicates components whose transcription is regulated by an MPL-receptor complex (DRN) binding to a GRE element in the nucleus and regulated by transcription mediated by MPL binding to an intermediate biosignal (BS) – interestingly this was dosing-dependent. In this direction we extend the concepts described in (Hazra, DuBois et al. 2008, Yao, Hoffman et al. 2008). The simpler mode of pathway regulation assumes a saturable induction of the pathway activity (Figure 4A, Equation 13) where k_s indicates the activation rate of pathway activity, IC_{50PAL} indicates the concentration of DRN responsible for 50% inhibition of the pathway activity activation rate, and k_d indicates the deactivation rate of pathway activity. This mode is expected to reflect "monophasic" dynamics with a transient (acute dosing) or persistent (chronic dosing) deviation of a pathway's activity following i.v. MPL administration. In addition, the emergence of regulation mediated through an MPL-regulated biosignal, is likely to exhibit a "biphasic" response (Figure 4B, Equations 14 and 15), describing the dynamics of an intermediate biosignal (BS) whose synthesis is directly related to DRN by k_e,S, is the stimulation constant for pathway activity due to DRN, IC_{50PAL} indicates the BS responsible for 50% inhibition of pathway activity activation rate, and γ indicates the factor of amplification of the influence of BS on the activation of pathway activity. These model equations are adapted from the transcription regulatory models of (Hazra, DuBois et al. 2008) where alternative models were also discussed, and could be easily accommodate. However, our analysis indicated that these simpler forms captured the essence of the pathway dynamics.

Monophasic Activity

$$\frac{dPAL}{dt} = k_s \left(1 \pm \frac{DRN}{IC_{50\,PAL} - DRN} \right) - k_d \cdot PAL \qquad 13$$

Biphasic Activity

$$\frac{dBS}{dt} = k_e \left(DRN - BS \right) \qquad 14$$

$$\frac{dPAL}{dt} = k_s \left(1 \pm S \cdot DRN \right) \left(1 \mp \frac{BS^{\gamma}}{IC_{50\,PAL}^{\gamma} - BS^{\gamma}} \right) - k_d \cdot PAL \qquad 15$$

Parameter estimation was performed using Matlab's optimization toolkit in a series of optimization stages. In all stages, we sought to minimize the residual sum of squares between the model prediction and the cluster centroid profile. In the first stage, it is assumed that the system is nonlinear and neither continuous nor differentiable for the entire parameter solution space. Therefore, as a rapid preliminary global search for a minimum, a stochastic direct method (simulated annealing) with bound constraints is employed. The result of this global search technique is taken as the initial parameter values for the second optimization stage using a direct pattern search method. In the final stage, a gradient-based method is used to probe this more limited space as the final optimization step. This stage uses the sequential quadratic programming as implemented through Matlab's *fmincon*. The model which results from this optimization process is visually inspected.

2.3 Discussion

Pharmacological time-series data, from comparative dosing studies, is critical to characterizing drug effects. Reconciling the data from multiple studies is inevitably difficult; multiple in vivo

high-throughput -omics studies are necessary to capture the global and temporal effects of the drug, but these experiments, though analogous, differ in (microarray or other) platforms, time-scales, and dosing regimens and thus cannot be directly combined or compared. This investigation addresses this reconciliation issue with a meta-analysis technique aimed at assessing the intrinsic activity at the pathway level (Acevedo, Berthel et al.).

The pathway-based analysis presented here is applicable to any type of expression data (temporal or across conditions) and is applied toward the analysis of the dosing-specific response of liver and muscle to methylprednisolone (Chapter 3), analysis of endogenous expression in drug-free tissues (Chapter 4), as well as comparison of drug-free endogenous expression across two essential pre-clinical animals (Chapter 4), rat and mouse.

The model-based analysis component of the pathway-based approach is designed to hypothesize regulatory relationships that would result in PAL dynamics. In the above chapter, this step is presented in the context of the PKPD of MPL and uses mathematical models describing this. However, this step is generalizable to any mathematical model and thus is generalizable. What is critical to this step is understanding its motivation. Changes in the dynamics of pathway activities are compared using the model-based assessment of pathway dynamics, both extending the principles of pharmacodynamics/pharmacokinetics (PKPD) to describe pathway activities and enabling us to hypothesize on the likely emergence (or disappearance) of regulatory interactions when comparing data sets against one another.

In summary, the pathway-based analysis approach presented above is sufficiently generalizable to process any high-throughput expression data (temporal or across conditions), capture and score both pathway occupancy and pathway dynamic information, describe these dynamics with a model-based assessment to enable discussion of regulatory relationships (generalizable for

different mathematical models), and via these techniques, the approach enables comparison across experiments (across platforms, tissues, organisms, time-scales).

Chapter 3: Pathway-based Analysis toward Investigating Tissue-specific and Dosing-specific Responses in Temporal Expression Data

3.1 Pathway-based Analysis of Liver Response to Intravenous Methylprednisolone (MPL) Administration in rats: Acute versus Chronic Dosing

3.1.1 Introduction

Synthetic glucocorticoids (GC), such as methylprednisolone (MPL), are widely used anti-inflammatory and immunosuppressive agents for the treatment of a variety of inflammatory and auto-immune conditions (Swartz and Dluhy 1978, Barnes 1998). GC drugs magnify the actions of endogenous glucocorticoids regulating pathways by binding of a drug-receptor complex to DNA glucocorticoid regulatory elements (GREs) or by signaling through receptors in a transcription-independent manner (Schaaf and Cidlowski 2002). Because of the diverse effects of GC and the multitude of molecular mechanisms involved, in vivo high-throughput transcriptomics has proven effective in better understanding the temporal and tissue-specific effects of MPL (Almon, DuBois et al. 2004, Almon, Dubois et al. 2005, Almon, Lai et al. 2005, Almon, DuBois et al. 2007, Almon, Yang et al. 2008, Yang, Almon et al. 2008, Yang, Almon et al. 2009, Nguyen, Almon et al. 2010, Nguyen, Almon et al. 2014).

However, while short-term CS use is beneficial for reducing inflammation, long-term use is associated with serious consequences including hyperglycemia, negative nitrogen balance, and fat redistribution leading to complications including diabetes, muscle wasting, osteoporosis, etc. (Andrews and Walker 1999, Morand and Leech 1999, Yang, Almon et al.). Therefore, and adding to the complexity of the physiological and pharmacological effects of corticosteroids (Almon, DuBois et al. 2004, Almon, Dubois et al. 2005, Almon, Lai et al. 2005), different dosing regimens

of GC administration induce different patterns of expression (Almon, DuBois et al. 2007, Almon, DuBois et al. 2007, Yao, Hoffman et al. 2008) likely indicative of dosing-dependent regulation. Thus, transcriptional dynamics under acute CS administration may not exhibit similar expression patterns during continuous infusion, pointing to the possibility of alternative regulatory mechanisms (Hazra, DuBois et al. 2008, Yao, Hoffman et al. 2008, Nguyen, Almon et al. 2010). Thus, an improved understanding of corticosteroid pharmacogenomic effects from multiple dosing regimens would be required to provide insight into the underlying molecular mechanisms of action. In this direction our earlier work had focused on assessing transcriptional dynamics in order to (1) identify transcriptional modules of characteristic mRNA dynamic features across multiple dosing regimens of corticosteroids; and (2) elaborate on their common regulatory controls (Hazra, DuBois et al. 2008, Yao, Hoffman et al. 2008, Nguyen, Almon et al. 2010).

In the following investigation, we apply the pathway-based analysis framework, presented in Chapter 2 (Acevedo, Berthel et al. , Acevedo, DuBois et al.), for the characterization of: 1) of the emerging transcriptional dynamics in response to MPL; and 2) of the dosing-dependent implications induced due to differences in drug exposure (acute versus chronic). We analyzed acute and chronic MPL dosing in male adrenalectomized rats and characterized the dosing-dependent differences in the dynamic response of MPL-responsive signaling and metabolic pathways, including: lipid metabolism (Macfarlane, Forbes et al. , Peckett, Wright et al.), amino acid metabolism (Ratnam, Maclean et al. 2002, Christiansen, Djurhuus et al. 2007), carbohydrate metabolism (McMahon, Gerich et al. 1988, Nader, Ng et al. 2012) metabolism of cofactors and vitamins (Pascussi, Drocourt et al. 2000), regulation of essential organelles (Wallace and Cidlowski 2001, Rhen and Cidlowski 2005, Cuzzocrea, Bruscoli et al. 2008), and xenobiotic metabolism pathway groups (Dvorak and Pavek 2010). To further elucidate, and consistently compare dosing-induced changes in the dynamics of pathway activities, we apply a novel model-

based assessment of pathway dynamics, extending the principles of pharmacodynamics/pharmacokinetics (PKPD) to describe pathway activities. The model-based approach enabled us to hypothesize on the likely emergence (or disappearance) of multiple dosing-dependent regulatory interactions, pointing to likely mechanistic implications of dosing of MPL upon transcriptional regulation.

3.1.2 Approach

Toward the analysis of the response of liver tissues to acute and chronic MPL dosing, we applied the pathway-based analysis approach presented in Chapter 2 (Acevedo, Berthel et al. , Acevedo, DuBois et al. 2019 (submitted)). Details specific to the liver analysis are presented herein, including the relevant data sets analyzed and notes on the version of the framework applied to liver data analysis (Acevedo, Berthel et al. , Acevedo, DuBois et al.).

Animal Model and Experimental Data use for MPL Liver Analysis

Acute dosing: 43 adrenalectomized male (ADX) Wistar rats were treated with a bolus dose of 50 mg/kg MPL intravenously (Jin, Almon et al.). This dose was established in previous investigations identifying biomarkers for gene-mediated effects of glucocorticoids within liver because it produces strong, but not saturating, effects on gene and protein expression within rat liver and for its comparability with large doses in human upon scale-up (Boudinot, D'Ambrosio et al. 1986). Liver is analyzed as a primary site of glucocorticoid action and contains a relatively high concentration of glucocorticoid receptors in comparison with other tissues (Ballard, Baxter et al. 1974). The animals were sacrificed at 17 timepoints (n = 2-4) from 0 to 72 hours post dosing. Affymetrix GeneChips Rat Genome U34A (Affymetrix, Inc.) was used to array the mRNA expression data collected at these time points (microarray contains 8799 probes). The

dataset was collected in a previous investigation, submitted to GEO (GSE490), and we have previously presented multiple analyses of the transcription responses (Almon, Yang et al. 2008, Almon, Yang et al. 2008, Yang, Almon et al. 2008, Nguyen, Almon et al. 2010, Ovacik, Sukumaran et al. 2010, Nguyen, Almon et al. 2014).

Chronic dosing: 40 ADX male Wistar rats were administered 0.3 mg/kg·h of MPL intravenously for 7 days (Almon, DuBois et al. 2007). As with the acute analysis, liver is analyzed as a primary site of glucocorticoid action and contains a relatively high concentration of glucocorticoid receptors in comparison with other tissues (Ballard, Baxter et al. 1974). Rats were sacrificed at 11 timepoints (n = 4) from 0 to 168 h (Almon, DuBois et al. 2007). As an additional timepoint at 0 h and as a control, four additional rats were used as a control group at various times throughout 7-day time period (Almon, DuBois et al. 2007). Affymetrix GeneChips Rat Genome 230A (Affymetrix, Inc., Santa Clara, CA) was used to analyze the data in the chronic study (microarray contains 15,967 probes). The dataset was collected in a previous investigation, submitted to GEO (GDS972), and we have previously presented multiple analyses of the transcription responses (Hazra, DuBois et al. 2008, Yao, Hoffman et al. 2008, Nguyen, Almon et al. 2010, Nguyen, Almon et al. 2014).

Notes on Framework for MPL Liver Analysis

To reconcile the temporal response of liver tissue to acute and chronic MPL dosing, the datasets were processed using our pathway activity analysis framework described in Chapter 2 (Acevedo, Berthel et al. , Acevedo, DuBois et al.). The liver analysis is recently published (Acevedo, Berthel et al.) and uses a slightly earlier version of the framework than the version described in Chapter 2. The differences between this version of the framework are minor and briefly listed here:

- Complete analysis of the liver data with the pathway-based analysis detailed in Chapter 2 is previously published (Acevedo, Berthel et al.).
- Data preprocessing steps include using row-average data imputation to supplement missing values in incomplete expression profiles. Only probes that registered as present or marginal were retained within the microarray for analysis.
- As of Jan 2018, the period in which the liver analysis was completed, the KEGG database contained 524 pathways that represent genomic and proteomic information across 5,646 organisms, 53 of which are mammals. 317 of the 524 possible KEGG pathways were relevant to Rattus norvegicus. Pathways unrelated to the liver are irrelevant to this study of MPL influence within the liver. For this reason, pathways unrelated to the liver (ex. Cardiac muscle contraction, Complement and coagulation cascades, Platelet activation), describing neurological diseases (ex. Non-alcoholic fatty liver disease, Alzheimer's disease, Parkinson's disease, Huntington's disease), irrelevant to the liver (Olfactory transduction), or redundant for all other metabolic pathways (KEGG's pathway entitled Metabolic pathways rno:01100 is the set of all other metabolism related pathways) were removed from the pathway set. The final list used for this investigation totals 209 pathways relevant to the liver.
- In early stages of the framework, multiple databases were used to convert Affymetrix probe identifiers to recognizable gene names and KEGG gene identifiers (Acevedo, Berthel et al.). To this end, a series of probe name conversions were completed and facilitated by additional databases: DAVID (Da Wei Huang and Lempicki 2009, Huang, Sherman et al. 2009) and Uniprot (Consortium 2018). Genes from rat pathways in KEGG are recognized by the identifier *rno*. Uniprot is used to convert from rno to Uniprot accession numbers. Only genes reported as reviewed in Uniprot were retained. These are

then converted to Affymetrix probe identifiers within the DAVID database. Affymetrix probes are redundant meaning multiple Affymetrix identifiers will refer to a single protein accession ID. However, one rno ID refers to a single unique protein accession number.

3.1.3 Results

Fractional coverage analysis of the 209 rat/liver-relevant KEGG pathways yields 56 and 57 pathways as significant, for acute and chronic dosing respectively. These are decomposed to their constitutive activities with the SVD approach described earlier. Each pathway yields multiple PAL profiles of varying significance. A fraction of total pathway activity (f_p) is identified for each PAL and only significant f_p indicate significant PAL. To assess the significance of the coverage we also calculate the confidence for each f_p value, defined as the f_p p-value and described in Chapter 2.

For consistency, the p-value threshold of 10^{-3} is used for selecting both the over-represented pathways and the significant f_p values. A significant f_p corresponds to a pathway activity level profile (PAL profile). A pathway is robustly active if its activity is described by at least one significant PAL. This analysis yields: 26 significant pathways in the acute and 27 in the chronic datasets (ST 3 and ST 4). Interestingly, we identify that the subset of 24 active pathways are shared across both dosing regimens, albeit the patterns of activity observed within the PAL are different – as will be discussed in greater detail in the following section.

Table 4 reports the details of the 24 pathways active in both the acute and chronic data. For each pathway, fractional coverage (f_c) is reported in the acute and chronic datasets. Also reported in this table are total f_p values for pathway datasets of different significance thresholds. In the

original gene set of each pathway, significant PAL are identified, each corresponding to an independent $f_p$value. The total of these significant f_p values indicates the fraction of pathway activity that is significant. This total fraction of pathway activity is what is reported as the total $f_p$value within this table.

Table 4 Significant pathways common to acute and chronic dosing data. These pathways exhibit significant fractional coverage (f_c p-value $\leq 10^{-3}$) and significant pathway activity (f_p p-value $\leq 10^{-3}$) in both the acute and chronic datasets.

Pathway (PW)	rno ID	Acute					Chronic				
		Unique Genes in PW from Dataset (rno)	Fractional PW Coverage (fc)	Total Significant Fraction of Pathway Activity (total fp)			Unique Genes in PW from Dataset (rno)	Fractional Pathway Coverage (fc)	Total Significant Fraction of Pathway Activity (total fp)		
				PWs pvalue <= 0.1	PWs pvalue <= 0.01	PWs pvalue <= 0.001			PWs pvalue <= 0.1	PWs pvalue <= 0.01	PWs pvalue <= 0.001
Amino Acid Metabolism											
Arginine biosynthesis	rno:00220	11	55%	76%	76%	76%	11	55%	54%	54%	54%
Biosynthesis of amino acids	rno:01230	27	32%	73%	73%	73%	33	39%	76%	76%	76%
Cysteine and methionine metabolism	rno:00270	17	36%	70%	70%	70%	19	40%	65%	65%	65%
Valine, leucine and isoleucine degradation	rno:00280	25	45%	58%	58%	58%	29	52%	51%	51%	51%
beta-Alanine metabolism	rno:00410	12	36%	66%	66%	66%	16	48%	75%	52%	52%
Tryptophan metabolism	rno:00380	16	34%	61%	61%	61%	25	53%	65%	65%	65%
Glutathione metabolism	rno:00480	17	26%	65%	65%	65%	22	34%	66%	66%	66%
Carbohydrate Metabolism											
Citrate cycle (TCA cycle)	rno:00020	13	39%	71%	71%	71%	19	58%	82%	82%	61%
Pyruvate metabolism	rno:00620	13	33%	68%	68%	68%	15	38%	68%	68%	42%
Carbon metabolism	rno:01200	39	31%	68%	68%	68%	57	45%	84%	72%	72%
Oxidative phosphorylation	rno:00190	37	26%	74%	74%	74%	49	34%	63%	63%	63%

Glycolysis / Gluconeogenesis	rno:00010	18	25%	72%	72%	72%	25	35%	64%	64%	64%
Propanoate metabolism	rno:00640	13	41%	57%	57%	57%	15	47%	45%	45%	45%
Glyoxylate and dicarboxylate metabolism	rno:00630	10	36%	49%	49%	49%	14	50%	51%	51%	27%
Essential Organelles											
Proteasome	rno:03050	18	38%	80%	64%	64%	20	42%	58%	58%	58%
Peroxisome	rno:04146	26	30%	59%	59%	59%	33	38%	63%	63%	63%
Ribosome	rno:03010	59	33%	81%	81%	81%	82	46%	78%	78%	78%
Protein processing in endoplasmic reticulum	rno:04141	32	19%	65%	65%	65%	54	33%	65%	65%	65%
Lipid Metabolism											
Fatty acid degradation	rno:00071	28	60%	56%	56%	56%	27	57%	63%	63%	43%
Fatty acid metabolism	rno:01212	26	48%	71%	56%	56%	25	46%	65%	46%	46%
Steroid hormone biosynthesis	rno:00140	27	33%	69%	55%	55%	26	31%	64%	64%	43%
PPAR signaling pathway	rno:03320	26	32%	52%	52%	52%	25	30%	66%	66%	66%
Xenobiotic Metabolism											
Metabolism of xenobiotics by cytochrome P450	rno:00980	22	30%	76%	76%	61%	23	32%	71%	71%	71%
Metabolism of cofactors and vitamins											
Retinol metabolism	rno:00830	24	28%	55%	55%	55%	25	29%	66%	66%	66%

Bootstrapping each pathway dataset allows us to identify, *in silico,* likely activity patterns from synthetic replications (bootstrapped) of the animal studies which yielded the transcriptomic datasets. 1000 bootstrapped datasets were generated for each pathway and significant pathway activities (PAL profiles) were identified, as described in the Methods section. We repeatedly identified significant pathway activities within the bootstrapped pathway gene sets and identified common patterns of activity despite the variability of the original data.

Pathways decomposed each into multiple PAL, indicating a likely codominance of activity patterns within the pathway and complex regulation of the pathways' components. To consistently characterize the dynamics of each individual PAL for a given pathway we hypothesize likely modes of regulation. Namely, we hypothesize a PAL component is either directly or indirectly regulated by MPL and possibly an intermediate biosignal. The dynamics of each PAL are fitted using either the monophasic or biphasic regulatory models, as described below. This step is critical as it allows us to compare PAL dynamics within, and across, dosing regimens in a model based, data-independent, manner.

Detailed analysis of the common pathways revealed very interesting trends. Using the acute response as the basis we identify two class groupings within the set of 24 significant pathways: **class 1**: (acute monophasic or acute biphasic response) pathways exhibiting either monophasic or biphasic regulation only; and **class 2**: (acute monophasic and acute biphasic, aka complex acute) pathways exhibiting both monophasic and biphasic activity, i.e. individual pathways that yield multiple PAL, some of which are acute monophasic and some of which are acute biphasic. Within these primary categories based on acute data, we further investigated the type of regulation each of the pathways under chronic dosing. Table 5 presents each pathway and its categorization by class and response type.

Table 5 Responses of significant (f_p p-value and f_c p-value $\leq 10^{-3}$) pathways to acute and chronic MPL administration.

Pathway	**Pathway Category**	**Acute MPL Response**	**Chronic MPL Response**	**Class**
Glyoxylate and dicarboxylate metabolism	Carbohydrate Metabolism	biphasic	monophasic	1
Tryptophan metabolism	Amino Acid Metabolism	monophasic	biphasic	1
Valine, leucine and isoleucine degradation	Amino Acid Metabolism	monophasic	monophasic/biphasic	1
Propanoate metabolism	Carbohydrate Metabolism	monophasic	biphasic	1
Peroxisome	Essential Organelles	monophasic	monophasic/biphasic	1
Fatty acid degradation	Lipid Metabolism	monophasic	monophasic/biphasic	1
Steroid hormone biosynthesis	Lipid Metabolism	monophasic	monophasic/biphasic	1
Fatty acid metabolism	Lipid Metabolism	monophasic	monophasic/biphasic	1
PPAR signaling pathway	Lipid Metabolism	monophasic	monophasic/biphasic	1
beta-Alanine metabolism	Amino Acid Metabolism	monophasic	monophasic	1
Glutathione metabolism	Amino Acid Metabolism	monophasic	monophasic	1
Proteasome	Essential Organelles	monophasic	monophasic	1
Retinol metabolism	Metabolism of cofactors and vitamins	monophasic	monophasic	1
Citrate cycle (TCA cycle)	Carbohydrate Metabolism	monophasic/biphasic	biphasic	2
Pyruvate metabolism	Carbohydrate Metabolism	monophasic/biphasic	biphasic	2
Ribosome	Essential Organelles	monophasic/biphasic	biphasic	2
Metabolism of xenobiotics by cytochrome P450	Xenobiotic Metabolism	monophasic/biphasic	biphasic	2
Arginine biosynthesis	Amino Acid Metabolism	monophasic/biphasic	monophasic	2
Oxidative phosphorylation	Carbohydrate Metabolism	monophasic/biphasic	monophasic	2
Biosynthesis of amino acids	Amino Acid Metabolism	monophasic/biphasic	monophasic/biphasic	2
Cysteine and methionine metabolism	Amino Acid Metabolism	monophasic/biphasic	monophasic/biphasic	2
Glycolysis / Gluconeogenesis	Carbohydrate Metabolism	monophasic/biphasic	monophasic/biphasic	2
Carbon metabolism	Carbohydrate Metabolism	monophasic/biphasic	monophasic/biphasic	2
Protein processing in endoplasmic reticulum	Essential Organelles	monophasic/biphasic	monophasic/biphasic	2

Class 1: Exclusively Monophasic or Biphasic Acute Response

Twelve pathways are identified with strictly acute monophasic responses and one pathway exhibits strictly acute biphasic response. The acute monophasic response pathways are classified by pathway families including **amino acid metabolism** (**beta-Alanine metabolism, Glutathione metabolism, Tryptophan metabolism,** and **Valine, leucine and isoleucine degradation**) (Ratnam, Maclean et al. 2002, Christiansen, Djurhuus et al. 2007), **carbohydrate metabolism** (**Propanoate metabolism**) (McMahon, Gerich et al. 1988, Nader, Ng et al. 2012), **essential organelle regulation** (**Peroxisome** and **Proteasome**) (Wallace and Cidlowski 2001, Rhen and Cidlowski 2005, Cuzzocrea, Bruscoli et al. 2008), **lipid metabolism** (**Fatty acid degradation, Fatty acid metabolism, PPAR signaling pathway,** and **Steroid hormone biosynthesis**) (Macfarlane, Forbes et al. 2008, Peckett, Wright et al. 2011), and **metabolism of cofactors and vitamins** (**Retinol Metabolism**) (Pascussi, Drocourt et al. 2000).

The majority of the monophasic responses in this set yield an early monophasic response, which consists of a single peak of activity corresponding to the direct effect of DRN between 2 and 5 h (also referenced as DRN effect peak) and subsequent return to initial baseline between 18 and 30 h. The Proteasome pathway exists as an outlier by exhibiting a late monophasic response consisting of a delayed DRN event peak between 7 and 15 h and a return to baseline between 32 and 65 hours, defining the late biphasic response category. Only the **Glyoxylate and dicarboxylate metabolism** pathway, within the carbohydrate metabolism family, exhibits a biphasic response to acute MPL administration, discussed further below.

Though many pathways exhibit monophasic behavior in response to either acute or chronic dosing, the **Glutathione Metabolism, Retinol Metabolism, Proteasome,** and **beta-Alanine**

Metabolism pathways exhibit exclusively monophasic behavior in response to both acute and chronic dosing. The acute response for each of these pathways reports a DRN event peak between 3 and 4 h followed by a return to baseline between 20 and 25 h. In the **Glutathione Metabolism** pathway, chronic MPL administration yields a steep and continuous incline and does not settle to a new steady state value within the 168 h of the experiment. The **beta-Alanine pathway** yields strictly one pattern of behavior in response to Chronic MPL, a steep incline until 25 h followed by a settling to a new steady state by 120 h. The **Retinol metabolism** pathway returns multiple chronic behavior responses: a steep continuous incline with no peak and no settling to a new baseline within the experiment time; steep incline until 25 h followed by settling at a new steady state by 120 h; and peak DRN activity event at 22 h followed by a settling at a new steady state by 55 h. The **Proteasome** pathway exhibits a slightly later acute DRN event peak at 9 h and returns to baseline by 50 h. The **Proteasome** pathway is singular in that it's response to chronic MPL administration yields DRN event peaks between 12 and 16 h followed by settling to a new steady state by 50 h.

Two pathways, **Propanoate metabolism** and **Tryptophan metabolism**, exhibit a DRN event peak at 3 h and a return to baseline by 20 to 25 h in response to acute MPL administration. In response to chronic MPL administration, these pathways exhibit strictly biphasic behavior. **Propanoate Metabolism** yields a DRN peak between 11 and 17 h, and a peak activity event due to an intermediate biosignal between 40 and 44 h. This pathway does not settle to a new steady state within the 168-h timeframe of the experiment, but the approach to an asymptote is implied. **Tryptophan metabolism** reports similar behavior, yielding a DRN event peak at 16 h, an intermediate biosignal peak between 44 and 54 h, and approaches an asymptote either by 150 h or is implied to approach steady state outside of the 168-hexperimental period.

The remaining six pathways (**Fatty acid degradation, Fatty acid metabolism, Peroxisome, PPAR signaling pathway, Steroid hormone biosynthesis, and Valine, leucine and isoleucine degradation**) exhibit the acute response (DRN peak between 3 and 4 h and return to baseline by 20 to 25 h), as well as both monophasic and biphasic responses to chronic MPL administration. Within the lipid metabolism pathways, **Fatty acid degradation** yields monophasic responses with DRN event peaks between 22 and 24 h followed by a rapid steady state achievement at 25 h or a delayed steady state achievement by 55 h. This pathway's biphasic responses yield peak DRN events at 15 to 16 h, intermediate biosignal events at 40 to 41 h, and settle to a new activity baseline by 155 h or after 168 h. **Fatty acid metabolism** returns monophasic reporting steep inclines in activity until 25 h and a similar settling to a new steady state achieved rapidly by 35 h or with delay by 90 h. **Fatty acid metabolism** pathway's chronic biphasic response reports DRN event peaks 14 h, intermediate biosignal event peaks at 33 to 36 h, and new steady state achievement either rapidly by 115 h or is implied to approach a new steady state after the 168 h.

Relatedly within the lipid metabolism family, **PPAR signaling pathway** and **Steroid hormone biosynthesis pathway** exhibit steep inclines until 30 to 35 h in their monophasic response to chronic MPL administration. This is followed by achievement of a new steady state of activity by 90 to 110 h. The chronic biphasic response within the **PPAR signaling pathway** describes DRN peaks from 15 to 16 h, intermediate biosignal peaks from 34 to 38 h, and new steady state achievement by 125 or 130 h or are implied to achieve steady state after 168 h by their approach to an activity asymptote. The **Steroid hormone biosynthesis** pathway exhibits one biphasic response that reports a DRN event peak at 1 h, an intermediate biosignal event peak at 30 h, and does not appear to achieve steady state within 168 h.

Glyoxylate and dicarboxylate metabolism pathway, exhibits strictly early biphasic response to acute MPL administration and represents the pathway family carbohydrate metabolism. Early

biphasic response is defined by pathways exhibiting DRN effect peaks between 1 and 5 h, an intermediate biosignal peak between 12 and 20 h, and return to baseline between 38 and 65 h. In response to acute MPL administration, this pathway exhibits DRN event peaks between 4 and 5 h, intermediate biosignal event peaks between 16 and 19 h, and return to baseline between 57 and 65 h. In response to chronic MPL administration Glyoxylate **and dicarboxylate metabolism** pathway yields a monophasic response reporting a steep incline until 25 h and a settling at a new steady state by 90 h.

Class 2: Complex Acute Response

Eleven pathways within the pathway groups of amino acid metabolism (Ratnam, Maclean et al. 2002, Christiansen, Djurhuus et al. 2007) (**Arginine biosynthesis, Biosynthesis of amino acids,** and **Cysteine and methionine metabolism**), carbohydrate metabolism (McMahon, Gerich et al. 1988, Nader, Ng et al. 2012) (**Pyruvate metabolism, Carbon Metabolism, Glycolysis / Gluconeogenesis, Citrate cycle**, and **Oxidative Phosphorylation**), regulation of essential organelles (**Ribosome** and **Protein processing in endoplasmic reticulum**) (Wallace and Cidlowski 2001, Rhen and Cidlowski 2005, Cuzzocrea, Bruscoli et al. 2008), and xenobiotic metabolism (Dvorak and Pavek 2010) (**Metabolism of xenobiotics by cytochrome P450**) also report complex responses to acute MPL administration. In this class, the PAL responses captured indicate that some components (i.e. subgroups of genes) of pathways respond with monophasic behavior while other components exhibit biphasic behavior. Acute MPL administration yields multiple profile patterns: both early and late phase of either monophasic or biphasic response. As previously defined, early monophasic response indicates DRN event peaks between 2 and 5 h followed by a return to baseline between 18 and 30 h. Late monophasic responses are defined by a DRN event peak between 7 and 15 h followed by a return to baseline between 32 and 65 hours. Early biphasic responses are defined by a DRN event peak between 1 and 5 h, an intermediate

biosignal peak between 12 and 20 h, and a return to baseline between 38 and 65 h. Only one pathway exhibited a late biphasic response (Arginine biosynthesis), defined by a DRN peak at 16 h, and intermediate biosignal event peak at 23 h and a return to baseline implied to occur after 72 h.

(**Acute Response: Early Monophasic and Early Biphasic**) Pathways in this subgroup (**Protein processing in endoplasmic reticulum, Metabolism of xenobiotics by cytochrome P450,** and **Ribosome)** exhibit both early monophasic and early biphasic response to acute MPL administration. In response to chronic MPL administration, **Protein processing in endoplasmic reticulum** exhibits both monophasic and biphasic responses. The chronic monophasic response exhibits a DRN event peak between 5 and 6 h followed by a settling to a new steady state by 45 h. The chronic biphasic response exhibits DRN event peak between 16 and 18 h, an intermediate biosignal peak between 58 and 60 h, and settles to a new steady state after 168 h. The **Metabolism of xenobiotics by cytochrome P450** and **Ribosome** pathways exhibit chronic biphasic behavior only. **Metabolism of xenobiotics by cytochrome P450** repots DRN effect peaks between2 and 4 h, a peak due to the intermediate biosignal between 36 and 38 h, and establishment of a new steady state is implied to occur after 168 h. The **Ribosome** pathways exhibits DRN effect peaks slightly later, between 16 and 29 h, followed by intermediate biosignal effects between 58 and 60 h, and establishment of a new steady state after 130 h.

(**Acute Response: Early and Late Monophasic and Early Biphasic**) **Oxidative phosphorylation** and **Carbon metabolism** exhibit early and late monophasic, as well as early biphasic, responses to acute MPL administration. In response to chronic MPL administration the **Oxidative phosphorylation** pathway exhibits a monophasic response, exhibiting a steep incline until 40 h with no clear event peak, but establishes a new steady state by 120 h. **Carbon metabolism** exhibits both monophasic and biphasic responses to chronic MPL administration. Its

chronic monophasic response reported a steep incline until 25 h with no peak, and establishes a new steady state by 30 h. Its chronic biphasic response reports a DRN event peak between 5 and 9 h, an intermediate biosignal peak between 35 and 40 h, and a settling to a new steady state after 150 h.

(**Acute Response: Late Monophasic and Early Biphasic**) Pathways **Cysteine and methionine metabolism**, **Pyruvate metabolism**, **Glycolysis / Gluconeogenesis**, **Biosynthesis of amino acids,** and **Citrate cycle** all exhibit this complex response to acute MPL administration, yielding both late monophasic and early biphasic responses. In response to chronic MPL administration, a combination of monophasic and biphasic responses is also observed. The **Cysteine and methionine metabolism** pathway reports chronic biphasic responses with DRN peaks between 2 and 9 h, intermediate biosignal peaks between 28 and 30 h, and establishment of a new steady state between 55 and 120 h. Its chronic monophasic response exhibits a steep incline until 35 h, no discernable peak, and establishment of a new steady state by 90 h. **Pyruvate metabolism** exhibits a chronic monophasic response with a steep continuous incline, no peak, and an implication that the system will settle after 168 h. It's chronic biphasic response exhibits a DRN event peak at 8 h, an intermediate biosignal peak at 47 h, and a new steady state is implied after 168 h. **Glycolysis / Gluconeogenesis** exhibits multiple chronic monophasic responses: one in which a peak is observed at 13 h and a new steady state is achieved by 50 h; as well as a monophasic response in which a steep incline is observed until 50 h, no peak is identifiable, and a new steady state is implied to occur after 168 h. Its biphasic response reports a DRN peak at 16 h, an intermediate biosignal event peak at 57 h, and establishment of a new steady state after 168 h. **Biosynthesis of amino acids** pathway yields monophasic responses that exhibit DRN event peaks between 4 and 15 h and settles to a new steady state between 35 and 45 h. Biphasic responses to chronic MPL within this pathway report DRN event peaks between 9 and 15 h,

intermediate biosignal peaks between 27 and 45 h, and settle to a new steady state by 80 to 120 h. Chronic MPL administration exhibits **Citrate cycle** only chronic biphasic response, reporting a DRN event peak between 9 and 13 h, and intermediate biosignal peak between 32 and 37 h, and establishment of a new steady state by 95 to 100 h.

(**Acute Response: Late Monophasic, Early and Late Biphasic**) Solely **Arginine biosynthesis** demonstrates this combination of responses to acute MPL administration: late monophasic, as well as early and late biphasic. In response to chronic MPL, **Arginine biosynthesis** exhibits monophasic behavior. Exhibiting activities with steep and continuous inclines until 30 or 40 h, no distinguishable peaks, and establishment of new steady states by 110 h or after 168 h.

3.1.4 Discussion

Synthetic glucocorticoids, such as MPL, are widely used anti-inflammatory drugs. Despite their widespread usage the actions and secondary effects are still under investigation. Dosing regimens further complicate the host's response to the drug. Of importance is the liver-response, being the organ of primary drug metabolism. Earlier studies have focused on liver-specific genome-wide transcriptomic analyses under acute and chronic dosing (Sun, DuBois et al. 1998, Ramakrishnan, DuBois et al. 2002, Ramakrishnan, DuBois et al. 2002, Jin, Almon et al. 2003, Almon, Dubois et al. 2005, Almon, DuBois et al. 2007, Almon, Yang et al. 2008, Hazra, DuBois et al. 2008, Yang, Almon et al. 2008, Nguyen, Almon et al. 2010, Nguyen, Almon et al. 2010, Nguyen, Almon et al. 2014, Nouri-Nigjeh, Sukumaran et al. 2014, Kamisoglu, Sukumaran et al. 2015, Ayyar, Almon et al. 2017). Transcriptional analyses focus on characterizing individual gene responses. Clustering and functional annotation enables a more complete characterization of the response. In this investigation, we approach the problem from another angle: we aim to characterize the dynamic response of functionally related *a priori* groupings of genes. We therefore aim to characterize the dynamic response of signaling and metabolic pathways following acute and chronic exposure to

MPL. Characterizing the dynamics at the pathway level, or at the level of functionally related genes in general, enables comparison across platforms and experiments since the approach does not require consistency across experiments.

The first step of the analysis requires that we identify pathway appropriately represented in the microarray data. This is a critical step, since we need to confirm that pathways whose activities will be further analyzed, are adequately represented in the experimental data. In doing so we define fractional coverage (f_c) as the metric characterizing the extent to which a pathway is represented in the probe set used and reported in the genome-wide transcriptomic studies, as previously defined in the Methods section. We further assess the statistical significance of this metric by associating with the fractional coverage of a pathway with a p-value communicating our confidence that the fractional coverage is statistically significant. The metric is very important particularly in cases like the one we analyzed where we are assessing and comparing experimental data using different platforms, or arrays as in our case. Since the initial set of genes whose activity is quantified are not the same across the two conditions (different animal studies make use of different microarrays), it is important to confirm that the pathways are appropriately represented because these pathways are identical across datasets and thus, can be compared. As expected, as the statistical significance of the reliability of the fractional coverage metric is increased, the set of significantly represented pathways decreases. Our results indicate that of 209 pathways represented in KEGG which are relevant to *Rattus norvegicus* and the liver, 56 and 57 have statistically significant fractional coverage in the acute and chronic experiments, respectively, at a confidence level of 10^{-3}.

The next critical step is to associate a coherent dynamic response with each of the represented pathways. Our hypothesis is that each pathway is effectively a high-dimensional dynamic system,

with each dimension corresponding to a gene in the pathway. We hypothesize that the multi-dimensional dynamics can be decomposed into intrinsic elements, identified via the SVD decomposition (Tomfohr, Lu et al. 2005, Ovacik, Sukumaran et al. 2010, Ovacik, Sen et al. 2013). SVD decomposition of the original data determined whether a pathway can generate at least one PAL, an indication that the pathway is active and should be further analyzed for multiple activity patterns in a manner that considers the inherent variability of the data. To account for the inherent variability in the experimental observations, the proposed bootstrap enabled us to identify likely intrinsic responses and further to assess a likelihood metric via corresponding p-values.

From within the sets of the 56 and 57 pathways identified to have statistically significant fractional coverage in the acute and chronic data respectively, 26 pathways in the acute and 27 in the chronic yielded at least one significant PAL profile, indicating their significant pathway activity. 24 of these pathways are common to both the acute and chronic significant pathway sets (Table 4). The chronic pathways exhibit consistently higher fractional coverage than their acute counterparts. Completed a few years after the acute study, the chronic study had access to a microarray platform (230A) previously unavailable. Because both experiments investigate MPL within the liver, a consistent set of significant pathways is anticipated to emerge when comparing these data with our framework. However, it is likely that the difference in platform contributes to this discrepancy between acute and chronic pathway fractional coverage. The chronic study has a larger probe set on its microarray and thus has more genes to occupy each pathway. Thus, a consistent core set of pathways emerges as significantly represented and active in response to MPL in both datasets. These pathways emerge from the amino acid metabolism (Ratnam, Maclean et al. 2002, Christiansen, Djurhuus et al. 2007), carbohydrate metabolism (McMahon, Gerich et al. 1988, Nader, Ng et al. 2012), essential organelle regulation (Wallace and Cidlowski

2001, Rhen and Cidlowski 2005, Cuzzocrea, Bruscoli et al. 2008), lipid metabolism (Macfarlane, Forbes et al. 2008, Peckett, Wright et al. 2011), metabolism of cofactors and vitamins (Pascussi, Drocourt et al. 2000), and xenobiotic metabolism pathway families (Dvorak and Pavek 2010).

Interestingly, the decomposition of the pathway dynamics to its intrinsic constituents verified that the emergent dynamics were consistent with likely mechanisms of regulation. Broadly, the intrinsic responses for the acute dosing reflects transient activity events due to DRN to GRE binding or transcription mediated via an intermediate biosignal influenced by MPL – while returning to baseline following the elimination of the drug. The chronic administration led to more complicated responses, including transient and persistent effects indicating both DRN to GRE binding or transcription mediated via intermediate biosignal. The bootstrapping step enabled us to investigate how the variability in a pathway dataset influences which pathway activity levels are dominant. The initial SVD step which determined whether a pathway can yield at least one PAL is a screening step which identifies if the pathway is at all active. The bootstrapping step is applied afterwards to ask the question, what kinds of significant activity emerge if the variability in the gene set is considered? For this investigation, this bootstrapping step is applied to pathways significant with p-values $\leq 10^{-3}$. It can be applied to pathway sets of any significance (i.e. pathway sets corresponding to p-value $\leq 10^{-1}$ and p-value $\leq 10^{-2}$), however this is not necessary for our investigation as we are only interested in pathways that pass the screening SVD test at the greatest significance. This process identified pathways indicating consistent activity under either acute or chronic drug administration. The first important observation from our analysis is that, regardless of dosing, the pathways encapsulating the MPL effects are similar. Interestingly, chronic administration leads to the emergence of complex dynamics, not necessarily expected based on analysis of the acute response.

To systematically compare across dosing regimens and time horizons (72 h in acute study, 168 h in chronic study), we compare the intrinsic dynamics in the space of regulatory models. We hypothesize that each intrinsic response can be represented by corresponding PKPD models. Following the regulatory mechanisms proposed in previous publications (Sun, DuBois et al. 1998, Ramakrishnan, DuBois et al. 2002, Hazra, DuBois et al. 2008) we develop a two-compartment PK model for both acute and chronic dosing (Figure 4) and hypothesized either monophasic (Equation 13) or biphasic (Equations 14 and 15) regulation of the intrinsic component of the activity of the pathway. We therefore extend the concept of PD dynamic to characterizing the intrinsic responses at the pathway level. Our analysis indicates that the acute response initiates pathway dynamics consistent with the nature of the acute dosing: since MPL half-life of 0.33 h in ADX rats with a total drug clearance observed in ADX rats by 4.6 h (Hazra, Pyszczynski et al. 2007).

We observed that the pathway responses emerging under acute dosing reflect monophasic or biphasic responses. However, the same pathway can lead to rather complicated dynamics under chronic administration. For consistency in our analysis, we examined pathways based on their response under acute administration. We therefore, broadly identified two major categories: Class 1 capturing pathways yielding strictly monophasic response or strictly biphasic response to acute MPL administration; and Class 2 reporting pathways yielding both monophasic and biphasic response to acute MPL administration. Within these categories (Table 5), pathway response to chronic MPL administration is compared.

Although PAL profiles resemble gene expression profiles, the features in these profiles do not necessarily correspond to up or down gene expression. The SVD linear combination technique preserves the relative magnitudes of gene expression profiles, but it does not preserve sign. For example, many genes which report an early upregulation event in their expression profiles will

contribute to a single unique PAL, which will contain an early event peak. This is because the PAL is a linear combination of those gene expression profiles. A set of gene expression profiles will "resolve" to a PAL with the same timing and relative magnitude of features, but which may appear as a reflection of the gene expression profiles. What is critical to our analysis is the timing and relative magnitude of the peak events, which SVD preserves. These features determine whether a monophasic of biphasic mechanism is proposed.

Class 1 includes pathways exhibiting exclusively monophasic or exclusive biphasic regulation under acute dosing. MPL induces a response which dies out as the drug is eventually eliminated from the system. Out of the 24 pathways, 13 pathways (**Tryptophan metabolism, beta-Alanine metabolism, Glutathione metabolism, Proteasome, Retinol metabolism, Valine, leucine and isoleucine degradation, Propanoate metabolism, Peroxisome, Fatty acid degradation, Steroid hormone biosynthesis, Fatty acid metabolism, PPAR signaling pathway,** and **Glyoxylate and dicarboxylate metabolism**) exhibited this response under acute dosing. Almost all of these pathways reported early acute monophasic response. Only Proteasome exhibited both early and late acute monophasic responses and only **Glyoxylate and dicarboxylate metabolism exhibited biphasic response to acute MPL.**

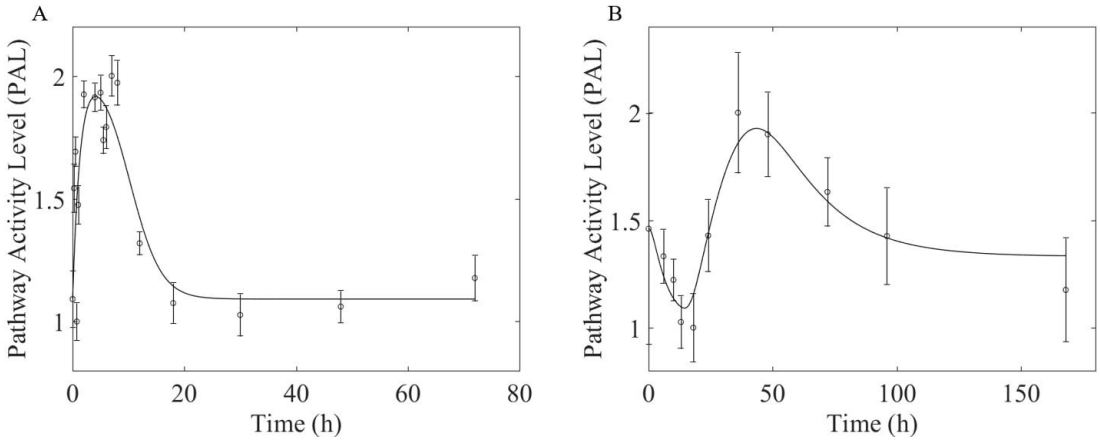

Figure 5 Tryptophan metabolism pathway response to (A) acute and (B) chronic MPL administration. Example of Class 1 pathway which yields monophasic response to acute MPL administration but varies in

its response to chronic MPL administration. The Tryptophan metabolism pathway yields a biphasic response to chronic MPL administration indicating an increased complexity across dosing studies.

Interestingly, the chronic response for the Class 1 pathways manifested itself in multiple ways. Some pathways (**Valine, leucine and isoleucine degradation, Tryptophan metabolism, Propanoate metabolism, Peroxisome, Fatty acid degradation, Steroid hormone biosynthesis, Fatty acid metabolism,** and **PPAR signaling pathway**) exhibited strictly early monophasic response but increased complexity in response to chronic MPL administration, exhibiting both monophasic and biphasic responses in different subcomponents of each pathway. **Tryptophan metabolism** (Figure 5), a pathway describing the processing of the amino acid tryptophan into biproducts catabolized by glycolysis, and other energy regulating pathways (Kanehisa and Goto 2000, Aoki and Kanehisa 2005, Christiansen, Djurhuus et al. 2007, Kanehisa, Furumichi et al. 2016) exemplifies the observed shift from acute monophasic response to a response of greater complexity, such as chronic biphasic. This shift indicates that the mechanism of regulation presumed appropriate for describing the pathway's response to acute MPL administration is insufficient for describing the pathway's actual mechanism of regulation, which is revealed with greater complexity in its biphasic response to chronic MPL administration. The **Peroxisome** pathway (Figure 6), which describes the biogenesis of peroxisome organelles, is crucial to redox signaling and lipid homeostasis (Kanehisa and Goto 2000, Aoki and Kanehisa 2005, Cuzzocrea, Bruscoli et al. 2008, Peckett, Wright et al. 2011, Kanehisa, Furumichi et al. 2016), yields strictly an acute monophasic response to acute MPL. However, the pathway reports multiple dominant activity patterns in response to chronic MPL. PAL profiles are linear combinations of the expression patterns of individual genes and if a pathway yields multiple significant PAL, it indicates that unique subgroups of genes within that pathway are responsible for each.

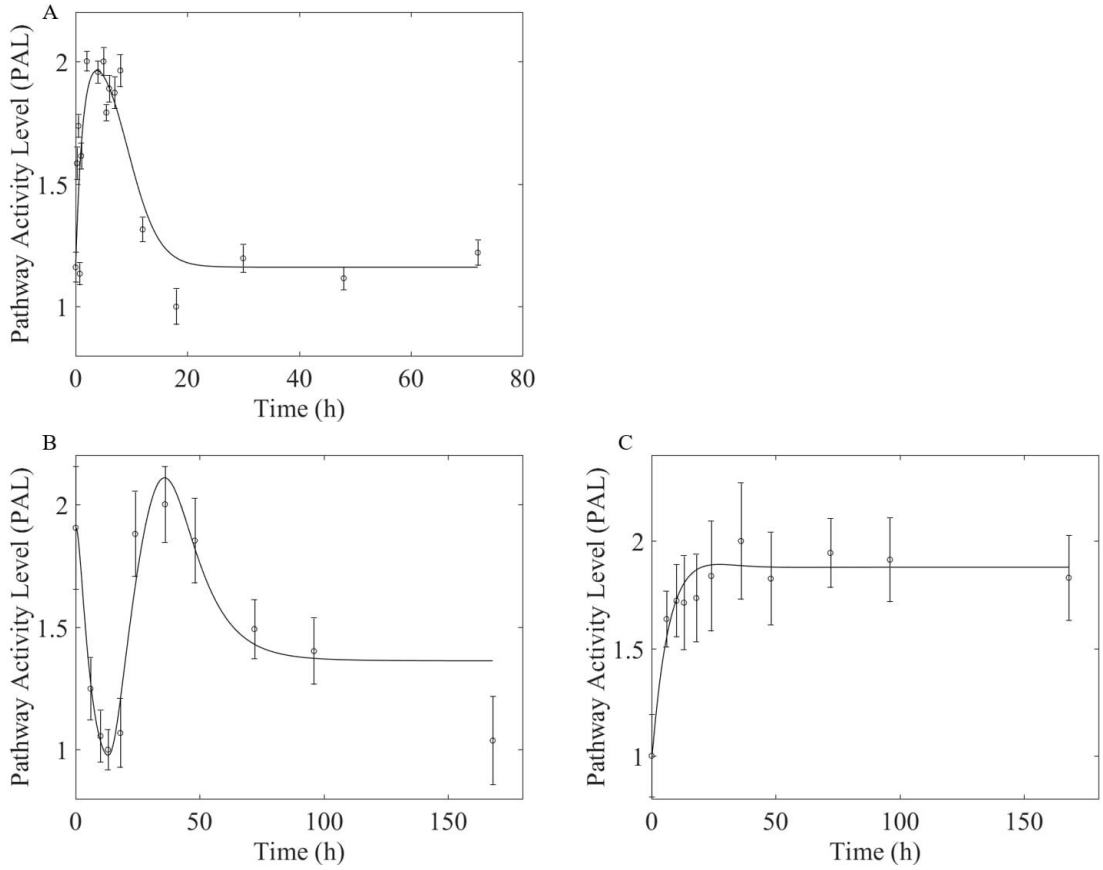

Figure 6 Peroxisome pathway response to (A) acute and (B and C) chronic MPL administration. Example of Class 1 pathway which yields monophasic response to acute MPL administration but varies in its response to chronic MPL administration. The Peroxisome pathway yields both monophasic and biphasic responses to chronic MPL administration indicating an increased complexity across dosing studies as well as an internal complexity to the pathway. This pathway exhibits multiple dominant patterns of activity, each corresponding to unique subgroups of genes within the pathway.

The **Peroxisome** pathway demonstrates this segregation of the pathway; within the gene set that composes the **Peroxisome** pathway, unique subgroups of genes behave differently, some prescribing to monophasic regulation and yielding a chronic monophasic response (Figure 6B) and some prescribing to a chronic biphasic response (Figure 6C). Thus, the **Peroxisome** pathway cannot be assumed homogenous, and in fact represents at least two subgroups of uniquely regulated gene sets. Other pathways maintained a strictly monophasic response (**beta-Alanine**

metabolism, Glutathione metabolism, Proteasome, and **Retinol metabolism**) to both acute and chronic MPL administration.

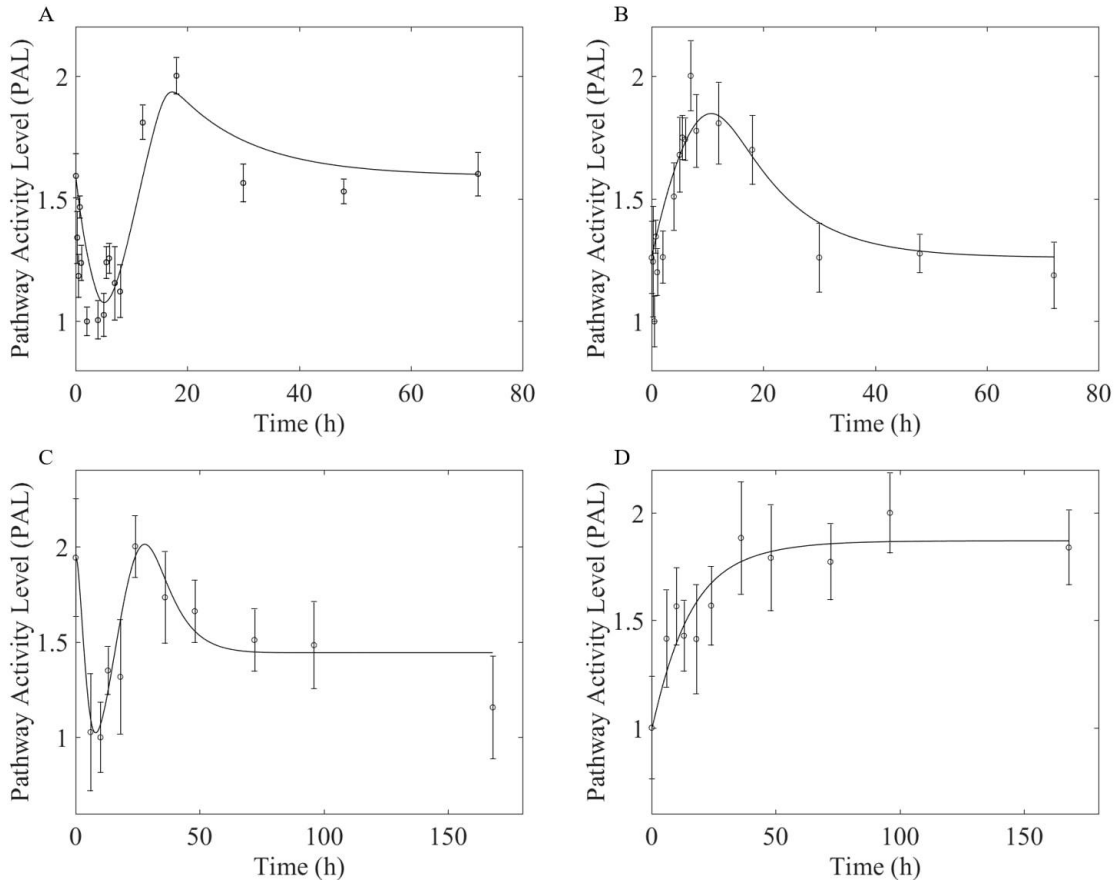

Figure 7 Cysteine and methionine metabolism pathway response to (A and B) acute and (C and D) chronic MPL administration. Example of Class 2 pathway which yields both monophasic and biphasic responses to acute MPL administration. This complexity indicates that multiple subgroups of genes within this pathway are regulated by different mechanisms. For the Cysteine and methionine pathway, this complexity is preserved across dosing types.

One pathway exhibited exclusively biphasic response to acute MPL, the **Glyoxylate and dicarboxylate metabolism** pathway. This pathway describes energy regulating biosynthesis reactions for synthesis of carbohydrates from acetyl-CoA and fatty acids (Kanehisa and Goto 2000, Aoki and Kanehisa 2005, Kanehisa, Furumichi et al. 2016). It yielded early biphasic

response to acute MPL administration but a prolonged monophasic response to chronic MPL administration.

The 11 pathways that yielded more complex acute responses were included within Class 2. Some pathways (**Cysteine and methionine metabolism, Glycolysis / Gluconeogenesis,** and **Carbon metabolism**) within this class remained complex between dosing regimens, exhibiting both monophasic and biphasic behavior in different subcomponents of the pathway, in response to both acute and chronic MPL administration. **Cysteine and methionine metabolism (**Figure 7**)**, a pathway which describes the metabolism of the eponymous amino acids into intermediates supplied to such processes as pyruvate metabolism and amino acid synthesizing pathways including **Valine, leucine, and isoleucine biosynthesis** pathway (Kanehisa and Goto 2000, Ratnam, Maclean et al. 2002, Aoki and Kanehisa 2005, Christiansen, Djurhuus et al. 2007, Kanehisa, Furumichi et al. 2016). It exemplifies the conservation of complex response between acute and chronic dosing. Regardless of dosing type, this pathway contains unique subgroups of genes who expression patterns are the foundation for the PAL profiles observed in the pathway's response. A complexity which indicates that multiple mechanisms of regulation are required to describe the activity of this pathway. Other pathways shifted their response, exhibiting complex acute behavior but resolving to either strictly chronic monophasic behavior (**Arginine biosynthesis** and **Oxidative phosphorylation**) or strictly chronic biphasic behavior (**Protein processing in endoplasmic reticulum, Citrate cycle (TCA cycle), Pyruvate metabolism, Metabolism of xenobiotics by cytochrome P450,** and **Ribosome**). The **Arginine biosynthesis** pathway describes the construction of the amino acid arginine as well as the overlap of this process with others including the Citrate cycle (catabolism of 2-Oxoglutarate and production of Fumarate), as well as the urea cycle (various steps including the generation of urea) (Kanehisa and Goto 2000, Aoki and Kanehisa 2005, Kanehisa, Furumichi et al. 2016). Acute MPL

administration provokes both an acute monophasic and acute biphasic response, indicating that the pathway can be decomposed into uniquely regulated subcomponents of genes (Figure 8A, B). However, this behavior resolves to a strictly monophasic response to chronic MPL administration (Figure 8C). This observation indicates that some regulatory structures within this pathway may be overwhelmed by chronic MPL administration and lose the phenotypes that distinguish monophasic from biphasic mechanisms.

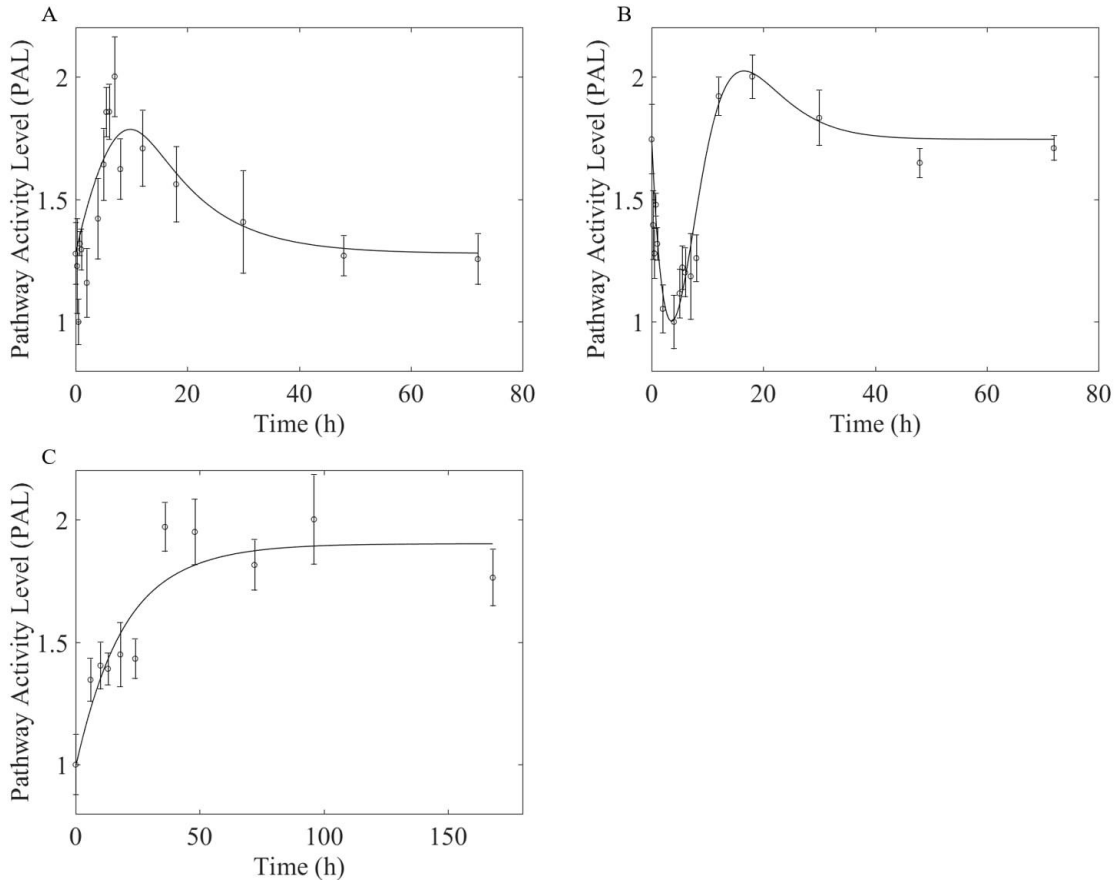

Figure 8 Arginine biosynthesis pathway response to (A and B) acute and (C) chronic MPL administration. Example of Class 2 pathway type which yields both monophasic and biphasic responses to acute MPL administration. This complexity indicates that multiple subgroups of genes within this pathway are regulated by different mechanisms. For the Arginine biosynthesis pathway, chronic MPL administration yields a shift to a monophasic response.

These results indicate that 16 of the 24 significant pathways exhibited a response pattern that changed between acute and chronic dosing. 8 of the 24 pathways **(Tryptophan metabolism, Valine, leucine and isoleucine degradation, Propanoate metabolism, Peroxisome, Fatty acid degradation, Steroid hormone biosynthesis, Fatty acid metabolism, and PPAR signaling pathway**) exhibit singularly monophasic or biphasic response to acute MPL administration but increase their complexity, exhibiting both monophasic and biphasic behavior, in response to chronic MPL administration. Increasing complexity indicates that a pathway's response to MPL is dosing-specific, and that different subcomponents (unique groups of genes within a pathway) exhibit purely DRN binding to GRE regulation, while other components exhibit both DRN to GRE binding as well as transcription regulation mediated by an intermediate biosignal. The pathway cannot be defined by simply one response type. For some pathways, the response does not change with changing dosing.

9 of the 24 pathways (**beta-Alanine metabolism, Glutathione metabolism, Proteasome, Retinol metabolism, Biosynthesis of amino acids, Cysteine and methionine metabolism, Glycolysis / Gluconeogenesis, Carbon metabolism, and Protein processing in endoplasmic reticulum**) exhibit no change in their dynamic, remaining monophasic in response to both dosing types or remaining chronic in response to both dosing types. This pathway's mechanism is sufficiently described by either strictly monophasic (DRN to GRE binding regulated transcription) or biphasic (DRN to GRE binding regulated transcription and MPL influenced intermediate biosignal mediating regulation of transcription). 4 pathways (**Citrate cycle, Pyruvate metabolism, Ribosome,** and **Metabolism of xenobiotics by cytochrome P450**) shift from a complex acute response to chronic biphasic behavior and 3 pathways (**Glyoxylate and dicarboxylate metabolism, Arginine biosynthesis, and Oxidative phosphorylation**) reduce from complex acute behavior to monophasic behavior in response to chronic MPL. This reduction

in complexity may indicate a dosing-dependence in which a system is overwhelmed by a particular magnitude of drug concentration. One mechanism may dominate in response to constant MPL administration.

The pathways that emerged within these classes exist within specific pathway families. Each of the pathways within the lipid metabolism (Macfarlane, Forbes et al. 2008, Peckett, Wright et al. 2011)family (**Fatty acid degradation, Steroid hormone biosynthesis, Fatty acid metabolism**, and **PPAR signaling pathway**) increased in complexity from acute monophasic to complex chronic responses. The amino acid metabolism family (Ratnam, Maclean et al. 2002, Christiansen, Djurhuus et al. 2007) yielded three pathways that increased in complexity from either monophasic or biphasic acute response to complex chronic response (**Tryptophan metabolism, Valine, leucine and isoleucine degradation,** and **Biosynthesis of amino acids**), three pathways that maintained either a monophasic response or a complex response to both dosing types (**beta-Alanine metabolism, Glutathione metabolism,** and **Cysteine and methionine metabolism**), and one pathway that shifted from a complex acute response to a singularly monophasic response (**Arginine biosynthesis**). Within the regulation of the essential organelles family, one pathway (**Peroxisome**) increased in complexity from acute monophasic to complex chronic response, two pathways maintained the same response across dosing types either both monophasic or both complex (**Proteasome** and **Protein processing in endoplasmic reticulum**), and one pathway shifted from a complex acute response to a chronic biphasic response (**Ribosome**). The **Retinol metabolism** pathway within metabolism of cofactors and vitamins maintained the same monophasic response to acute and chronic MPL. The **Metabolism of xenobiotics by cytochrome P450** pathway within the xenobiotic metabolism family shifted from complex acute response to chronic biphasic.

This investigation uses meta-analysis technique to capture and compare physiological dynamics at the pathway level. This method provides a more comprehensive survey of physiological activity than do strictly gene-centric approaches, while capable of predicting likely regulatory structures. Designed to facilitate comparison of experiments that differ in platform, time scale, and dosing, this framework enabled a multiple dosing to identify and compare the influence of MPL within the liver. Significant influence of MPL is observed within five pathway families: amino acid metabolism (Ratnam, Maclean et al. 2002, Christiansen, Djurhuus et al. 2007), carbohydrate metabolism (McMahon, Gerich et al. 1988, Nader, Ng et al. 2012), regulation of essential organelles (Wallace and Cidlowski , Rhen and Cidlowski , Cuzzocrea, Bruscoli et al.), lipid metabolism (Macfarlane, Forbes et al. , Peckett, Wright et al.), metabolism of cofactors and vitamins (Nader, Ng et al. 2012), and xenobiotic metabolism (Dvorak and Pavek). Within each family, most pathways demonstrate changed dynamics across dosing regimens. Further, all pathways exhibit some form of dosing-dependence easily identified when comparing acute to chronic responses within a pathway. Deconstruction of the activity of a pathway using SVD reveals multiple, temporally related, and co-dominant patterns of activity for each pathway, activity patterns which correspond to unique subcomponents within a pathway. Thus, this investigation not only identifies pathways with physiological relevance to the liver and MPL but provides a complex, but defined, systemic characterization of the consequences of MPL within the liver and the possible regulatory structures that govern these pathways.

3.2 Pathway-based Analysis of the Skeletal Muscle Response to Intravenous Methylprednisolone (MPL) Administration in Rats: Acute versus Chronic Dosing

3.2.1 Introduction

Corticosteroids, such as methylprednisolone (MPL), are synthetic glucocorticoids ubiquitously used as an anti-inflammatory and immune-suppressive therapy applied to various autoimmune diseases, asthma, used as supplements after organ transplantation and to cancer treatment (Swartz and Dluhy 1978, Barnes 1998). Analogues of the endogenous glucocorticoid cortisol, corticosteroids regulate transcription via the same mechanisms as this adrenal hormone, by either binding of a drug-receptor complex to DNA glucocorticoid regulatory elements (GREs) and by signaling through receptors in a manner independent of transcription (Schaaf and Cidlowski 2002). Glucocorticoid effects are pervasive and involve multiple molecular mechanisms. Investigation via *in vivo* high-throughput transcriptomics has proven a useful tool in capturing and understanding tissue and dosing-specific effects of MPL (Sun, DuBois et al. 1998, Sun, McKay et al. 1999, Ramakrishnan, DuBois et al. 2002, Ramakrishnan, DuBois et al. 2002, Almon, DuBois et al. , Almon, Dubois et al. , Almon, Lai et al. 2005, Almon, DuBois et al. , Hazra, Pyszczynski et al. 2007, Almon, Yang et al. 2008, Almon, Yang et al. , Hazra, DuBois et al. 2008, Yang, Almon et al. , Yao, Hoffman et al. 2008, Yang, Almon et al. 2009, Nguyen, Almon et al. 2010, Nguyen, Almon et al. , Acevedo, Berthel et al. 2019).

Acute administration is generally beneficial for reducing inflammation temporarily. However, chronic administration of corticosteroids, though necessary for chronic conditions, has deteriorative consequences including hyperglycemia, negative nitrogen balance, and fat redistribution leading to complications including diabetes, muscle wasting, osteoporosis (Morand

and Leech 1999, Liu, Wang et al. 2017). These consequences are notably observed within muscle; continuous use of corticosteroids leads to muscle atrophy and insulin resistance (Schakman, Kalista et al. 2013, Bodine and Furlow 2015).

Corticosteroids influence physiology at the regulatory level, leading to multifactorial and systems-influencing consequences further complicated by the observed differences in response dynamics to differing dosing regimens of glucocorticoid administration (Almon, DuBois et al. , Yao, Hoffman et al.). These changing dynamics are indicative of likely differences in regulatory mechanisms, further revealing that regulatory structures implied in by acute administration are not consistent with regulatory structures implied by chronic MPL administration (Hazra, DuBois et al. 2008, Yao, Hoffman et al. , Nguyen, Almon et al.).

In our previous analyses in liver, we developed a meta-analysis approach in order to better understand these complex pharmacogenomic effects of corticosteroids captured in temporal high-throughput transcriptomic data (Acevedo, Berthel et al.). This approach applies a pathway-based analysis, which filters transcriptomic data into tissue- and organism-relevant pathways, decomposes these pathways for gene expression activity, and uses a model-based assessment of activity to assess pathway dynamics, thus endeavoring to analyze and interpret data sets separately and subsequently compare the analysis. With this approach, we are able to compare across pharmacological time-series obtained from different (transcriptomic or other) platforms and time-scales, including multiple dosing regimens (Almon, DuBois et al. 2007, Almon, DuBois et al. 2007), and across different tissues.

In the following sections, we apply the pathway-based analysis approach (Acevedo, Berthel et al. , Acevedo, DuBois et al.) to analyze acute and chronic MPL dosing response in gastrocnemius muscle of male adrenalectomized rats and characterize the dosing-dependent differences in the

dynamic response of MPL-responsive pathways capturing: amino acid metabolism, lipid metabolism, signal transduction, endocrine regulation, regulation of cellular functions including growth, death, motility, transport, protein degradation, and catabolism. To consistently compare across dosing-induced changes, we applied a model-based approach for the assessment of pathway dynamics, extending the principles of pharmacokinetics and pharmacodynamics (PKPD) to characterize pathway activity (Acevedo, Berthel et al.). With this approach, we hypothesized dosing-dependent regulatory interactions in order to understand the mechanistic implications of MPL dosing in muscle. Further, we compared acute and chronic MPL response in muscle with previously established acute and chronic MPL response in liver (Acevedo, Berthel et al.). Such comparison revealed that dynamics are frequently inconsistent across dosing regimen and across tissues, though the same regulatory mechanisms capture these different dynamics.

3.2.2 Approach

Toward the analysis of the response of muscle tissue to acute and chronic MPL dosing, we applied the pathway-based analysis approach presented in Chapter 2 (Acevedo, Berthel et al. , Acevedo, DuBois et al.). Details specific to the muscle analysis are presented herein, including the relevant data sets analyzed and notes on the version of the framework applied to muscle data analysis (Acevedo, Berthel et al. , Acevedo, DuBois et al.).

Animal Model and Experimental Data

Two deteriorative consequences of continued application of corticosteroid therapy are muscle wasting and insulin resistance. These motivate investigation into the dosing-dependent effects of corticosteroids within muscle tissue. The temporal transcriptomic data used for this analysis was collected from extracted gastrocnemius muscle in two temporal large rat studies presented here (Sun, McKay et al. , Ramakrishnan, DuBois et al.).

For acquisition of acute MPL response data, 39 adrenalectomized male (ADX) Wistar rats treated with a bolus dose of 50 mg/kg MPL intravenously (Sun, McKay et al.). This dose was established

previously for identifying biomarkers for gene-mediated effects of glucocorticoids within liver tissue because of its induction of strong, but not saturating, effects on gene and protein expression and comparability with large doses in human upon scale-up (Boudinot, D'Ambrosio et al.). The animals were sacrificed at 17 timepoints (n = 2-4) from 0 to 72 hours post dosing and isolated RNA were hybridized with Affymetrix GeneChips Rat Genome U34A (Affymetrix, Inc.) (microarray contains 8799 probes).

Acquisition of chronic MPL administration response data in muscle tissue was isolated from another longitudinal study in which 40 ADX male Wistar rats were administered 0.3 mg/kg·hr of MPL intravenously for 7 days (Nguyen, Almon et al.). Animals were sacrificed at 11 time points over this period. Isolated RNA from excised gastrocnemius muscle tissue was hybridized with Affymetrix GeneChips Rat Genome 230A (Affymetrix, Inc., Santa Clara, CA) (microarray contains 15,967 probes). Both the acute and chronic datasets were submitted to GEO (acute: GSE490 and chronic: GSE5101) and we have previously presented analyses of the transcription responses (Sun, DuBois et al. , Almon, DuBois et al. 2002, Ramakrishnan, DuBois et al. , Almon, DuBois et al. , Almon, DuBois et al. 2005, Almon, DuBois et al. , Almon, Yang et al. 2008, Yao, Hoffman et al. , Fang, Sukumaran et al. 2013, Nguyen, Almon et al. 2014).

Application of Pathway-based Analysis Framework

To reconcile the temporal response of muscle tissue to acute and chronic MPL dosing, the datasets were processed using our pathway activity analysis approach described in depth in Chapter 2 (Acevedo, Berthel et al. , Acevedo, DuBois et al. 2019 (submitted)). The most recent version of the framework was used to analyze muscle data *(Acevedo, DuBois et al. 2019 (submitted))* and details specific to the analysis of muscle data are listed briefly here:

Details of this analysis of specific to the muscle data include:

- Active genes are then identified using differential expression analysis with the software Extraction and Analysis of Gene Expression (EDGE) (Leek, Monsen et al. 2006). Differentially expressed genes are identified by p-value. Differentially expressed profiles are then z-scored with respect to the individual profile mean and standard deviation. Replicate profiles are then averaged together, yielding averaged z-scored profiles.
- As of June 2019, the time of submission of the skeletal muscle manuscript, this database contains 326 pathways relevant to rat tissues and used for our analysis. Only pathways relevant to muscle tissue are relevant to this analysis motivating the removal of the pathways relevant to other tissues (ex. pathways relevant to the digestive, excretory, circulatory systems), disease pathways (ex. Neurodegenerative disease, cancers, and infectious disease pathways), or redundant pathways (KEGG's pathway entitled Metabolic pathways, rno:01100, is the set of all other metabolism related pathways). This elimination step left 179 remaining pathways for consideration in our analysis.
- Affymetrix probe identifiers are translated into their NCBI Entrez IDs and Gene Symbols using the Bioconductor packages for each Affymetrix Platform: Package rae230a.db containing the annotation data for Affymetrix Rat Expression Set 230A used with the chronic data; and Package rgu34a.db containing the annotation data for Affymetrix Rat Genome U34 Array annotation data used with the acute data.
- Some pathways with low fractional occupancy yield inconclusive p-values as an artifact of the Fisher's Exact Test and were eliminated from the analysis, discussed further in ST 2.

- PAL profiles were captured by our “monophasic” or “biphasic” model types (Acevedo, Berthel et al.) and developed as an extension of the concepts presented in (Hazra, DuBois et al. 2008, Yao, Hoffman et al.).

3.2.3 Results

Of the 179 pathways determined rat- and muscle- relevant pathways, fractional coverage analysis yielded 51 significantly covered pathways in the acute dataset and 61 in the chronic dataset. Pathway activity analysis, as described above, was used to process these pathways. Multiple PAL profiles emerged from each pathway and yielded f_p and f_p p-values indicate the fraction of activity captured by that PAL profile and the significance of that activity profile, respectively. Only pathways that yielded at least one significant PAL profile were retained as significant. For consistency, a consistent p-value threshold of 0.05 was used to determine significance for f_p and f_c.

Pathways which yielded at least one significant PAL (f_p p-value ≤ 0.05) were considered significantly active. From the acute dataset, 49 pathways emerged as significant. The chronic dataset yielded 61 pathways as significant (identical to the list of pathways that exhibited significant fractional coverage). Discussed in greater detail below, we identified a subset of 29 pathways both significant and common to the acute and chronic datasets. Within these pathways, PAL profiles exhibit different features across dose. Further, when compared against the list of significant pathways in liver (Acevedo, Berthel et al.), we identified a subset of pathways that were also significant in liver in response to acute and chronic MPL administration, detailed further in the Discussion section.

In order to account for variability within the data, a bootstrapping step was applied to each pathway. This step allowed us to predict *in silico* likely activity patterns from muscle tissue, had the experiment been repeated. As described in the Methods section above, bootstrapped pathway gene sets (n=1000) were generated for each pathway and significant PAL were identified from each. Multiple significant PAL frequently emerged from each bootstrapped pathway gene set. Despite variability in the data, we repeatedly identified significant pathway activities within the bootstrapped pathway gene sets and identified common patterns of activity. When comparing across pathways, we frequently observed common patterns of activity in response to a common dose. We also observed common patterns of activity across liver and muscle response within the same pathway.

The emergence of multiple significant PAL from original and bootstrapped pathway gene sets indicates a codominance of activity patterns, and complex regulatory structures, within the pathway. To characterize these activity dynamics consistently, we applied a model-fitting technique previously described (Acevedo, Berthel et al.) and adapted from previous investigations into corticosteroid influence in muscle tissue (Sun, DuBois et al. , Almon, DuBois et al. 2002, Ramakrishnan, DuBois et al. , Almon, DuBois et al. , Almon, DuBois et al. 2005, Almon, DuBois et al. , Almon, Yang et al. 2008, Yao, Hoffman et al. , Fang, Sukumaran et al. 2013, Nguyen, Almon et al. 2014). Models that describe direct and indirect regulation by MPL and an intermediate biosignal were fitted to PAL profiles, referred to as monophasic or biphasic models. This step served to hypothesize likely modes of regulation within a pathway. This step is also essential to our analysis as it enables comparison of drug response in a data-independent manner, i.e. without concern for differences in experimental platform, animal, tissue, dosing regimen, or time horizon. Table 6 reports the coverage, pathway activity, and model fitting results for each of the 29 pathways.

We discretized the results from perspective of the acute response data, as it became evident that two classes of response existed within this set of significant pathways. **Class 1:** The majority (26 pathways) emerged with PAL described by strictly either acute monophasic or acute biphasic models. **Class 2:** The smaller subset (3 pathways) emerged with a more complex response exhibiting significant PAL described by both acute monophasic and acute biphasic models simultaneously. These classes were further analyzed for chronic response activity and revealed an interesting consistency between all 29 common significant pathways. In response to chronic MPL administration, pathways varied whether they yielded one or more PAL profile types. However, every pathway exhibited what we define as a "tolerance" behavior at a minimum. This behavior is characterized by PAL profiles which exhibit activity that deviates from baseline for the majority of the 168 h of chronic MPL administration, but which ultimately begins to return to baseline despite continued administration of the drug. Specific examples are detailed further below.

Class 1: Exclusively Monophasic or Biphasic Acute Response

Twenty-six pathways exhibit either strictly monophasic or strictly biphasic responses to acute MPL administration. Many pathway families are represented in this subset including amino acid metabolism pathway family (**Arginine and proline metabolism**, **Glutathione metabolism**), pathways related to cell motility, cell growth and death, cellular events such folding, sorting, and degradation of genetic material and proteins, transport, and catabolism (**Regulation of actin cytoskeleton, Apoptosis, Cellular senescence, Ferroptosis, Proteasome, Autophagy, Peroxisome**), endocrine regulation (Signaling pathways for **Glucagon, GnRH, Insulin, Oxytocin, Prolactin, PPAR, and Thyroid hormone**), signal transduction (Signaling pathways for **TGF-beta, AMPK, cGMP-PKG, ErbB, Fox-O, HIF-1, PI3K-Akt, and Rap1**), lipid metabolism (**Fatty acid degradation and Fatty acid metabolism**). Interestingly, all monophasic

responses to acute MPL administration in muscle tissue exhibit a consistent response of an initial peak in activity due to DRN action between 5 and 15 h followed by a return to baseline between 20 and 40 h. Similarly, pathways exhibiting any biphasic response to acute MPL administration exhibit a first peak due to DRN action at approximately 5 h, a second and opposite peak in activity due to BS action from 15 to 25 h, and a return to baseline within between 30 and 60 h. Response to chronic administration yielded similar consistency in profile activity events a cross pathways. Though pathways varied in their complexity of response to chronic administration by exhibiting monophasic and/or biphasic behavior, all pathways exhibited a biphasic response that we define as tolerance. A tolerance profile is characterized by: (1) a biphasic model in which effect due to DRN and effect due to BS regulate the activity in opposite direction (i.e. positive effect due to DRN combined with a negative effect due to BS, or the reverse); and (2) a return of the PAL profile to baseline after approximately 100 h despite continued administration of MPL.

The pathways that exhibit strictly biphasic response to MPL administration (**Proteasome, Fatty acid degradation, TGF-beta signaling pathway**) yield greater complexity in response to chronic administration. The Proteasome and Fatty acid degradation pathways exhibit exclusively tolerance response to chronic MPL administration. This models for these predict a steep increase in activity until 20 to 25 h, a subsequent shallower incline in activity until 85 to 100 h, a defined a peak in activity at that time, and ultimately a continuous return to baseline through the end of the experiment at 168 h. The TGF-β signaling pathway exhibits this tolerance response to chronic MPL administration, as well as a chronic monophasic response characterized by a steep incline in activity until 5 to 10 h, a small overshoot at that time, and a subsequent settling to a new steady by approximately 40 h.

Acute MPL monophasic response only

Most significant pathways in muscle tissue exhibit strictly monophasic response to acute MPL administration. The significant PAL of these pathways are characterized monophasic models that yield an initial peak in activity between 5 and 15 h, due to DRN action, followed by a return to baseline between 25 and 30 h. Response to chronic MPL administration is again more complex.

Some pathways yield strictly tolerance response to chronic MPL (**AMPK signaling pathway, Thyroid hormone signaling pathway, Autophagy, ErbB signaling pathway, Ferroptosis, and Fatty acid metabolism**). The tolerance behavior exhibits profiles consistent with those previously described: a steep increase in activity until 20 to 25 h, a subsequent shallower incline in activity until 85 to 120 h and a defined a peak in activity at that time, and then a return to baseline for the remainder of the experiment at 168 h. Other pathways exhibit both monophasic and tolerance responses to chronic MPL administration (**HIF-1 signaling pathway, Regulation of actin cytoskeleton, Oxytocin signaling pathway, PI3K-Akt signaling pathway, Apoptosis, Cellular senescence, Peroxisome, Insulin signaling pathway, Rap1 signaling pathway, Glucagon signaling pathway, cGMP-PKG signaling pathway**, **Arginine and Proline metabolism, Glutathione metabolism, PPAR signaling pathway**). The tolerance and monophasic response profiles are identical to those previously described.

An additional set of pathways (**Fox-O signaling pathway, Prolactin signaling pathway, GnRH signaling pathway**) exhibit tolerance behavior in response to chronic administration consistent with previously described tolerance profiles, as well as an additional form of biphasic behavior. The Fox-O and Prolactin signaling pathways yield biphasic profiles exhibiting an initial peak between 15 and 20 h due to DRN action, a secondary and opposite peak by 40 or 60 h primarily due to BS action, and an approach to a new steady state far from baseline as the experiment continues to 168 h. The GnRH signaling pathway exhibits a slightly different profile in which a

first peak is observed at 25 h, a steep deviation from baseline in the direction opposite the first peak, and ultimately approaches a new steady state until 168 h.

Class 2: Complex Acute Response

Three pathways exhibit both monophasic and biphasic responses to acute MPL administration. These pathways represent the endocrine regulation (**Adipocytokine signaling pathway**) and signal transduction (**MAPK signaling pathway and VEGF signaling pathway**). The monophasic responses to acute MPL administration are similar to those previously described: an initial peak due to DRN action from 5 to 10 h and a return to baseline by 20 to 30 h for all pathways. Similarly, the biphasic responses of these pathways to acute MPL administration report consistent activity events including an initial peak due to DRN action at 5 h, a secondary peak due to BS action from 15 to 20 h, and a return to baseline thereafter between 40 and 50 h. The Adipocytokine signaling pathway exhibits only tolerance behavior in response to chronic MPL administration. The remaining pathways exhibit chronic monophasic response characterized by a steep incline in activity until 10 to 15 h, a shallow overshoot at that time, followed a settling to a new steady state by 45 to 50 h.

3.2.4 Discussion

Ubiquitously used anti-inflammatory and immune-suppressing drugs, corticosteroids exhibit both deleterious and beneficial effects, notably within muscle; continuous use of corticosteroids leads to muscle atrophy and insulin resistance (Schakman, Kalista et al. 2013, Bodine and Furlow 2015). Despite its continued use, its induced responses are not entirely characterized. To this end, we seek to reconcile data capturing MPL response across multiple tissues using a meta-analysis pathway-based approach (Acevedo, Berthel et al.). Though foundational, gene-centric analyses do not capture the complexity of the multi-genomic consequences of MPL. Further, reconciling data

from multiple studies that explore the influence of MPL is not straightforward, as this data was collected using different experimental platforms, on different time scales, within different tissues, and across different dosing regimens (Ghosh, Barette et al. 2003, Ramasamy, Mondry et al. 2008, Tseng, Ghosh et al. 2012). To compare results across studies and capture the multi-genomic consequences of MPL administration in muscle, it becomes necessary to first analyze the MPL response in each data set independently in the context of functional groups, i.e. pathways, and characterize this in the space of regulatory models. We then compare these model results across data sets and observed dosing-dependence.

We first analyzed response of muscle tissue to acute and chronic MPL administration independently through the application of the pathway activity analysis previously published (Acevedo, Berthel et al.). The first step of this analysis sorts temporal expression data into functional pathways harvested from KEGG (Kanehisa and Goto 2000, Kanehisa, Furumichi et al. 2016, Kanehisa, Sato et al. 2018), using only rat-relevant and muscle-relevant pathways. These pathway gene sets were analyzed for fractional coverage (f_c). Pathways that exhibited significant fractional coverage (f_c p-value ≤ 0.05) were retained for subsequent pathway analysis. Of the 179 pathways considered, fractional coverage analysis yielded 51 pathways in the acute dataset and 61 in the chronic dataset selected for subsequent pathway activity analysis.

Pathway activity analysis identifies pathways that are significantly active in response to MPL administration in the liver. This step hypothesizes that a pathway is a high-dimensional system that we can decompose in order to identify significant trends. With singular value decomposition (SVD), we decompose the pathway into constituent singular values and singular vectors. The singular vectors are linear combinations of the original transcript expression over time. Thus, they capture trends in the activity of the pathway and we define these Pathway Activity Level (PAL)

profiles. The fraction of variability of each PAL profile is calculated from the singular values and is defined as the fraction of pathway activity (f_p). Alternatively, a PAL profile can be thought of as the expression of a metagene over time, where the metagene is a representation of common trends in gene expression within a pathway.

Pathways exhibiting at least one significant PAL profile (f_p p-value ≤ 0.05) are considered significant, a threshold step which yields 49 and 61 significant pathways from the acute and chronic data sets, respectfully (

ST 5 and ST 6). The discrepancy in number of significant pathways between data sets is likely due to the difference in size of the chronic data set compared to the acute. The chronic study was completed later than the acute and thus had access to the Affymetrix microarray platform 230A which is considerably larger than the U34a microarray platform used to generate the acute data set. However, because both data sets investigate the influence of MPL in muscle tissue, a consistent subset of significant pathways is reasonably expected to emerge. Our investigation yields a subset of 29 significant pathways common to both acute and chronic data sets (Table 6) including pathways relevant to amino acid metabolism, lipid metabolism, signal transduction, endocrine regulation, regulation of cellular functions including growth, death, motility, transport, protein degradation, and catabolism.

Decomposition of these pathways yielded emergent activity dynamics consistent with established mechanisms of regulation. More specifically, previously established mechanisms of CS regulation including events due to DRN binding to GRE elements or transcription mediated by an intermediate BS (Sun, McKay et al. , Ramakrishnan, DuBois et al. , Ramakrishnan, DuBois et al. , Hazra, Pyszczynski et al. , Yao, Hoffman et al.). Given that the animals in these experiments were adrenalectomized, acute MPL administration would activate what was once directly or indirectly regulated by cortisol. In the case of acute MPL administration, these effects would be transient while chronic administration yields more persistent effects. Though the consistency of the activity profiles of the original pathway gene set is interesting, it is important to consider the influence of inherent variability of the original transcript expression data when characterizing a pathway's response. To this end, the aforementioned bootstrapping technique is applied to replicate the experiments *in silico* and so predict alternative response profiles for each pathway. Each significant pathway was thus bootstrapped, and significant PAL profiles were determined from each of 1000 bootstrapped gene sets for each pathway. We observed strikingly consistent

response profiles across pathways and within the same dosing regimen and that chronic administration yielded more complex pathway dynamics for most pathways than did acute administration.

The issue of reconciling data set captured within different time horizons, dosing regimens, microarray platforms, and tissues is overcome by analyzing the PAL profiles in the space of regulatory models. Based on previous analyses of MPL response in muscle, we hypothesize that the PAL response profiles observed can be captured with previously established regulatory mechanisms (Sun, McKay et al. , Ramakrishnan, DuBois et al. , Ramakrishnan, DuBois et al. , Hazra, Pyszczynski et al. , Yao, Hoffman et al.). A two-compartment PK model describes the administration of CS intravenously and transfer from plasma to muscle tissue compartment for both acute and chronic dosing. It is important to note that our analysis indicates that the acute response initiates pathway dynamics consistent with the nature of the acute dosing: as MPL half-life of 0.33 hours in ADX rats with a total drug clearance observed in ADX rats by 4.6 hours (Hazra, Pyszczynski et al. 2007). The PD is described by previously proposed relationships between drug, receptor, and the drug-receptor complex transferring to the nucleus initiating transcription activity. This traditional PD model is extended to characterize activity at the pathway level by the hypothesized monophasic and biphasic regulation. Though PAL profiles resemble gene expression profiles, the features in these profiles do not correspond necessarily to up or down gene expression (Acevedo, Berthel et al.). A consequence of the linear algebra of the SVD technique is loss of sign but preservation of relative magnitude in a PAL profile; a PAL profile will predict a change from up- to down- regulation in a pathway's activity but will report this as either an up/down profile or a down/up profile. For example, a PAL that reports a peak around 5 h in its profile is indicating that its reference pathway either has an upregulation or downregulation transcription event at 5 h. The PAL does not communicate which. A pathway

gene set will resolve to a PAL that captures the timing and relative magnitude of activity events which is the information critical to our analysis as these features determine whether a monophasic of biphasic model is proposed.

Analysis of the response dynamics of the common pathways yielded definite dosing-dependence in muscle tissue with increased complexity in the case of chronic administration. We define the classes of pathway response by response to acute administration first.

Class 1: Simple acute response

Class 1 consists of pathways that exhibit exclusively monophasic or biphasic response to acute MPL administration. These pathways exhibit strikingly consistent patterns of activity and corresponding times for events due to DRN effect. All 23 pathways that yield monophasic behavior in response to acute MPL exhibit a single event between 5 and 15 h due to DRN action followed by a return to baseline (**Arginine and proline metabolism, Glutathione metabolism, Apoptosis, Cellular senescence, Ferroptosis, Regulation of actin cytoskeleton, Prolactin signaling pathway, GnRH signaling pathway, Glucagon signaling pathway, Insulin signaling pathway, Oxytocin signaling pathway, PPAR signaling pathway, Thyroid hormone signaling pathway, Fatty acid metabolism, Fox-O signaling pathway, cGMP-PKG signaling pathway, HIF-1 signaling pathway, PI3K-Akt signaling pathway, Rap1 signaling pathway, AMPK signaling pathway, ErbB signaling pathway, Peroxisome, Autophagy**).

Analysis of the three pathways that exhibit biphasic response to acute MPL administration (**Adipocytokine signaling pathway, MAPK signaling pathway, VEGF signaling pathway**) reveals that action due to DRN initiates a peak at approximately 5 h for each, an event time which corresponds to the DRN peak in the acute monophasic pathway response. This is where the correspondence ends, however. The settling time of the acute monophasic profiles is much earlier

than that of biphasic profiles, ranging from 20 to 40 h. This corresponds to neither the range of event times for the event due to BS action (20 to 40 h) or the return to steady state time range (50 to 60 h) for acute biphasic pathways.

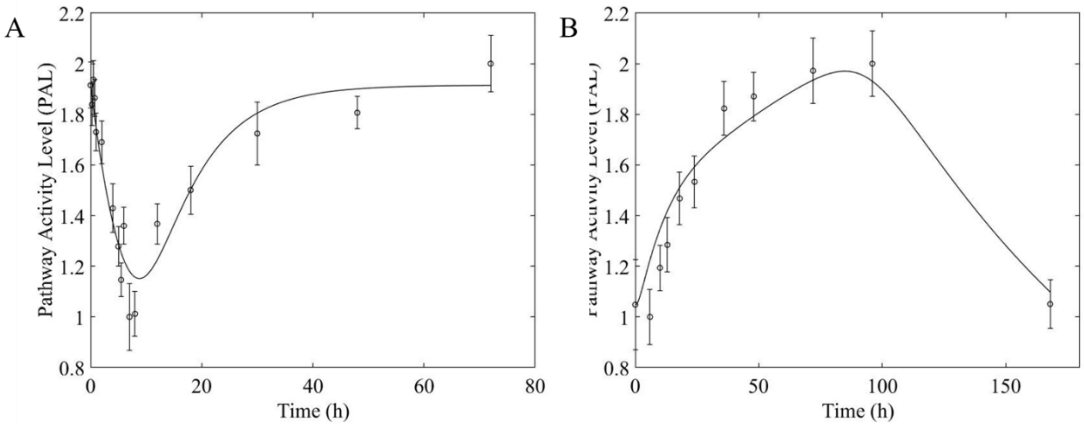

Figure 9 AMPK signaling pathway response to (A) acute and (B) chronic MPL administration. Example of Class 1 pathway which yields monophasic response to acute MPL administration but varies in its response to chronic MPL administration. The AMPK pathway yields biphasic response to chronic MPL administration indicating an increased complexity across dosing studies. This format of biphasic response indicates the development of tolerance to MPL within this pathway of the muscle tissue because the system returns to baseline by the end of the experiment despite continued administration of MPL.

In response to chronic administration, all pathways in this class exhibited, at minimum, a biphasic response. For some pathways (**Ferroptosis, Proteasome, Fatty acid degradation, Thyroid hormone signaling pathway, Fatty acid metabolism, AMPK signaling pathway, ErbB signaling pathway, Autophagy**), only one format of biphasic behavior was observed exemplified by the AMPK signaling pathway (Figure 9), an energy metabolism regulator and is responsible for inhibiting energy-consuming pathways (anabolic functions) and activating ATP-generating catabolic pathways (KEGG 2019). Activation of this pathway is unsurprising because it is previously observed that corticosteroid treatment causes mitochondrial dysfunction in muscle cells, which induces a state of ATP deprivation and subsequent activation of AMPK signaling to

counteract this, ultimately leading to muscle atrophy (Liu, Peng et al. 2015). In response to chronic MPL, the AMPK pathway yields biphasic response - an increased complexity only revealed by experimenting with multiple dosing regimens. This format of biphasic response indicates the development of tolerance to MPL because despite continuous administration of MPL over the course of the experiment, the pathway begins to return to baseline after 100 h. The model that captures this response is biphasic and the demand placed on the system is such that intermediate biosignal must be continuously generated in order to drive the PAL back to baseline, a presumable energy drain on the pathway and tissue (Figure 10C).

Chronic MPL administration yielded another format of biphasic response for other pathways (**Prolactin, GnRH, and Fox-O signaling pathways**). The Fox-O signaling pathway consists of a series of transcription factors that regulate multiple events within the cell including “apoptosis, cell-cycle control, glucose metabolism, oxidative stress resistance, and longevity (KEGG 2019).” Fox-O transcription factors including Foxo1 and Foxo3a are upregulated in response to the corticosteroid dexamethasone and are key regulators of gene expression leading to muscle atrophy (Waddell, Baehr et al. 2008, Zhao, Qin et al. 2009, Schakman, Kalista et al. 2013). In response to chronic MPL administration, the Fox-O pathway (Figure 11) yields two formats of biphasic response revealing an increased complexity across dosing studies as well as an internal complexity to the pathway. Subgroups of genes within this pathway respond differently to the same chronic dosing regimen. One subgroup of genes (Figure 11B) indicates the development of tolerance to MPL because the system returns to baseline by the end of the experiment despite continued administration of MPL. An additional subgroup of genes yields another format of biphasic response (Figure 11C) which settles to a new steady state far from its original baseline.

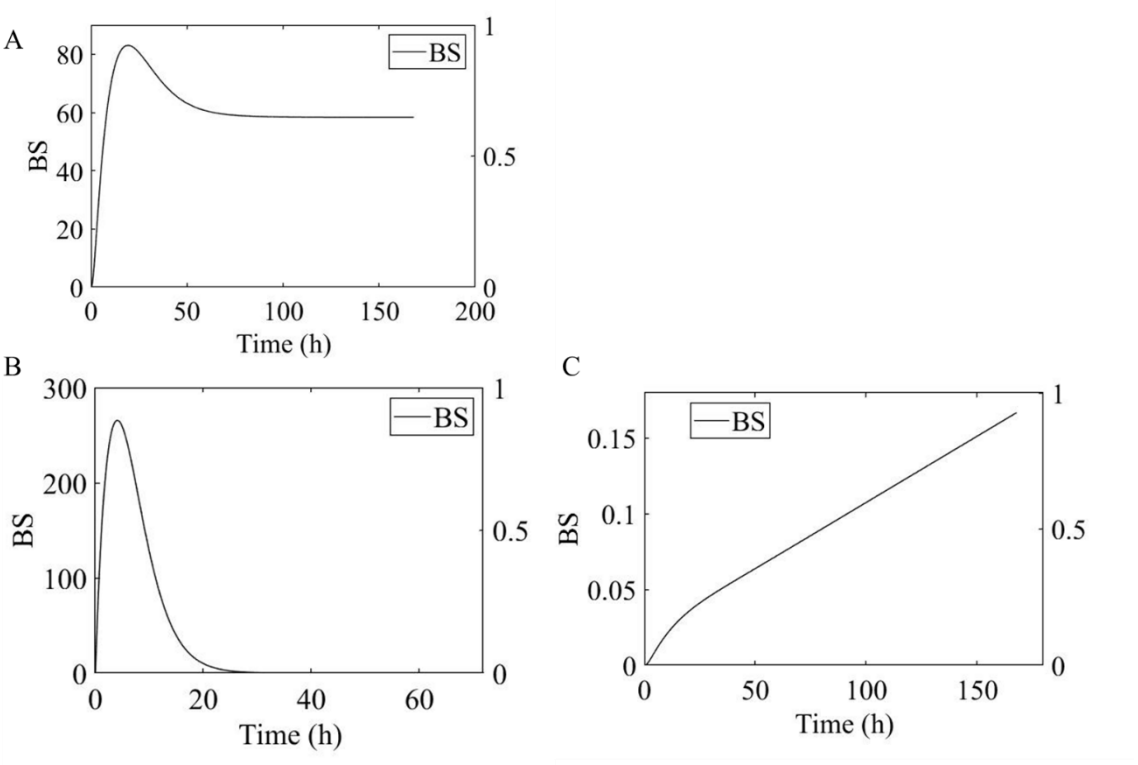

Figure 10 Expression of intermediate biosignal in different response cases. (A) BS signaling in case of acute biphasic response (generated from the Fatty acid degradation pathway). (B) Chronic biphasic response characterized by two opposite PAL peaks. (C) Chronic biphasic response characterized by tolerance. (B and C are generated from the Fox-O signaling pathway.)

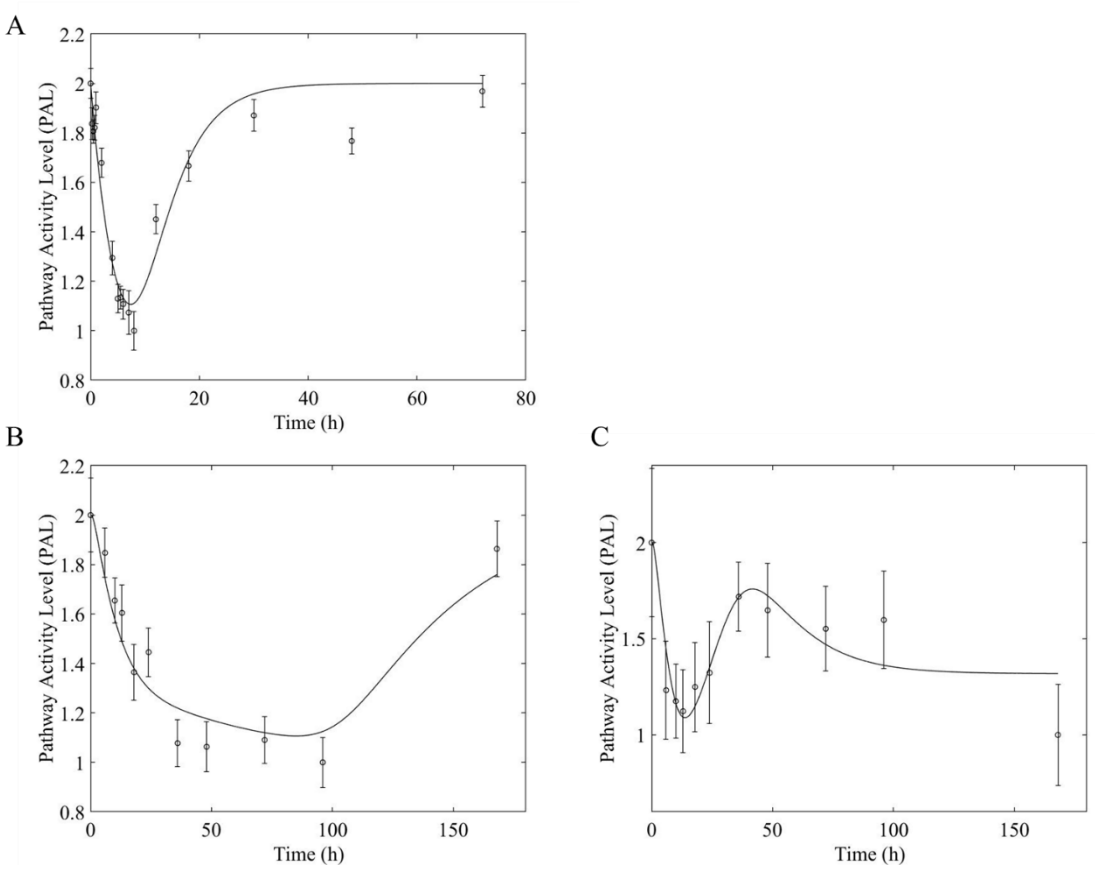

Figure 11 Fox-O signaling pathway response to (A) acute and (B, C) chronic MPL administration. Example of Class 1 pathway which yields monophasic response to acute MPL administration but varies in its response to chronic MPL administration. The Fox-O pathway yields two formats of biphasic response to chronic MPL administration indicating an increased complexity across dosing studies as well as an internal complexity, i.e. subgroups of components within the pathway subject to different regulatory structures. The response of (B) indicates the development of tolerance to MPL because the system returns to baseline by the end of the experiment despite continued administration of MPL. This is as opposed to the response format in (C) which settles to a new steady state far from baseline.

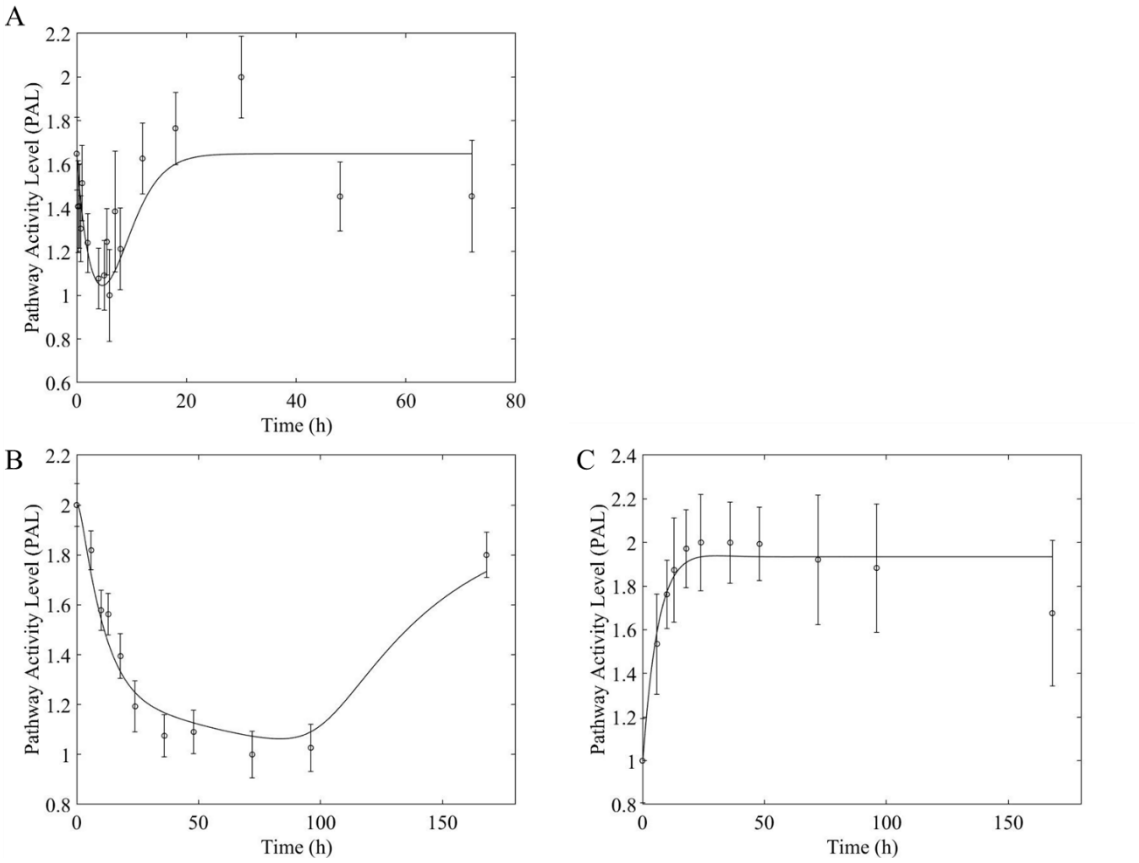

Figure 12 PPAR signaling pathway response to (A) acute and (B, C) chronic MPL administration. Example of Class 1 pathway which yields monophasic response to acute MPL administration but varies in its response to chronic MPL administration. The PPAR pathway yields biphasic (B) and monophasic (C) response formats to chronic MPL administration indicating an increased complexity across dosing studies as well as an internal complexity, i.e. subgroups of components within the pathway subject to different regulatory structures. The response of (B) indicates the development of tolerance to MPL because the system returns to baseline by the end of the experiment despite continued administration of MPL. This is as opposed to the response format in (C) which settles to a new steady state far from baseline.

The remaining pathways within Class 1 also yield two modes of response to chronic MPL administration indicating similar complexity within the pathway: a combination of the biphasic tolerance response and a monophasic response, exemplified by the PPAR signaling pathway (Figure 12). This pathway helps to regulate lipid metabolism in liver and skeletal muscle (Burri, Thoresen et al. , KEGG 2019) and is observed to cause muscle atrophy in response to

corticosteroid dexamethasone treatment via the mechanism of PPAR upregulation of Fox-O transcription factor expression in muscle (Castillero, Alamdari et al. 2013). These authors further established that interruption of PPAR signaling helps ameliorate loss of muscle in cases of glucocorticoid- and sepsis-induced muscle atrophy. Much like the Fox-O pathway example, the PPAR pathway demonstrates two modes of response to chronic administration, one in which the system seeks to return to baseline thus exhibiting tolerance of MPL administration over time (Figure 12B) and another in which the system remains deviated from baseline (Figure 12C).

Class 2: Complex acute response

Class 2 consists of pathways that exhibit both monophasic or biphasic responses to acute MPL administration indicating that subgroups of genes within these pathways respond to separate regulatory mechanisms in response to acute MPL administration. These pathways also exhibit consistent patterns. All acute monophasic response modes are characterized by a peak from 5 to 10 h (due to DRN effects) and a return to baseline by 20 to 30 h. Within the biphasic response profiles, the initial peak due to DRN effect is also observed at approximately 5 h. The biphasic response profiles settle slightly later, however, by 40 to 50 h. All pathways in this class exhibit at least a biphasic response profile that captures the tolerance behavior previously described. The **Adipocytokine signaling pathway** exhibits only this biphasic tolerance response whereas the other two pathways in this class (**MAPK and VEGF signaling pathway**) exhibit both monophasic and tolerance behavior identical to that exemplified by the PPAR signaling pathway of Class 1. Model results for all pathways in Table 6 are included as Supplementary Figures.

3.3 Comparison of Response to Acute and Chronic MPL Dosing Across Multiple Tissues

We have previously analyzed the dosing-dependent consequences of MPL within liver pathways (Acevedo, Berthel et al.). We anticipate this tissue-specificity extends to analyses at the pathway level based on previous analysis of corticosteroid influence in multiple tissues, the ubiquity of glucocorticoid responsiveness observed in multiple tissues, and the tissue-specific deteriorative effects of corticosteroid treatment (Ballard, Baxter et al. 1974, Sun, DuBois et al. , Sun, McKay et al. , Yao, Hoffman et al. , Nguyen, Almon et al. 2014). To compare liver and muscle response, the sets of significant pathways in muscle tissue in response to acute (49 significant pathways) and chronic (61 significant pathways) MPL administration were compared with the list of significant pathways reported in liver (

ST 5 and ST 6) (Acevedo, Berthel et al.).

Comparison of significant pathways in response to acute MPL administration between muscle and liver yielded significant pathways describing: regulation of essential organelles (**Peroxisome and Proteasome pathways**); lipid metabolism (**Fatty acid degradation, Fatty acid metabolism, and PPAR signaling pathway**), and amino acid metabolism (**Glutathione metabolism**). Comparison of significant pathway results in response to chronic MPL administration yielded significant pathways capturing: carbohydrate metabolism (**Glyoxylate and dicarboxylate metabolism, Propanoate metabolism, Citrate cycle, Pyruvate metabolism, Oxidative phosphorylation, Glycolysis/Gluconeogenesis, Carbon metabolism**); amino acid metabolism (**Tryptophan metabolism, Valine, leucine and isoleucine degradation, Glutathione metabolism, Arginine biosynthesis, Biosynthesis of amino acids, Cysteine and methionine metabolism**); regulation of essential organelles (**Peroxisome, Proteasome, Protein processing in endoplasmic reticulum**); and lipid metabolism (**Fatty acid degradation, Fatty acid metabolism, PPAR signaling pathway**). The greater number of significant pathways in the chronic data set, as compared to the acute data set, is likely due to its larger size (larger microarray platform).

3.3.1 Comparison of Acute Response across Liver and Muscle

In response to acute MPL administration, there is an overwhelming number of Case 1 (simple acute) pathway responses in muscle tissue. The list of significant pathways from the acute muscle data was compared against the significant list of 24 pathways found in liver (Acevedo, Berthel et al.), revealing multiple pathways and dynamics help in common between the groups. Seven pathways emerged including **Peroxisome, Fatty acid degradation, Fatty acid metabolism, PPAR signaling, Glutathione metabolism, Proteasome, and Metabolism of xenobiotics by cytochrome P450**. Some pathways exhibited the same dynamic response in liver and muscle

(**Peroxisome, Fatty acid metabolism, PPAR signaling, and Glutathione metabolism**) (Figure 13A). Although captured by the same regulatory model, these pathways do not correspond in their DRN event peak times. Liver exhibits DRN peak event times at approximately 5 h for each pathway in Figure 13A, which is slightly ahead of the observed peaks in muscle which occur nearer 10 h. The closest correspondence in peak time within this example set of pathways is the peroxisome proliferator-activated receptor (PPAR) signaling pathway. In this pathway, we observe that muscle tissue exhibits its peak near 5 h, however liver peaks slightly before the peak in muscle. This difference of a few hours is not marginal when we consider the 4.6 h total drug clearance time of MPL. Comparison across tissues in the context of these pathways reveals that MPL administration induces an activity response slightly before muscle tissue, when predicting drug response with our established models. It may be that this time difference is marginal. However, this observed lag in response may also speak to greater sensitivity to MPL in liver compared to muscle.

Comparison across tissues in the acute reveals that some pathways exhibit a monophasic response in liver but a biphasic response in muscle (**Fatty acid degradation and Proteasome**) (Figure 13B). Although the DRN peak times align for these pathways, responses in muscle indicate a secondary activity event in response to the action of an intermediate biosignal. Both the Fatty acid degradation pathway and the pathway that regulates Proteasome subunit expression are sensitive to corticosteroid action within the liver and muscle tissues, contributing to the development of metabolic syndrome, muscle wasting, among other harmful consequences of corticosteroids (Du, Mitch et al. 2000, Short, Nygren et al. 2004, Macfarlane, Forbes et al. 2008), but clearly exhibit difference expression dynamics in different tissues.

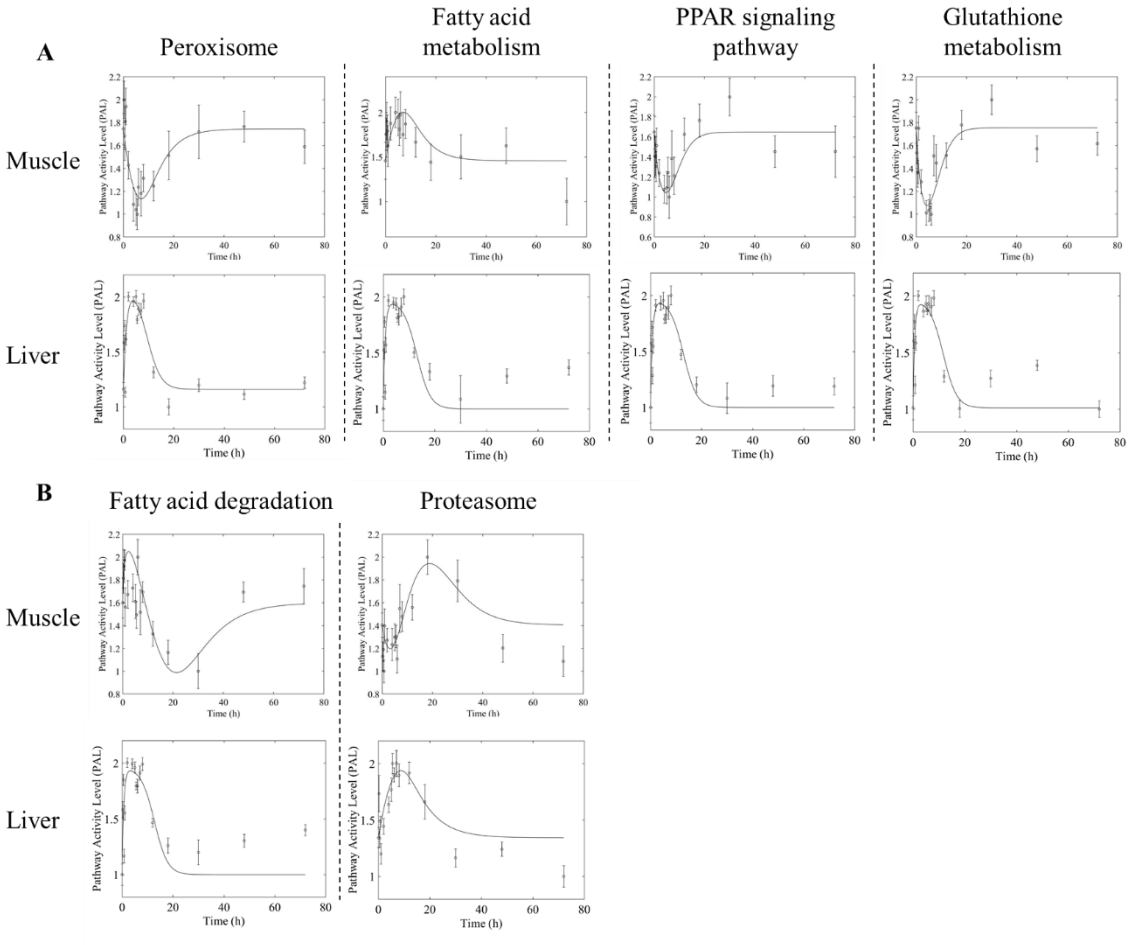

Figure 13 Comparison of acute MPL administration in liver and muscle. (A) Pathways exhibiting monophasic response in liver and muscle. (B) Pathways exhibiting monophasic response in liver and biphasic in muscle.

3.3.2 Comparison of Chronic Response across Liver and Muscle

In response to chronic MPL administration, liver and muscle tissue share 19 significant pathways, many of which exhibit different response profiles to chronic MPL administration discussed in detail below. The most striking observation is that the tolerance response observed in muscle tissue is rarely found in the liver (see exceptions in the discussion below of Biosynthesis of amino acid pathway, Figure 14A, and Tryptophan metabolism, Figure 15B). This suggests that in response to chronic MPL administration, muscle tissue is capable of making functional

adjustments in order to return to its original set point, whereas liver remains modified and settles to a new set point in most cases.

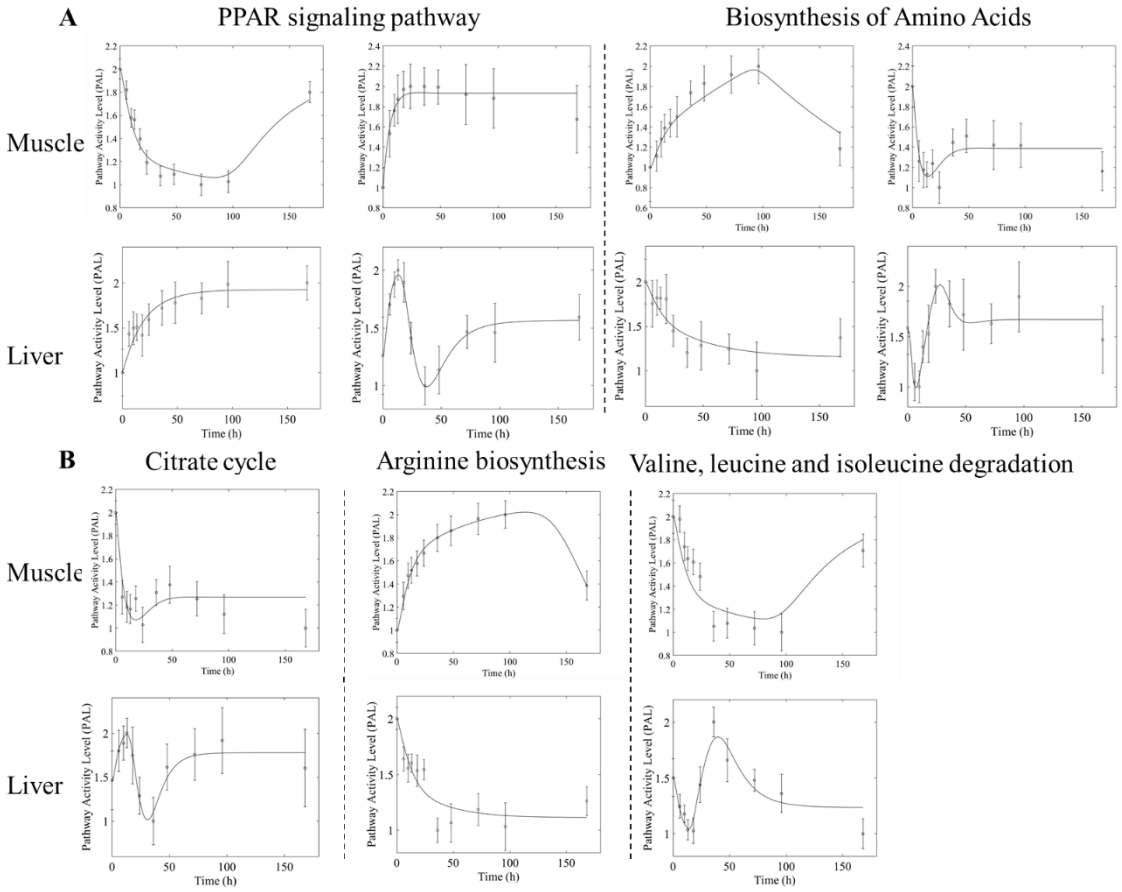

Figure 14 Comparison of response to chronic MPL administration in liver and muscle. (A) Pathways exhibiting both monophasic and biphasic response. (B) Pathways exhibiting either monophasic or biphasic response.

Figure 14A presented pathways that exhibit a complex response to chronic MPL administration in both liver and muscle (**Peroxisome, PPAR signaling pathway, Biosynthesis of amino acids, Cysteine and methionine metabolism, Glycolysis / Gluconeogenesis, Carbon metabolism, and Protein processing in endoplasmic reticulum**). Within the PPAR signaling pathway, we observe a chronic monophasic response similar to the chronic monophasic response observed in liver. We also observe biphasic responses in both tissues. In muscle, this biphasic response

manifests as the tolerance behavior characteristic of muscle tissue, whereas the biphasic response in liver is characterized by two peaks in opposite directions corresponding to an initial event due to DRN and subsequent action due to BS. Relating to the activity of the biosynthesis of amino acid pathway, glucocorticoids (and corticosteroids by extension) are observed to increase protein degradation and suppress protein synthesis in muscle (Kuo, Harris et al. 2013). Interestingly, the biosynthesis of amino acid is one of the few liver response pathways that exhibits a biphasic response that appear to return to its initial set point. This may indicate that the liver exhibits some tolerance as well according to the model predictions. However, the error observed within the biphasic response of liver in this pathway may also contradict this possibility.

Some pathways in liver and muscle exhibit a singular response to chronic MPL administration in both tissues, either monophasic or biphasic response (**Propanoate metabolism, Proteasome, Citrate cycle, Arginine biosynthesis, and Valine, leucine, and isoleucine degradation**) (Figure 14B). The citrate cycle pathway is essential to the oxidation of carbohydrates and fatty acids, a function of liver and muscle tissue (Koves, Ussher et al. 2008, Rui 2011). The citrate cycle in muscle exhibits a chronic monophasic response, settling to a new baseline in response to chronic MPL administration. The liver tissue exhibits a biphasic response with opposing peak events due to the action of DRN and BS. It is important to note that the liver response to chronic MPL administration predicts that the model will settle to a new set point, unlike in the Biosynthesis of amino acid pathway. The arginine biosynthesis pathway indicates additional contrast between tissues. Tolerance response is observed in muscle tissue, while the liver response is captured by a monophasic model. Valine, leucine, and isoleucine degradation pathways captures the degradation of these amino acids for the purposes of protein metabolism, reported in muscle and liver (Nair, Schwartz et al. 1992, Campos-Ferraz, Bozza et al. 2013) (Holeček 2002). This pathway exhibits a biphasic tolerance response in muscle and a biphasic (opposite DRN and BS

events) response in liver. The response in muscle drives toward its original activity set point, however this is not observed in the liver response. These three pathways exemplify another striking difference between liver and muscle tissue; although both liver and muscle require the functions of these two pathways, they regulate their activity with entirely different mechanisms and thus experience different responses to chronic MPL administration.

Pathways that exhibit a complex response to chronic MPL administration in one tissue but a singular response in another tissue are presented in Figure 15, and provide examples of changes in drug response complexity as we move across tissues. These include pathways with a singular response in liver and a complex response in muscle (**Fatty acid degradation and Fatty acid metabolism**) (Figure 15A) and pathways that exhibit a complex response in liver and a singular response in muscle (Glyoxylate and dicarboxylate metabolism, **Tryptophan metabolism,** Glutathione metabolism, Pyruvate metabolism, and **Oxidative phosphorylation**) (Figure 15B). The oxidative phosphorylation pathway describes the coupling of respiration and generation of ATP along the mitochondrial matrix, a function which is observed to be modified by glucocorticoids (Roussel, Dumas et al. 2004). In response to chronic MPL administration, this pathway exhibits complexity in muscle but a singular response in liver. Similarly, tryptophan metabolism pathway exhibits complexity in muscle but singularly biphasic response in liver. It is interesting that the biphasic response observed in liver does appear to settle near to its original set point. We may then include tryptophan alongside biosynthesis of amino acids as examples in which the liver does appear to return to its initial set point while MPL is continuously administered, i.e. possible tolerance behavior. Fatty acid degradation (Short, Nygren et al. 2004, Macfarlane, Forbes et al. 2008) also exhibits the tolerance behavior in muscle, but exhibits complexity in liver which yields two distinct regulatory structures, both of which settle to new set points.

Comparison of muscle and liver response to acute and chronic MPL administration indicates that few pathways exhibit consistent responses across tissues. Even when pathway responses can be described by the same regulatory mechanism, the peak events do not necessarily align, as with the comparison of acute response profiles across liver and muscle. Similarly, even when a biphasic model captures response to chronic MPL administration in both liver and muscle, muscle frequently exhibits a tolerance behavior in which pathway activity returns to the initial set point. This tolerance behavior is arguably observed in some liver pathways (Biosynthesis of amino acids and Tryptophan metabolism chronic responses), but not at the level of consistency observed in muscle tissue. The differences in dynamics observed across tissues within the same pathways follows the expectation that corticosteroids have tissue-specific consequences. Our analysis expands on this expectation by establishing temporal dynamics and characterizing these in the context of established regulatory mechanisms.

Such characterization of drug response from the perspective of a functional groups or pathways enables us to capture the unavoidably multifactorial consequences of drug administration, a systems pharmacology perspective essential to translational research and drug development. Practical implementation of this knowledge relies on translation of this information from preclinical understanding to selection of potential drug targets. For example, in order to implement a theoretical action such as manipulating the PPAR signaling pathway to disrupt muscle atrophy (Burri, Thoresen et al. , Castillero, Alamdari et al.), the functional response of the PPAR signaling pathway and connected pathways, in addition to potential drug targets, can be identified with this framework. The nature of singular value decomposition is such that PAL profiles are associated with each gene in the gene set with varying magnitude. In the decomposition of a pathway gene set by singular value decomposition, PAL correspond to each gene in the gene set by varying magnitudes, previously identified as the translational matrix U

(Acevedo, Berthel et al.). Via applying the meta-analysis technique that is the pathway-based analysis framework, we understand the consequences of the drug in the context of the physiological systems. We can then isolate subgroups within the network that correspond to hypothetical regulatory mechanisms (have large U coefficients corresponding to a PAL), then target these with further preclinical and clinical studies.

In summary, this investigation uses a pathway-based meta-analysis technique to compare the physiological dynamics of muscle tissue in response to acute and chronic MPL administration. As with our previous analysis in liver (Acevedo, Berthel et al.), we seek to enhance a conventional gene-centric approach and characterize a complex multi-genomic drug response in the context of functional groups that can reflect that complexity, i.e. functional pathways. We analyze data sets capturing the response of muscle tissue to acute and chronic dosing regimens of MPL and identify significant pathways representative multiple pathway families. All pathways exhibit a dosing dependence, moving from an acute response characterized by consistent and transient activities captured by monophasic and biphasic models, to a more complex chronic response. Interestingly, all significant pathways exhibited at least a tolerance biphasic response format indicating the tendency of muscle tissue to drive to its original set point. This analysis compared responses across liver and muscle, extending the discussion of activity to tissue-dependence. Comparison with liver revealed that tolerance behavior is pervasive in muscle tissue, though some pathways within liver present a biphasic response that settles near the original set point echoing tolerance behavior. Through characterization of MPL influence in muscle and subsequent comparison with liver, we endeavor to characterize the differences in functional response of the same pathway to different dosing regimens and across multiple tissues. It is evident that for a corticosteroid therapy, the differences in functional behavior of CS-sensitive tissues must be

considered as they exhibit consistently different mechanisms of regulation and response dynamics across the same pathways.

Table 6 Significant pathways common to acute and chronic dosing data and their response type to acute and chronic MPL administration. These pathways exhibit significant fractional coverage (f_c p-value ≤ 0.05) and significant pathway activity (f_p p-value ≤ 0.05) in both the acute and chronic datasets.

Pathway (PW)	rno ID	Genes in KEGG PW	Acute				Chronic				Class
			Unique Genes in PW from Dataset	Fractional PW Coverage (fc)	Total Fraction of PW Activity (total fp)	Acute MPL Response	Unique Genes in PW from Dataset	Fractional PW Coverage (fc)	Total Fraction of PW Activity (total fp)	Chronic MPL Response	
Amino acid metabolism											
Arginine and proline metabolism	rno00330	52	9	17%	42%	monophasic	17	33%	56%	monophasic/tolerance	1
Glutathione metabolism	rno00480	69	10	14%	69%	monophasic	22	32%	72%	monophasic/tolerance	1
Cell growth and death											
Apoptosis	rno04210	141	23	16%	61%	monophasic	38	27%	55%	monophasic/tolerance	1
Cellular senescence	rno04218	189	24	13%	57%	monophasic	44	23%	69%	monophasic/tolerance	1
Ferroptosis	rno04216	41	9	22%	49%	monophasic	15	37%	72%	tolerance	1
Cell motility											
Regulation of actin cytoskeleton	rno04810	223	21	9%	47%	monophasic	48	22%	71%	monophasic/tolerance	1
Endocrine system											

Adipocytokine signaling pathway	rno04920	74	14	19%	57%	monophasic/biphasic	20	27%	55%	tolerance	2
Glucagon signaling pathway	rno04922	103	11	11%	65%	monophasic	32	31%	58%	monophasic/tolerance	1
GnRH signaling pathway	rno04912	94	12	13%	60%	monophasic	29	31%	76%	biphasic/tolerance	1
Insulin signaling pathway	rno04910	138	18	13%	50%	monophasic	43	31%	73%	monophasic/tolerance	1
Oxytocin signaling pathway	rno04921	157	21	13%	58%	monophasic	40	25%	57%	monophasic/tolerance	1
PPAR signaling pathway	rno03320	82	15	18%	61%	monophasic	21	26%	61%	monophasic/tolerance	1
Prolactin signaling pathway	rno04917	74	13	18%	61%	monophasic	18	24%	48%	biphasic/tolerance	1
Thyroid hormone signaling pathway	rno04919	118	21	18%	41%	monophasic	30	25%	55%	tolerance	1
Folding, sorting and degradation											
Proteasome	rno03050	48	14	29%	62%	biphasic	30	63%	87%	tolerance	1
Lipid metabolism											
Fatty acid degradation	rno00071	47	11	23%	44%	biphasic	18	38%	70%	tolerance	1
Fatty acid metabolism	rno01212	59	12	20%	59%	monophasic	19	32%	68%	tolerance	1
Signal transduction											
AMPK signaling pathway	rno04152	127	16	13%	50%	monophasic	36	28%	58%	tolerance	1

cGMP-PKG signaling pathway	rno04022	172	19	11%	54%	monophasic	38	22%	53%	monophasic/tolerance	1
ErbB signaling pathway	rno04012	88	11	13%	70%	monophasic	23	26%	61%	tolerance	1
FoxO signaling pathway	rno04068	134	16	12%	61%	monophasic	43	32%	68%	biphasic/tolerance	1
HIF-1 signaling pathway	rno04066	107	16	15%	55%	monophasic	35	33%	67%	monophasic/tolerance	1
MAPK signaling pathway	rno04010	300	39	13%	59%	monophasic/biphasic	68	23%	81%	monophasic/tolerance	2
PI3K-Akt signaling pathway	rno04151	349	45	13%	51%	monophasic	73	21%	56%	monophasic/tolerance	1
Rap1 signaling pathway	rno04015	213	28	13%	54%	monophasic	44	21%	67%	monophasic/tolerance	1
TGF-beta signaling pathway	rno04350	93	11	12%	47%	biphasic	23	25%	54%	monophasic/tolerance	1
VEGF signaling pathway	rno04370	58	14	24%	57%	monophasic/biphasic	20	34%	83%	monophasic/tolerance	2
Transport and catabolism											
Autophagy - animal	rno04140	134	16	12%	70%	monophasic	45	34%	59%	tolerance	1
Peroxisome	rno04146	88	11	13%	47%	monophasic	24	27%	77%	monophasic/tolerance	1

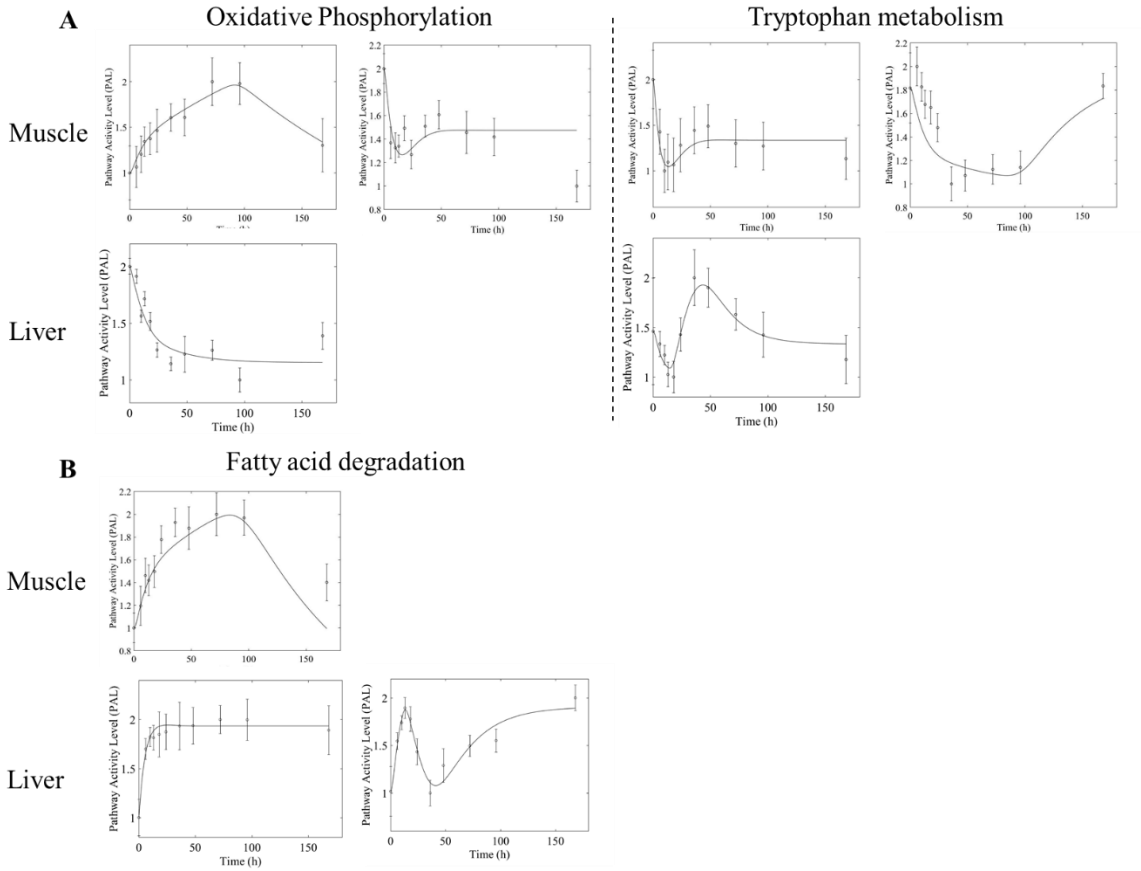

Figure 15 Comparison of response to chronic MPL administration in liver and muscle. (A) Pathways that exhibit both biphasic (tolerance) and monophasic response in muscle but either monophasic or biphasic in liver. (B) A pathway exhibiting biphasic (tolerance) response in muscle but exhibits both biphasic and monophasic response in liver.

Chapter 4: Endogenous Circadian Activity Across Multiple Tissues in Rat and Mouse

4.1 Introduction

The biological time-keeping machinery which maintains 24 h oscillations in cellular and physiological processes in mammals is organized as a hierarchical, interconnected, network of clocks (Albrecht 2012). The master, or central, clock in the suprachiasmatic nuclei (SCN) is mainly linked to light/dark cycle, and synchronizes a network of peripheral clocks, distributed across tissues, by controlling timing of feeding and activity cycles (Cassone 1990, Cardone, Hirayama et al. 2005). Homeostasis is maintained through rhythmic hormonal and metabolic signals that establish the phase relationships among the various clocks (Skarke, Lahens et al. 2017). The circadian rhythms coordinate the interactions between endocrine, immune, autonomic, and central nervous systems (Cutolo and Masi 2005) so that these are regulated in a precise temporal manner by the central and peripheral circadian clocks (Buijs, van Eden et al. 2003, Dibner, Schibler et al. 2010), thus coordinating the time-of-day variation of important physiological mediators playing a major role in immune (Lee and Edery 2008, Paladino, Leone et al. 2010, Silver, Arjona et al. 2012) and metabolic functions (Feillet, Albrecht et al. 2006) and conferring adaptive advantages (Edery 2000).

Recent genome-wide studies have confirmed that a substantial fraction of the mammalian genes is expressed with 24-hour periodicity (Zhang, Lahens et al. 2014, Mavroudis, DuBois et al. 2018, Mure, Le et al. 2018). Additional studies have indicated that circadian regulation organizes the metabolic fingerprint as well (Dyar, Lutter et al. 2018). Interestingly, the strong connections between circadian rhythms, and their disruption, in health and disease have not only been recognized and established (Bishehsari, Levi et al. 2016, Kaczmarek, Thompson et al. 2017,

Doherty 2018, Khaper, Bailey et al. 2018, Varcoe 2018, Zaki, Spence et al. 2018) but also the idea of pharmacologically, and non-pharmacologically, targeting the circadian rhythms directly is gaining acceptance (Fang, Guo et al. 2015, Cunningham, Ahern et al. 2016, Nakamura, Nakano et al. 2016).

In view of these recent findings, genome-wide studies (Zhang, Lahens et al. 2014, Mavroudis, DuBois et al. 2018, Mure, Le et al. 2018) have a profound impact in that they enable us to decipher the details of circadian regulation at a very fundamental level. As such, the aforementioned studies have established a number of key conclusions: (1) periodicity in gene expression is widespread across the host's genome; (2) rhythmic gene expression appears to have strong tissue-specific characteristics; and (3) despite tissue-specific rhythmic patterns, the "core clock machinery" - a small group of mutually regulated genes/transcription factors maintaining periodicity at the cell level (Buhr and Takahashi 2013) – is coherently expressed across tissues. The latter is very interesting, indicating that despite the fact the underlying time-keeping mechanism is consistent across tissues, its effects are manifested in a tissue-specific manner.

Recognizing not only the importance of genome-wide studies, but also the wealth of information they provide, in this work we establish a computational framework to enable the characterization of circadian dynamics at the level of "functional groupings of genes" and do so within two organisms essential to preclinical research, rat and mouse (Consortium 2002, Consortium 2004, Bryda 2013, Denayer, Stöhr et al. 2014, Ellenbroek and Youn 2016). Without loss of generality, the functional groupings in our study are based on KEGG pathways (Kanehisa and Goto 2000, Kanehisa and Goto , Aoki and Kanehisa , Kanehisa, Sato et al.). In other words, we aim to identify how individual genes come together to generate rhythmic patterns in the context of signaling and metabolic pathways (or any other networked functional grouping of interest), capitalizing on our earlier work on pathway activity analyses (Ovacik, Sukumaran et al. 2010,

Euling, White et al. 2011, Euling, White et al. 2013, Acevedo, Berthel et al. , Acevedo, DuBois et al.). By mapping genome-wide transcriptional data onto pathways, we characterize the tissue-specific circadian dynamics at the pathway level to assess how individual genes come together. Our analysis focuses on four rat and mouse tissues (adipose, liver, lung and muscle) recently analyzed in (Zhang, Lahens et al. , Mavroudis, DuBois et al. 2018). Interestingly, we identify alternative tissue-specific and organism-specific cascading and non-cascading circadian behavior within immune and signaling, metabolic, and cell regulatory pathways. A genome-wide pathway-centric analysis enables us to develop a more complete picture on how the observed circadian variation at the individual gene level, orchestrates functional responses at the pathway level. Finally, such "meta-data" analysis that the pathway approach offers enables the rational integration and comparison across organisms, platforms and experimental designs since we evaluate emergent dynamics as opposed to comparing individual elements.

4.2. Approach

Toward the analysis of the endogenous circadian expression within multiple tissues across rat and mouse, we applied the pathway-based analysis approach presented in Chapter 2 (Acevedo, Berthel et al. , Acevedo, DuBois et al.). However, this data is not an analysis of drug response, thus the corticosteroid modeling component is not used in this part of the analysis. This investigation remains ongoing and modeling may be incorporated in investigations related to this work in the thesis work of future graduate students in our lab.

4.2.1 Animal Model and Experimental Data

The data capturing the endogenous circadian expression of liver, muscle, adipose, and lung within rat is described in great detail in (Mavroudis, DuBois et al. 2018). In brief, normal male Wistar rats acclimatized to a constant 22˚C environment, were equipped with a 12:12 h light-dark cycle with free access to standard rat chow and water. The animals were sacrificed at 9 timepoints:

0.25, 1, 2, 4, 6, 8, 10, 11, and 11.75 h after lights on (ZT=0 at 8 am) for the light period, and 9 sample times at 12.25, 13, 14, 16, 18, 20, 22, 23, and 23.75 h after lights off (ZT=12 at 8 pm) for the dark period. Livers, gastrocnemius muscles, abdominal fat pads, and lungs were excised. mRNA expression data from the tissue samples were obtained using Affymetrix Rat Expression Set 230A for liver and muscle tissue, and Affymetrix Rat Genome 230 2.0 for adipose and lung tissue (Affymetrix, Santa Clara, CA). Datasets were submitted to Gene Expression Omnibus (GEO) (GSE8988 for liver, GSE8989 for muscle, GSE20635 for adipose, and GSE25612 for lung), and were previously published (Almon, Yang et al. 2008, Almon, Yang et al. 2008, Sukumaran, Xue et al. 2010, Sukumaran, Jusko et al. 2011, Mavroudis, DuBois et al. 2018, Mavroudis, DuBois et al. 2018).

The data capturing the endogenous expression of liver, muscle, adipose, and lung within mouse is described in (Zhang, Lahens et al. 2014). In brief, C57/BL6 mice were entrained to a 12:12 h light-dark schedule then released in constant darkness. Beginning at CT18, three mice were sacrificed every 2 h for 48 h (24 samples over 2 days). Many organs were harvested from each mouse for analysis in previous publications (Zhang, Lahens et al. 2014). Our analysis seeks to compare activity across a consistent set of organs common to available rat and mouse analyses, so we use the data sets specific to liver, muscle, lung, and brown adipose collected by (Zhang, Lahens et al. 2014).mRNA expression was quantified using Affymetrix MoGene 1.0 ST arrays and submitted to the Gene Expression Omnibus (GEO) (GSE54652 for all tissues) (Zhang, Lahens et al. 2014).

4.2.2 Application of Pathway-based Analysis Framework

To characterize endogenous circadian expression across multiple organisms and tissues, we applied our pathway activity analysis approach described in depth in Chapter 2 (Acevedo, Berthel

et al. , Acevedo, DuBois et al. 2019 (submitted)), but did not include the corticosteroid modeling component as it was not relevant to analyzing drug-free tissue. The most recent version of the framework was applied for this analysis (Chapter 2)(Acevedo, DuBois et al. 2019 (submitted)) and details specific to this analysis are listed here:

Data Preprocessing

Active genes were identified using differential expression analysis accomplished with the software Extraction and Analysis of Gene Expression (EDGE) (Leek, Monsen et al. 2006). Differentially expressed genes are identified by p-value. Differentially expressed profiles are then z-scored with respect to the individual profile mean and standard deviation. Replicate profiles are then averaged together, yielding averaged z-scored profiles.

Mapping Data onto Pathways

As of June 2019, the KEGG database contains approximately 300 pathways relevant to rat and/or mouse tissues and used for our analysis. Only pathways relevant to each tissue (liver, lung, muscle, adipose) are used in the independent analysis of each. However, many pathways are removed for each pathway including (ex. pathways relevant to the digestive, excretory, circulatory systems), disease pathways (ex. Neurodegenerative disease, cancers, and infectious disease pathways), or redundant pathways (KEGG's pathway entitled Metabolic pathways, rno:01100, is the set of all other metabolism related pathways). This elimination step left about 178 pathways to consider in this analysis.

Affymetrix probe identifiers are translated into their NCBI Entrez IDs and Gene Symbols using the Bioconductor packages for each Affymetrix Platform: Package rae230a.db containing the annotation data for Affymetrix Rat Expression Set 230A used with the rat liver and muscle tissue; Package rat2302.db containing the annotation data for Affymetrix Rat Genome 230 2.0 Array

annotation data used with the rat adipose and lung tissue; Package mogene10sttranscriptcluster.db containing the annotation data for Affymetrix MoGene 1.0 ST Array used for all tissues in mouse.

Some pathways with low fractional occupancy yield inconclusive p-values as an artifact of the Fisher's Exact Test and were eliminated from the analysis, discussed further in ST 2.

Pathway Activity Analysis

Active genes are identified using differential expression analysis with the software Extraction and Analysis of Gene Expression (EDGE) (Leek, Monsen et al. 2006). Differentially expressed genes are identified by p-value, $p \leq 0.05$.

All pathways yielding fractional occupancy f_c p-value ≤ 0.05 with at least one significant PAL profile f_p p-value ≤ 0.05 are defined as significant.

4.3 Analysis of Endogenous Circadian Activity in Rat

4.3.1 Results

A computational framework was developed to enable the characterization of genome-wide, multi-tissue circadian dynamics at the level of "functional groupings of genes" defined in the context of signaling, cellular/genetic processing and metabolic pathways. Our aim is to identify how individual genes come together to generate orchestrated rhythmic patterns and how these may vary within and across tissues. We focus our analysis on four tissues in rat (adipose, liver, lung, and muscle). Interestingly, we identify alternative tissue-specific cascading and non-cascading circadian behavior within immune and signaling, metabolic, and cell regulatory pathways. A genome-wide pathway-centric analysis enables us to develop a comprehensive picture on how the observed circadian variation at the individual gene level, orchestrates functional responses at the pathway level. Such "meta-data" analysis that the pathway approach enables the rational

integration and comparison across platforms and/or experimental designs since we evaluate emergent dynamics as opposed to comparing individual elements. One of our key findings is that when considering the dynamics at the pathway level, a complex behavior emerges, as it is not likely that a pathway will exhibit a pattern of activity indicative of "rush hours" as occurs with individual gene expression patterns. Rather tissues tend to coordinate activity in a way that optimizes tissue-specific activity depending of each tissue's broader role in homeostasis.

The mapping of rat gene expression data onto pathways reveals interesting patterns of activity. Characteristics examples are presented in Figure 16, Figure 17, and Figure 18 for TCA, mTOR and glycolysis/gluconeogenesis pathways in liver. Unlike earlier studies which appear to emphasize the clustering of gene expression data around specific "rush hours" (Zhang, Lahens et al. 2014, Mavroudis, DuBois et al. 2018), pathways manifested dynamics indicating a flow of activity with individual genes' phases that span a wide range during the 24-h period. These results suggest that multiple processes coordinate appropriately in the context of a pathway and that pathways are not characterized by a coordinated burst of activity.

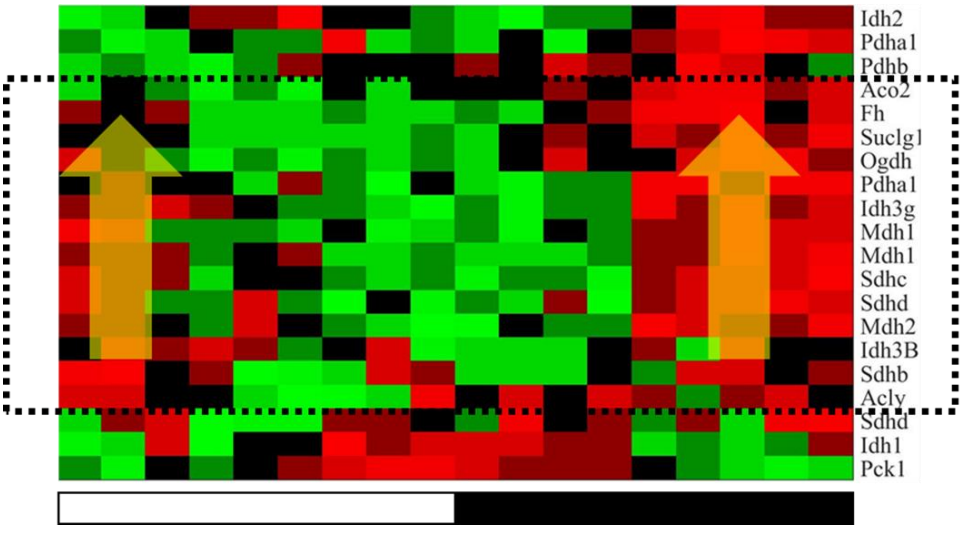

Figure 16 Circadian pathway activity pattern (TCA cycle in liver). The peak expression activities of the genes coordinating a function is focused during specific period of the circadian cycle for most of the genes

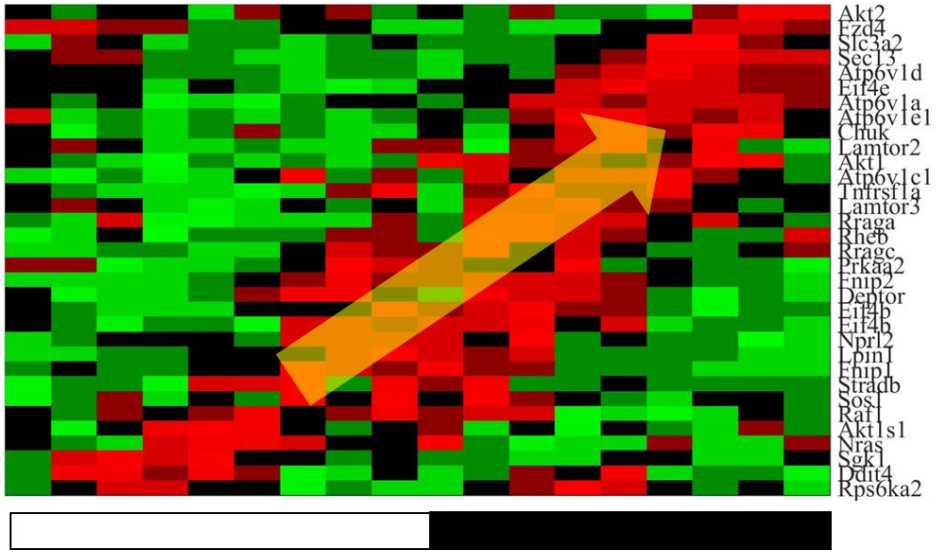

Figure 17 Circadian pathway activity pattern (mTOR in liver) The peak expression activity of each gene is different, resulting in a "wave" of activity across the pathway during the circadian cycle.

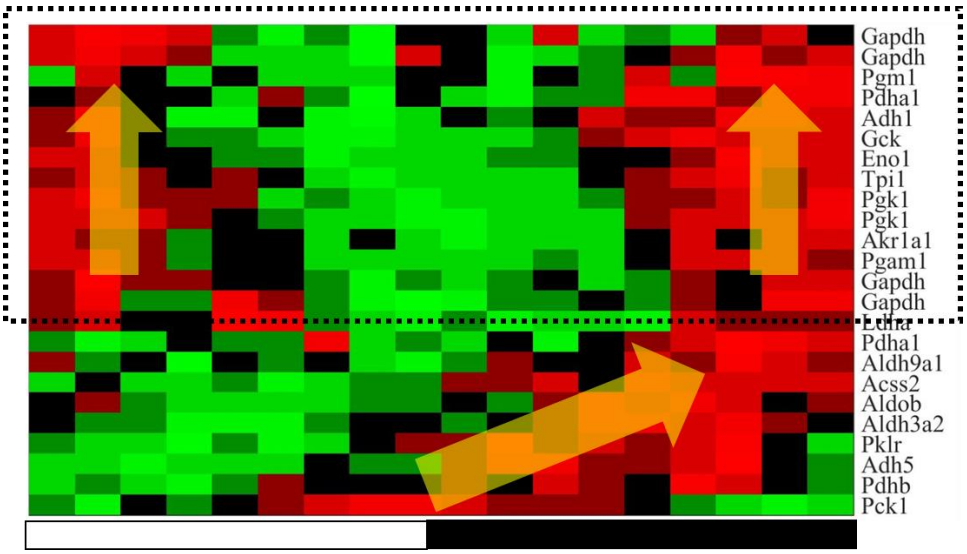

Figure 18 Circadian pathway activity pattern (Glycolysis/gluconeogenesis in liver). The peak activities of the genes in a pathway result in the emergence of complex dynamics.

Once mapped onto pathways, the tissue-specific transcriptional data were analyzed to assess the emergence of pathways with well-defined dynamics. The fractional occupancy and activity criteria described earlier were applied to all four tissues and coherently active pathways were

identified. Interestingly the active pathways exhibit structured patterns of activity over the course a 24-hour period. A comprehensive list of the significant pathways that emerged from each tissue is presented in the Appendix (ST 7). In summary, the tissues are characterized as follows:

In **liver**, 6796 unique Affymetrix probes contained at least one measurement recorded as Present. Differential expression analysis using EDGE (Leek, Monsen et al. 2006) yielded 2,636 probe profiles. 57 pathways were identified representing a plethora of signaling and metabolic functions including, but not limited to: metabolism of amino acids, TCA cycle, fatty acid metabolism and degradation, glycolysis/gluconeogenesis, oxidative phosphorylation, pentose phosphate metabolism, bile biosynthesis, pyruvate, purine metabolism, as well as a multitude of signaling pathways including mTOR, PPAR, and insulin. The dynamics within each pathway are complex and reflected in the characteristic examples in Figure 19, with the mTOR signaling pathway (top) exhibiting expression of its elements in a form of "wave" with phases of individual genes distributed during the course of a 24-hour period. Whereas the cysteine and methionine metabolism pathway (bottom) exhibits primarily two blocks of activity, both concentrated around the light/dark and dark/light transition periods. Mapping the expression patterns on the network representation of the pathway provides an overall view of the distribution of activity across the pathway, Figure 20.

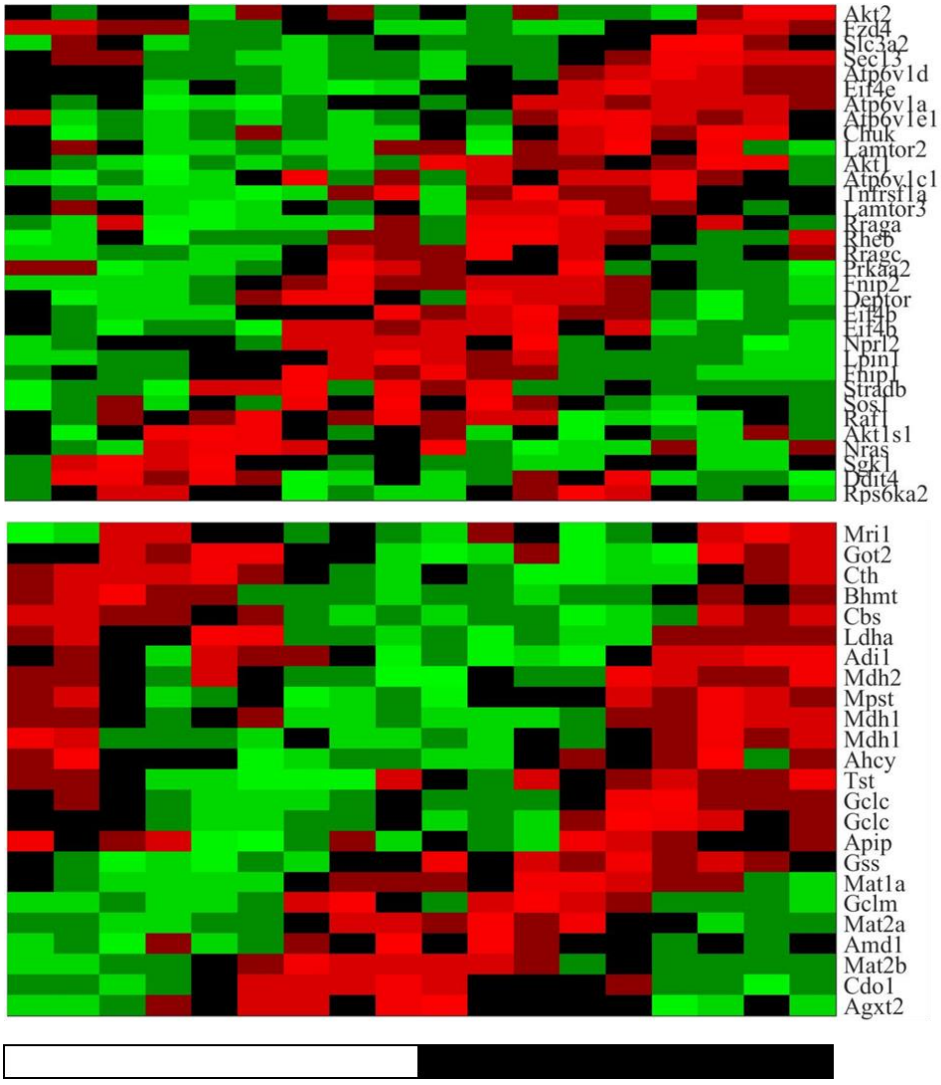

Figure 19 (top) mTOR and (bottom) Cysteine/Methionine Metabolism activity maps in liver

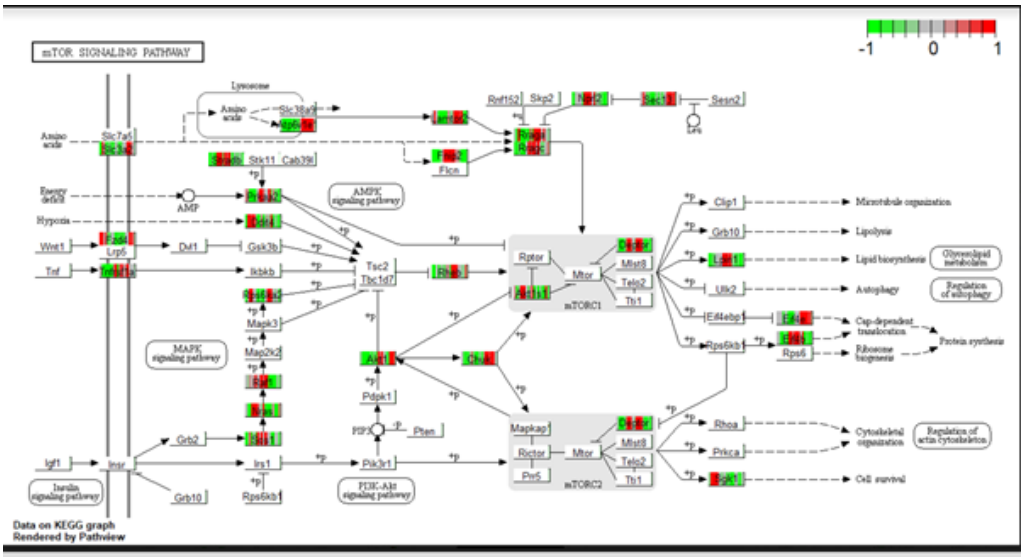
mTOR SIGNALING PATHWAY
-1
0
1
Lysosome
Amino acid
Slc38a9
Slc7a5
Slc1a5
Rragc/d
Rragb
Rheb
Rptor
Mtor
Mlst8
Telo2
Tti1
mTORC1
Rictor
Pm5
mTORC2
Rnf152
Skp2
Fbxl2
Sesn2
Stk11
Cab39l
Flcn
AMPK signaling pathway
AMP
Energy deficit
Hypoxia
Wnt1
Lrp6
Tnf
Dvl1
Gsk3b
Ikbkb
Tsc2
Tbc1d7
Rhb
Mapk3
Map2k2
MAPK signaling pathway
Pdpk1
PIP3
Pten
Igf1
Insr
Irs1
Pik3r1
Grb2
Grb10
Rps6kb1
Insulin signaling pathway
PI3K-Akt signaling pathway
Clip1
Grb10
Lipolysis
Lipid biosynthesis
Glycerolipid metabolism
Ulk2
Autophagy
Regulation of autophagy
Eif4ebp1
Rps6kb1
Rps6
Cap-dependent translocation
Ribosome biogenesis
Protein synthesis
Rhoa
Prkca
Cytoskeletal organization
Regulation of actin cytoskeleton
Cell survival
Microtubule organization
Data on KEGG graph
Rendered by Pathview

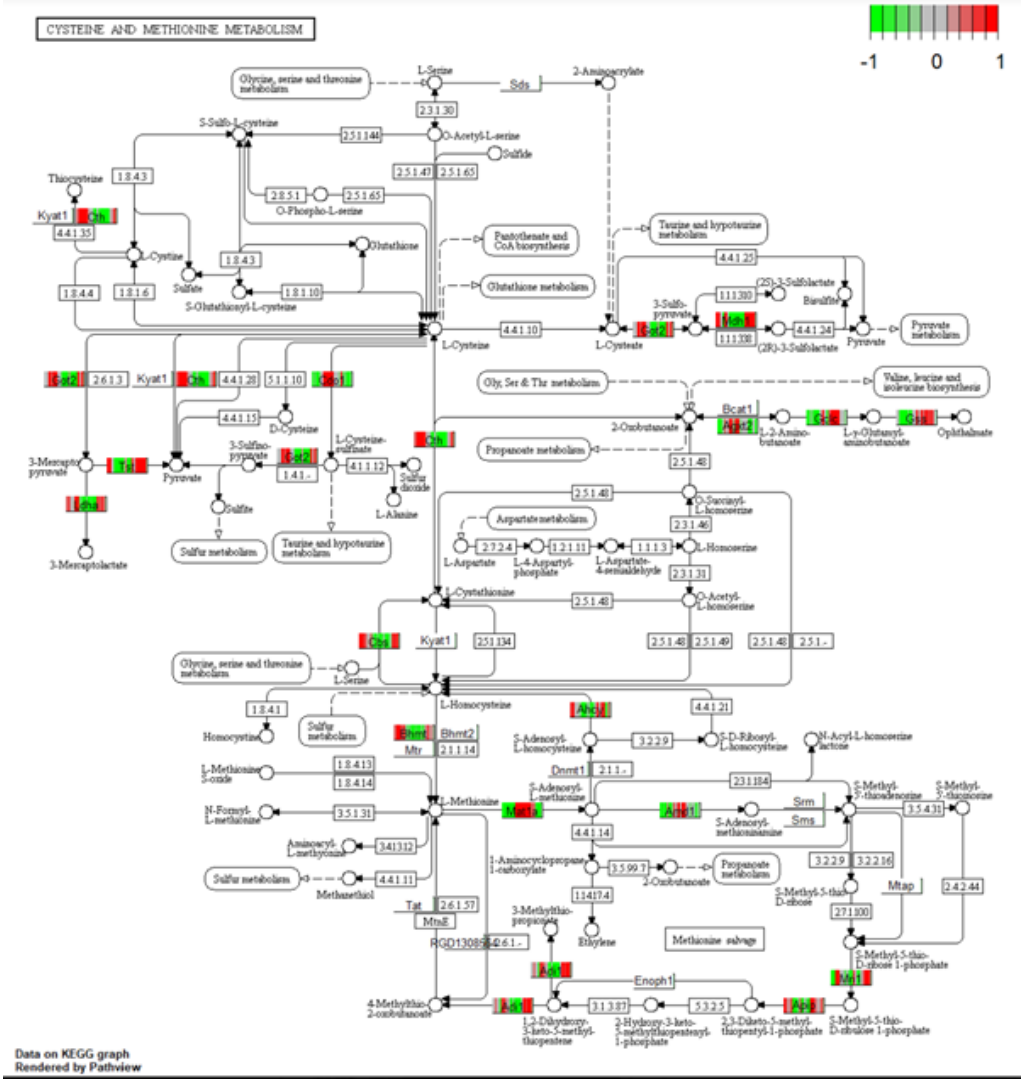
CYSTEINE AND METHIONINE METABOLISM
-1
0
1
Glycine, serine and threonine metabolism
L-Serine
Sds
2-Aminoacrylate
2.3.1.30
S-Sulfo-L-cysteine
2.5.1.140
O-Acetyl-L-serine
Sulfide
2.5.1.47
2.5.1.65
Thiocysteine
1.8.4.3
Kyat1
Cth
4.4.1.35
2.8.5.1
O-Phospho-L-serine
L-Cysteine
Glutathione
Pantothenate and CoA biosynthesis
Glutathione metabolism
1.8.4.4
1.8.1.6
Sulfate
1.8.1.10
S-Glutathionyl-L-cysteine
Taurine and hypotaurine metabolism
4.4.1.25
1.11.1.30
(2S)-3-Sulfolactate
Bisulfite
3-Sulfo-pyruvate
Cbs
1.11.1.31
(2R)-3-Sulfolactate
4.4.1.24
Pyruvate
Pyruvate metabolism
4.4.1.10
L-Cysteate
Gly, Ser & Thr metabolism
Valine, leucine and isoleucine biosynthesis
Bcat1
Bcat2
2-Oxobutanoate
1-2-Amino-butanoate
L-γ-Glutamyl-aminobutanoate
Ophthalmate
Propanoate metabolism
2.5.1.48
4.4.1.28
5.1.1.10
D-Cysteine
4.4.1.15
3-Sulfino-pyruvate
L-Cysteine-sulfinate
4.1.1.12
Sulfur dioxide
L-Alanine
3-Mercapto-pyruvate
Pyruvate
Sulfite
3-Mercaptolactate
Sulfur metabolism
Taurine and hypotaurine metabolism
Aspartate metabolism
2.7.2.4
L-Aspartate
L-4-Aspartyl-phosphate
1.2.1.11
L-Aspartate-4-semialdehyde
1.1.1.3
L-Homoserine
2.3.1.46
O-Succinyl-L-homoserine
2.3.1.31
L-Cystathionine
O-Acetyl-L-homoserine
2.5.1.49
2.5.1.-
Kyat1
2.5.1.34
Glycine, serine and threonine metabolism
L-Serine
L-Homocysteine
1.8.4.1
Homocystine
Sulfur metabolism
Bhmt
Bhmt2
Mtr
2.1.1.14
S-Adenosyl-L-homocysteine
3.2.2.9
S-D-Ribosyl-L-homocysteine
N-Acryl-L-homoserine lactone
Dnmt1
2.1.1.-
L-Methionine S-oxide
1.8.4.13
1.8.4.14
L-Methionine
S-Adenosyl-L-methionine
Mat2a
Mat1a
2.3.1.184
Srm
Sms
S-Methyl-5'-thioadenosine
S-Methyl-5'-thioinosine
3.5.4.31
S-Adenosyl-methioninamine
N-Formyl-L-methionine
3.5.1.31
Aminoacyl-L-methionine
3.4.13.12
4.4.1.14
1-Aminocyclopropane-1-carboxylate
3.5.99.7
2-Oxobutanoate
Propanoate metabolism
3.2.2.9
3.2.2.16
S-Methyl-5-thio-D-ribose
Mtap
2.4.2.44
Sulfur metabolism
4.4.1.11
Methanethiol
Tat
2.6.1.57
MtnE
RGD1308564
2.6.1.-
3-Methylthio-propionate
1.13.11.53
Ethylene
Methionine salvage
2.7.1.100
S-Methyl-5-thio-D-ribose 1-phosphate
Aco1
Eno1
Eno2
Eno3
Enoph1
4-Methylthio-2-oxobutanoate
Aldh1a1
3.1.3.87
5.3.2.5
Aldh1a3
1,2-Dihydroxy-3-keto-5-methyl-thiopentene
2-Hydroxy-3-keto-5-methylthiopentenyl-1-phosphate
2,3-Diketo-5-methyl-thiopentyl-1-phosphate
S-Methyl-5-thio-D-ribulose 1-phosphate
Data on KEGG graph
Rendered by Pathview

Figure 20 Mapping of liver onto KEGG pathway schematics (top: mTOR; bottom: Cysteine/Methionine Metabolism)

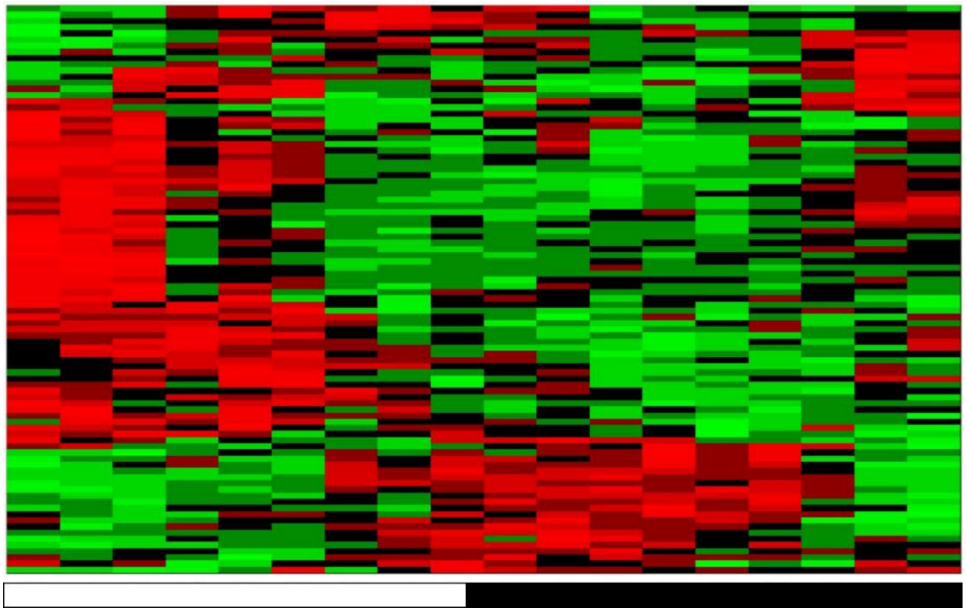

Figure 21 mTOR activity in lung.

In **lung**, 20,126 unique Affymetrix probes contained at least one measurement recorded as Present. Differential expression analysis using EDGE (Leek, Monsen et al. 2006) yielded 11,979 probe profiles. Occupancy and pathway activity analysis yielded 60 significant pathways. Liver and lung generated the richest set of circadian pathways, in line with earlier studies that observed similar trends in the context of circadian gene expression (Zhang, Lahens et al. 2014, Mavroudis, DuBois et al. 2018). Interestingly, most coordinate responses in lung were related to signaling pathways, including mTOR, MAPK, Rap1, Ras, TGF-β, TNF, HIF, and Fox-O. It must be emphasized that the number of genes eventually considered in lung were about 5 times more than those in liver (due to the different arrays used). However, it is still interesting that in lung, signaling pathways dominated as opposed to metabolic pathways. Comparing the dynamics across tissues, notable observations emerge. It is noteworthy to consider the difference at the tissue level of mTOR between liver (Figure 19) and lung (Figure 21). In lung, strong activity

appears to emerge during the early stages of the light (rest) period, unlike the broader distribution in liver. Lung, unlike the other three tissues, exhibited some notable exceptions to the structure of the pathway dynamics by yielding high activity during the early rest period. Interestingly, lung-specific gene expression patterns were is generally observed to be broadly different in lung than in other tissues in both the mouse (Zhang, Lahens et al. 2014) and rat (Mavroudis, DuBois et al. 2018). The mapping of expression data onto the mTOR pathway in lung is shown in Figure 22.

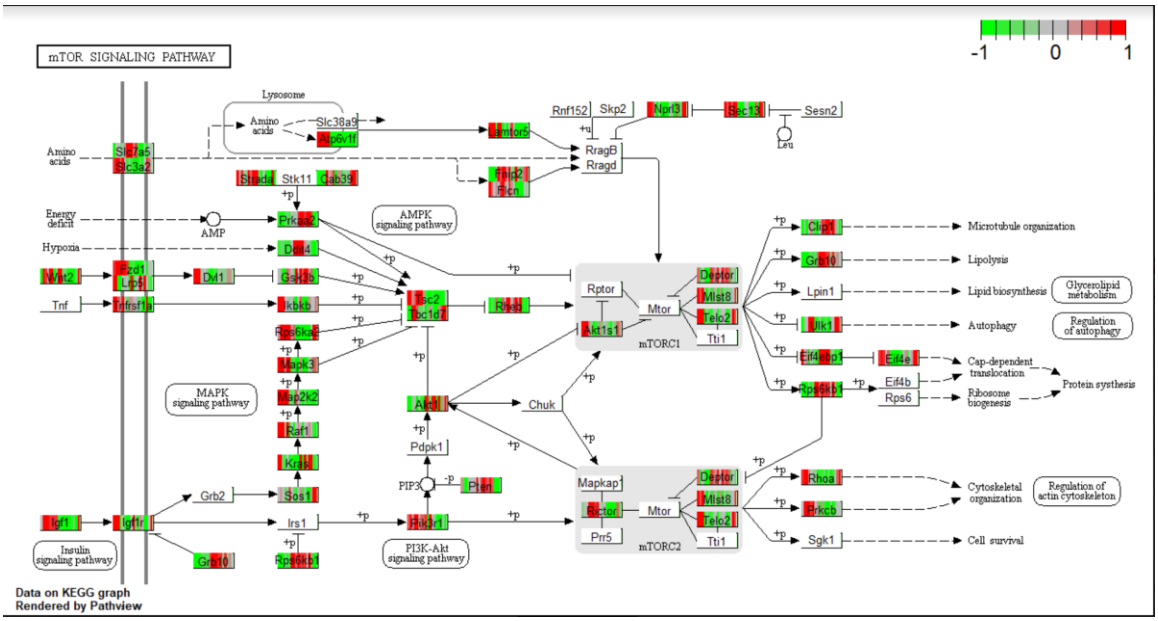

Figure 22 Mapping of mTOR gene expression patterns onto KEGG schematic in lung.

In **muscle**, 7,086 unique Affymetrix probes contained at least one measurement recorded as Present. Differential expression analysis using EDGE (Leek, Monsen et al. 2006) yielded 2,233 probe profiles (p value ≤ 0.05). 47 pathways were identified as significant in muscle. Muscle emerged as relatively active metabolically, including pathways within amino acid, carbohydrate, and lipid metabolism pathway subgroups (families) (ST 7). Muscle also exhibited robust activities within endocrine signaling and signal transduction.

Within **adipose**, 17,246 unique Affymetrix probes contained at least one measurement recorded as Present. Differential expression analysis using EDGE (Leek, Monsen et al. 2006) yielded 4,851 probe profiles (p value ≤ 0.05). Adipose tissue yielded 47 significant pathways (ST 7). Consistent with earlier studies at gene expression levels (Zhang, Lahens et al. 2014, Mavroudis, DuBois et al. 2018), both muscle and adipose expressed far fewer rhythmic genes, and by extension, exhibited less coherent activity at the pathway level. Similar to lung, the muscle and adipose tissues primarily revealed the importance of signaling pathways including, but not limited to, cGMP-PKG, insulin, ErbB, AMPK, and Fox-O.

All tissues appear to share broadly similar activities in term of pathways related to genetic and cellular information processing. An overview of the broad distribution of processes active in each tissue is presented in Figure 23 and the detailed list of significant pathways is provided in the Appendix (ST 7).

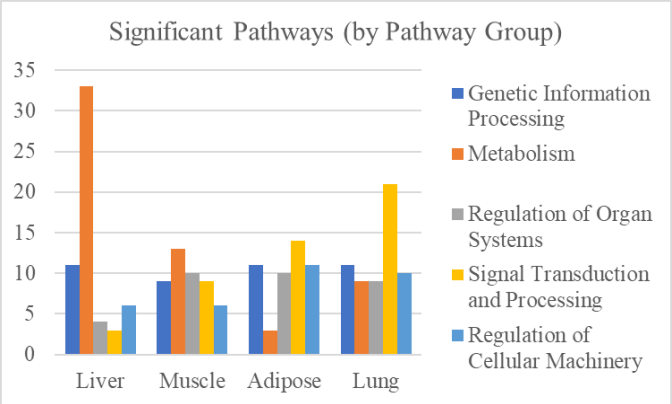

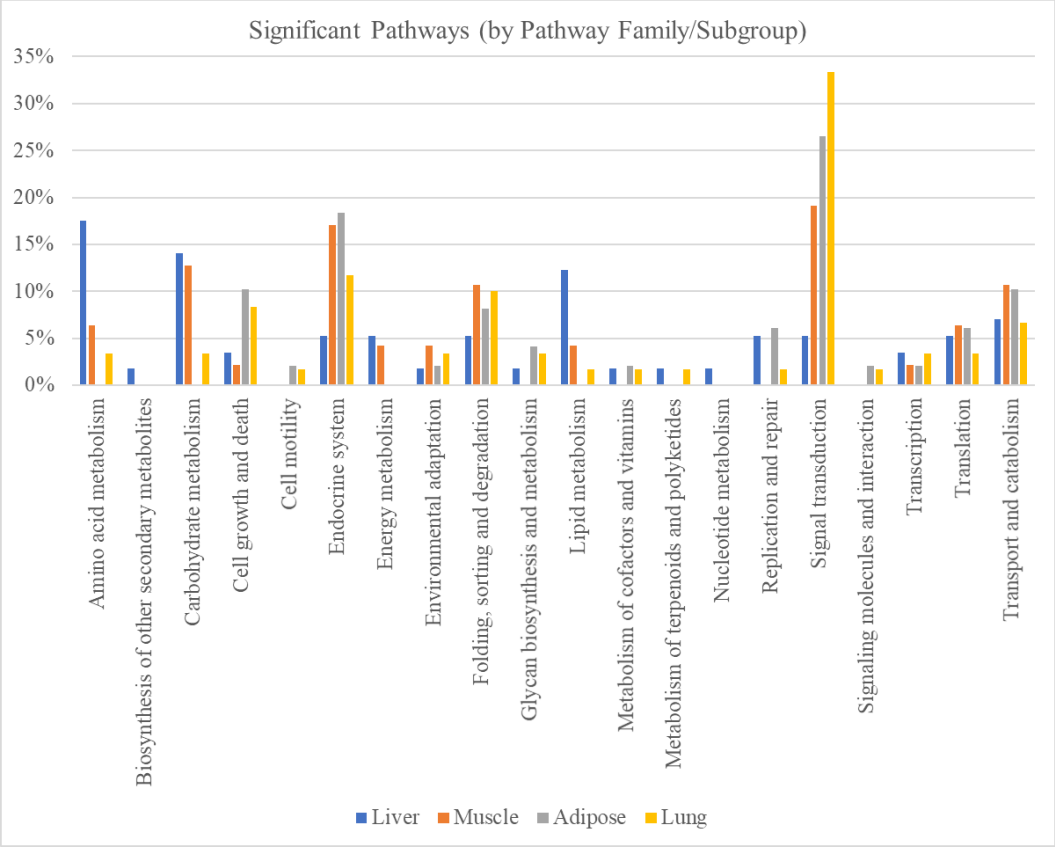

Figure 23 Distribution of pathways with robust circadian activity across tissues in rat. Pathways are grouped by the (top) group and (bottom) subgroup (family) labels (ST 7). The percentages (bottom) indicate the fraction of total pathways for the corresponding tissue.

4.3.2 Discussion

Circadian rhythms play a critical role in homeostasis and health (Zvonic, Floyd et al. 2007, McEachron 2012, Portaluppi, Tiseo et al. 2012, Tan and Scott 2014, Bishehsari, Levi et al. 2016, Zhou, Wang et al. 2016, Gnocchi and Bruscalupi 2017, Doherty 2018, Khaper, Bailey et al. 2018). Both managing and restoring circadian rhythms are emerging as major therapeutic approaches (Sulli, Manoogian et al. 2018). Recent evidence has shown that not only is timing of drug administration relative to circadian rhythms of drug targets significant (Kanemitsu, Tsurudome et al. 2017), but directly targeting components of the molecular clock is also a powerful pharmacological approach (He, Nohara et al. 2016). As such, numerous recent studies have started to map out genomic elements under the regulation of the molecular clock and have successfully identified numerous genes that exhibit, under homeostatic conditions, robust circadian oscillations. Our study explores the emergent coordination of circadian rhythmicity among various genomic components when viewed as parts of functional groups. We do so by examining circadian pathway activity across tissues by analyzing *a priori* groupings of functionally related genes in the context of biochemical pathways and within the four rat tissues. Characterizing the dynamics at the pathway level, or at the level of any set of functionally related genes, enables an extension of the gene-centric perspective. A meta-analysis technique was applied in which each tissue is analyzed separately for pathway activity. Via this analysis, we developed a more systemic view of circadian regulation, assisting in understanding inherent circadian behavior across tissues and in developing treatments for conditions which are interdependent with circadian-regulated functions.

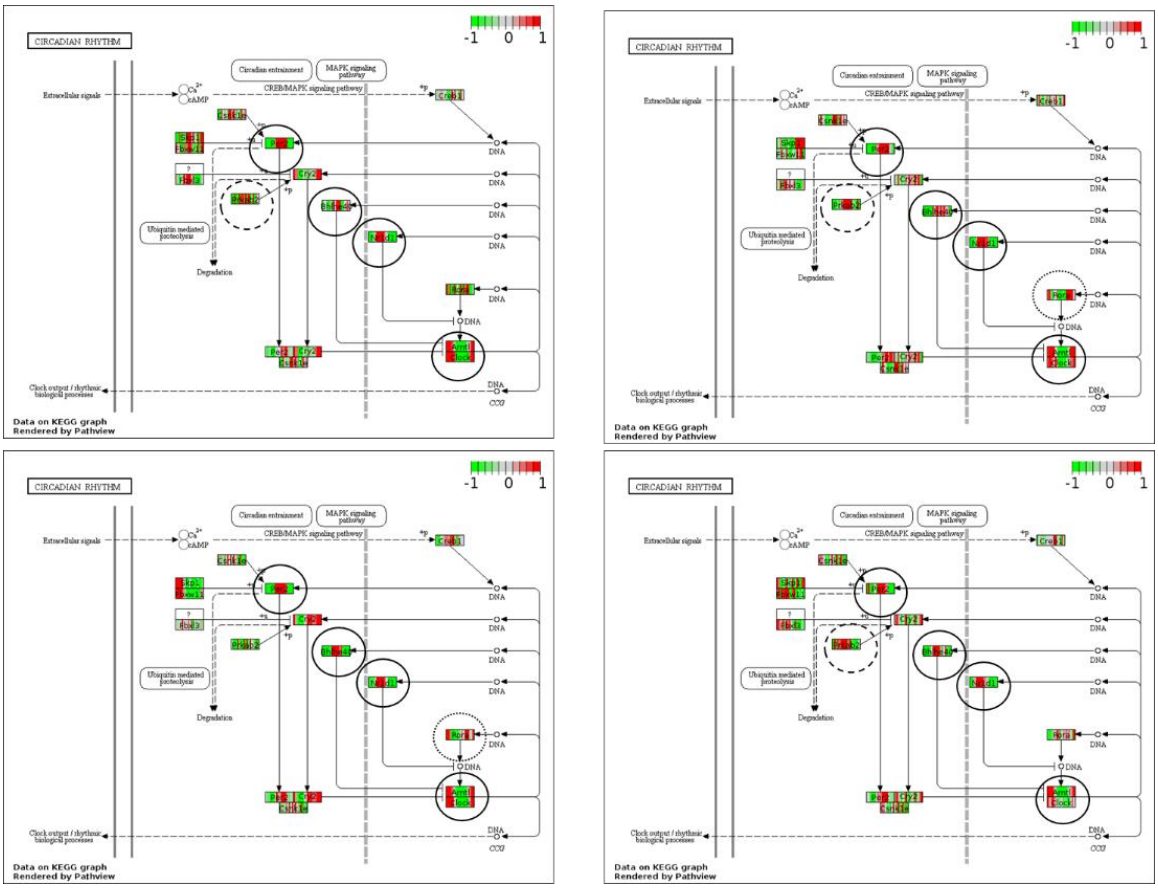

Figure 24 The circadian clock mechanism consists of cell-autonomous transcription-translation feedback loops that drive rhythmic 24-hour expression patterns of core clock components. Comparison of the corresponding pathways in (top) adipose, liver; (bottom) lung, muscle.

Peripheral circadian expression is regulated both globally by the central clock (SCN) delivering a uniform signal throughout the body (Pett, Kondoff et al. 2018), as well as locally by endogenous clock mechanisms of peripheral tissues (Panda, Antoch et al. 2002, Liu, Lewis et al. 2007, Mirsky, Liu et al. 2009, Doherty and Kay 2010). Interestingly, the peripheral clocks are coordinated across tissues, with major components of the clocks exhibiting aligned patterns of activity, as noted in Figure 24. Despite the peripheral clock machine being similar across tissues and the fact that all tissues are exposed to systemic levels of humoral signals, the perception and translation of these signals is dependent on each tissue, pointing to likely tissue-dependent

regulation (Pett, Kondoff et al. 2018). Therefore, the mechanism by which the tissue-specific regulation of the peripheral clocks is implemented may be the presence of tissue-specific transcription factors and translational/post-translational mechanisms, though as yet unknown (Nguyen, Almon et al. 2014, Yeung, Mermet et al. 2018). We have recently hypothesized that tissue-specific regulatory mechanisms are the likely drivers behind this type of tissue-specificity (Nguyen, Almon et al. 2014), whereas in (Korencic, Kosir et al. 2014) alternative models are suggested that could enable translation of common circadian signals to tissue-specific responses.

One of the key realizations of the analysis of the four rat tissues in the context of individual gene expression patterns was that tissues tend to coordinate gene expression is such a way that apparent dominant phases ("rush hours") within a tissue emerge (Mavroudis, DuBois et al. 2018). These emerging structures were presumed to indicate tissue-specific activity depending of each tissue's broader role in homeostasis. The patterns of individual gene expression, as noted in (Mavroudis, DuBois et al. 2018), appear concentrated in a tissue-specific manner, namely: in liver, the peak of activity was broadly observed during the active (dark) period; muscle and adipose exhibited a more uniformly distributed activity; and lung maintained high transcriptional activity during the active (light) period. Similar studies often identify and discuss events of increased activity focusing on transition periods characterized by peak expression, usually during transitions from dark to light period (Zhang, Lahens et al. 2014). However, when considering the dynamics at the pathway level, in other words in the context of a coordinated expression of functionally related genes, a more complex behavior emerges as it is not likely that a pathway will exhibit a pattern of activity indicative of "rush hours".

Rather, a group of functionally related genes coordinate their activities in a way that, potentially, optimizes the pathway's function. Some pathways may exhibit an overall dynamic indicative of a dominant peak expression phase, usually during the active/inactive transition. An example of that

is depicted in Figure 16, portraying the 24-hour dynamic fingerprint of TCA cycle in liver. The PAL analysis indicates the presence of a single dominant pattern, which is further decomposed into two broad gene sub-groups within the pathway: the dominant with expression peaking during the dark/light (ZT=0 h) transition, and a secondary with peak expression during the light/dark (ZT=12 h) transition. A mapping of the expression patterns onto the KEGG representation of the pathway enables us to allocate specific patterns across the pathway. This type of response is more in line with earlier studies that assign peak expression to specific points during the circadian cycle and by extension, following functional enrichment of the gene set, peak activity of the corresponding enriched pathway would be assumed at similar time intervals (Mavroudis, DuBois et al. 2018). Similar observations strictly based on gene expression patterns were also reported for diurnal animal where peak expression clustered around “dawn and dusk” (Mure, Le et al. 2018).

What is further observed for the overwhelming majority of pathways is that circadian gene expression profiles generate a cascade of events resulting in a distribution of information across the pathway throughout the light/dark periods. The example of mTOR signaling in liver (Figure 17) best exemplifies this pattern. The genes that comprise this signaling pathway are each characterized by their individual phase (location of peak expression), however, the activities “flow” through the pathway in a wave-like function. This is an important observation as it challenges the more traditional view of a circadian pattern defined primarily by the phase of the constituents. The PAL analysis indicates the emergence of multiple dominant profiles which reveal that the peak activity is not concentrated at specific time intervals, such as during the dark/light transition. Rather, each component of the pathway peaks at its own phase through the circadian cycle, but in such a way that the overall functional impact of the pathway is harmonized with the broader homeostasis goals.

Pathways may also manifest dynamics expressing a combination of the two patterns indicated earlier. For example, glycolysis/gluconeogenesis in liver (Figure 18) exhibits functional activity decomposed in two parts: elements of the pathway with peak activity during the light/dark transition period, as well as elements of the pathway exhibiting peak activity in the form of a cascade of events encompassing almost the entire dark (active) period. The decomposition of the intrinsic dynamics into three components (PALs) is a manifestation of this behavior.

The emergence of disparate patterns of functional activity is indicative of the likely distinct role that pathways play within a tissue as a function of the time-of-day. Figure 19 clearly depicts the distinct organization the mTOR and cysteine/methionine (CYS/MET) metabolism pathways in liver. Whereas mTOR exhibits a uniform distribution of phases of individual genes, the CYS/MET pathway indicates a rush of activity for part of the pathway during the light/dark transition and for another part of the pathway mostly during the dark/light transition. The distribution of activity is also clearly indicated in the corresponding pathway schematics (Figure 20).

Comparison of liver, gastrocnemius muscle, lung, and adipose tissue gene expression reveals that clock-controlled genes exhibit tissue-specific expression patterns that group by functional enrichment including genes relevant to metabolism, transcription/translation, and signaling events that peaked at different times across tissues (Mavroudis, DuBois et al. 2018). Mapping of expressed genes onto KEGG pathways yielded evidence of robust circadian activity in pathways related to immune and signaling functions, metabolism, and regulation of cellular events including transcription, translation, protein processing and packaging for all tissues. The lung and liver datasets yielded the greatest number of significant pathways, a finding consistent with earlier works that have also determined the, relative to liver and lung, smaller number of circadian regulated genes in other tissues (Zhang, Lahens et al. 2014, Mavroudis, DuBois et al.

2018). Liver tissue is established as a primary target of metabolism and circadian regulation, so robust circadian activity in the pathway analysis is expected in pathways related to metabolism and the immune system's inflammatory response (Almon, Yang et al. 2008, Yang, Almon et al. 2008, Ovacik, Sukumaran et al. 2010, Nguyen, Almon et al. 2014). Circadian regulation is also present in lung tissue an understanding of which is essential to the treatment of lung diseases, such as asthma (Gibbs, Beesley et al. 2009). Despite a relatively small list of significant circadian pathways identified in adipose and muscle, these tissues exhibit circadian regulation and are influenced by drug administration (Almon, DuBois et al. 2004, Almon, Dubois et al. 2005, Almon, DuBois et al. 2007, Almon, Yang et al. 2008, Nguyen, Almon et al. 2014).

In terms of the tissue-specific circadian activity, we observe that while tissues share similarities, they also express individual characteristics. As indicated in Figure 23, liver is undoubtedly the most metabolically-driven tissue, followed by muscle. The genetic and cellular information processing footprint during the day appears to be more uniform across tissues. Interestingly, the lung appears to be substantially more active within signaling pathways, an observation that is supported by the knowledge that the lung is an organ that constantly interacts with the environment and is exposed to foreign materials.

Earlier analyses that focused exclusively on liver-specific gene expression circadian patterns (Almon, Yang et al. 2008) note the importance of oscillating genes related to metabolism and emphasize the importance of individual genes peaking at specific times. However, the pathway view of the dynamics communicates different information. The genes composing the metabolic pathways do not exhibit synchronized expression patterns. On the contrary, activity across the pathway proceeds in a wave-form, with different genes peaking at different point in time. Therefore, rhythmic characteristics of individual genes do not properly describe the overall dynamics of the pathway.

Lung is an active organ, constantly interacting with the environment. We observe that significant circadian activity is observed in signaling pathways (Figure 23, ST 7). Unlike liver, lung appears more consistent with earlier observations on the nature of gene dynamics, where lung pathways appear to have phase distribution across the 24-h period, as well as activity concentrated during the early phases of the light (rest) period (Sukumaran, Jusko et al. 2011). This is likely related to the circadian characteristics of pulmonary function which generally exhibit lower activity during the rest period, likely purposed to optimize use of resources.

Signaling and cellular processing pathways appear to be the most active during the 24-h period, for adipose tissue. Adipose tissue also appears to exhibit complex dynamics characteristics, with a concentration of coherent pathway activity during the dark (active) period, consistent with earlier observations (Sukumaran, Xue et al. 2010). While adipose tissue did not exhibit coherent circadian metabolic activity, adipose appears to be active in signaling and cellular processes, as well as the regulation of its immune response. This includes the regulation of chemokines and TNF signaling. This was an interesting observation as it is well established that low-grade chronic inflammation in adipose is a hallmark of obesity (Xu, Barnes et al. 2003, Heilbronn and Campbell 2008, Cooke, Connaughton et al. 2016).

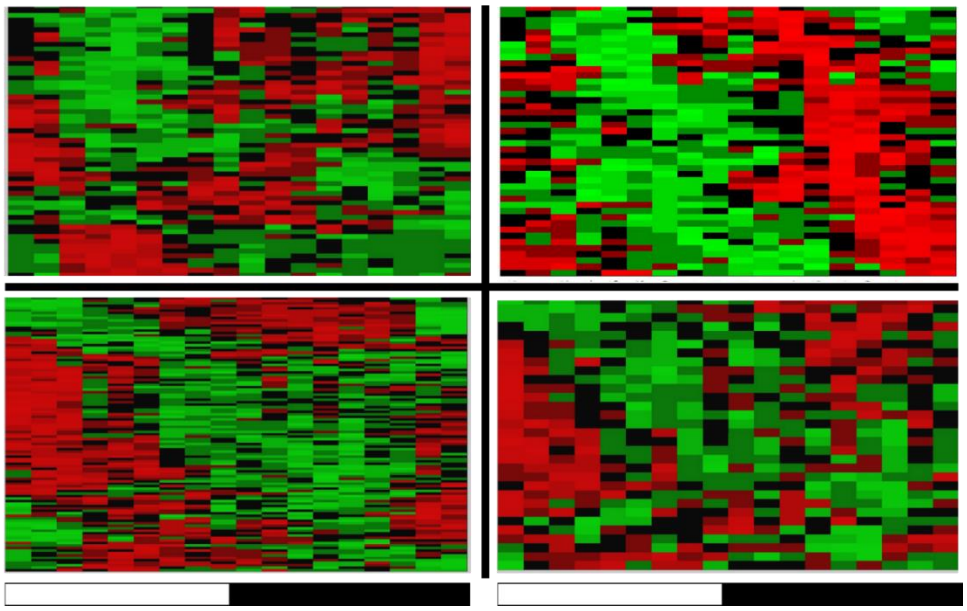

Figure 25 Activity maps for RNA transport (top: adipose - liver; bottom: lung - muscle)

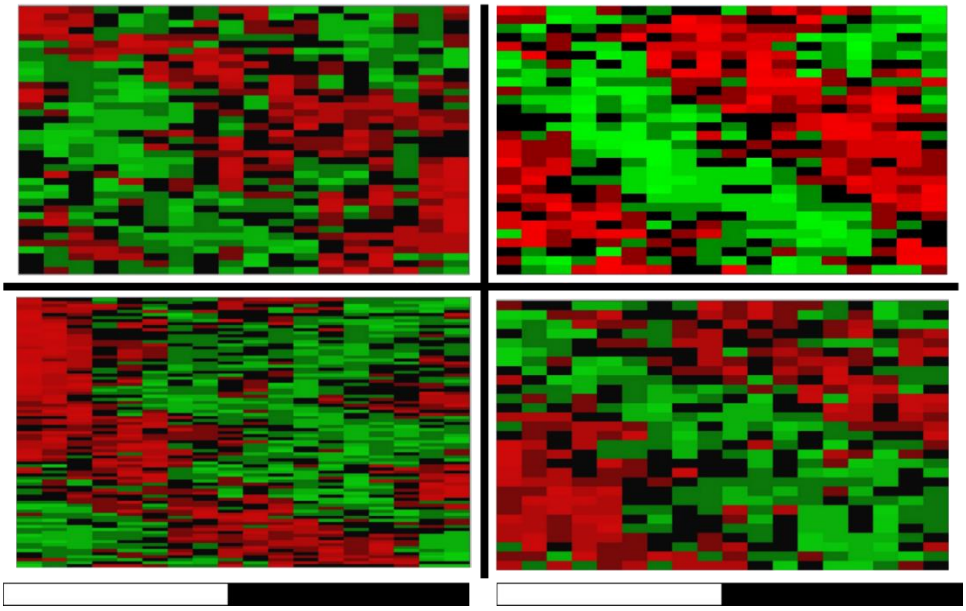

Figure 26 Activity maps for Insulin signaling (top: adipose – liver; bottom: lung – muscle)

As noted in Figure 23, the processing of cellular and genetic information appears to be an active function in all tissues. However, the processing of this information appears to take different forms in each tissue. Consider the example of RNA transport between the nucleus and the cytoplasm

(Figure 25). In liver, activity appears prominent during the active (dark) period. In adipose the activity appears more uniformly distributed throughout the day. Alternatively, lung again exhibits increased activity during the early stages on the light (rest) period and again during the light/dark transition, whereas muscle exhibits activity primarily during the early light period. These observations indicate that each tissue attempts to optimize the dynamics of their corresponding cellular functions in a tissue-specific manner. The cross-tissue differences and similarities are easily observed. Figure 26 depicts the emergent dynamics of the insulin signaling pathway in all four tissues. Liver and muscle appear to be active during the transition (dark/light and light/dark) periods, adipose expresses dynamics with a wave of activity during the 24-h period, and lung exhibits activity during the early hours of the light (rest) period and again during the light/dark (inactive/active) transition. However, the arginine and proline metabolism pathway in liver (Figure 27) exhibits characteristically different dynamics in liver and muscle, between which the periods of activity/inactivity seem opposite.

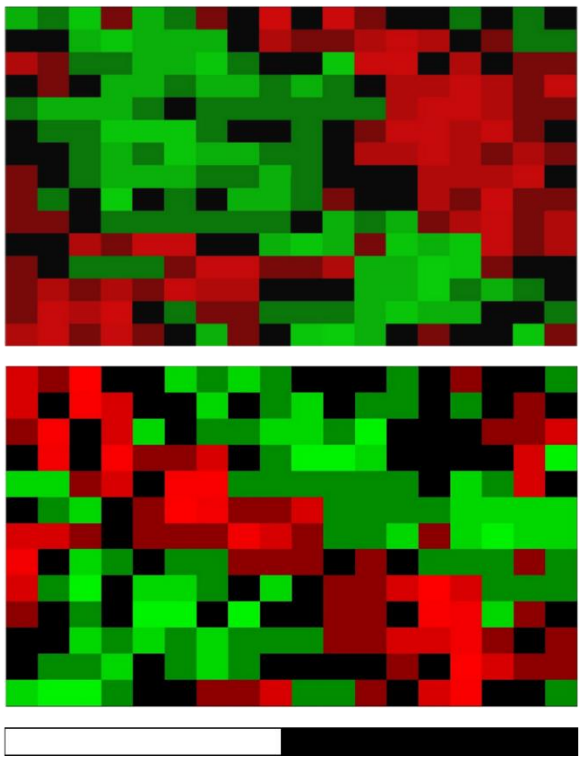

Figure 27 Activity maps for Arginine Proline Metabolism (top: liver; bottom: muscle)

Finally, it should be noted that the lack of a plethora of metabolic and signaling pathways exhibiting coordinated circadian rhythmicity at the pathway level in muscle and adipose tissues, in comparison to lung and liver, does not point to a lack of circadian components within those tissues, or the criticality of circadian regulation. Instead, it likely indicates a lack of strong circadian coordination at the pathway level. However, this should not diminish the importance of individual components. Even though it is recognized that clock-controlled genes in different tissues have little overlap in terms of peak phases (Korencic, Kosir et al. 2014), we hypothesize that analysis of individual genes does not necessarily convey coordination of biological and physiological functions. Even though individual components of a broader function may differ, their integrated response may communicate coordination.

4.4 Comparison of Endogenous Circadian Activity Across Multiple Species

4.4.1 Motivation

Comparative (translational) research is highly dependent on rat and mouse models in that we first seek to understand a process in these organisms before extending to high-order organisms, including humans (Bryda 2013).Rats and mice are historically used because of their economic advantages including their relatively (as compared to larger experimental organisms such as pigs, dogs, and primates) small living space requirements and size, rapid gestation period, large number of offspring, rapid development and short life spans (Bryda 2013). They are valued in contemporary scientific research for these economic advantages as well as their ability to be genetically modified through transgenic, knock-out, and knock-in techniques (Consortium 2002, Bryda 2013). Rat and mouse share sufficiently high genomic relationships with each other, and with humans, to justify retaining their place as primary pre-clinical model organisms (Consortium 2002, Consortium 2004).

Despite the advantages of these model organisms, translation from pre-clinical rodent studies to successful clinical studies in humans has low success rate (Denayer, Stöhr et al. 2014). There are many reasons for this. Many drug studies fail in Phase II and Phase III clinical trials because lack of characterization of drug targets (lack of sufficient translational research) leads to reduced drug efficacy (Denayer, Stöhr et al. 2014). This failure is not necessarily the result of a lack of similarity between human and rodent models, but of a lack of understanding of the function of the selected animal model (Denayer, Stöhr et al. 2014, Ellenbroek and Youn 2016). Selection of the correct animal model for your pre-clinical research is critical. As previously stated, rodent organisms share sufficient genetic similarity with humans to merit their use as pre-clinical model organisms (Consortium 2002, Bryda 2013). Further, the ability to genetically modify rat and mouse models in contemporary biomedical research is effectively equal, thus it becomes

necessary to focus on the functional differences in model organism in order to support successful translational research (Ellenbroek and Youn 2016).

Discussed in detail in Chapter 1, multifactorial conditions (diabetes, cancers, rheumatoid arthritis, metabolic syndrome, and other chronic inflammatory conditions and auto-immune diseases) require a systems pharmacology approach, a characterization of physiology at the systems level, in order to be understood and addressed. Circadian regulation drives a diverse set of biological processes and disruption of circadian regulation leads to and/or exacerbates these multifactorial conditions (Mavroudis, Scheff et al. 2013, Bae and Androulakis 2018, Rao, Scherholz et al. 2018, Bae and Androulakis 2019, Rao and Androulakis 2019, Scherholz, Schlesinger et al. 2019). It is important, therefore, to focus our investigation on endogenous circadian activity, and see how it compares across model organisms. Such investigations inform selection of appropriate animal models for investigating multifactorial disease.

Thus, we seek to investigate the underlying endogenous circadian activity within this data to better understand how drug-free and intact model organisms' function in a state of health. In this investigation, we endeavor to characterize and compare mouse and rat model organisms at the systemic level using our pathway-based analysis approach (Acevedo, Berthel et al. , Acevedo, DuBois et al.). We believe that such an investigation will help direct pre-clinical decision-making relevant to translational research.

4.4.2 Additional Pre-processing Steps Enables Comparison Across Species

Extra pre-processing steps needed to be taken so that pathway activity dynamics could be appropriately compared across species. This is not necessarily true if we were to extend into the space of indirect modeling as with the MPL research in previous chapters (Acevedo, Berthel et al. , Acevedo, DuBois et al.). Such steps include comparing temporal expression across a consistent

set of sample times between experiments. To achieve this, the mouse and rat data were additionally processed as follows:

- The mouse data was sampled every 2 h over a 48-h period. Expression data corresponding to the same circadian time was averaged together. For example, gene expression from the two microarrays sampled at CT18 on subsequent days were averaged. This resulted in 12 time points of data (CT0, 2, 4, 6, 8, 10, 12, 14, 16, 18, 20, 22) used for subsequent analysis of expression over a single day.
- The rat data was collected within an experiment that lasted a single day. In order to coordinate with mouse expression data time points, only data from the following time points were considered for analysis: 0.25 h, 2, 4, 6, 8, 10, 12.25, 14, 16, 18, 20, 22.

4.4.3 Preliminary Results

Application of the pathway-based framework (Chapter 1) to temporal transcriptomic expression data enabled the characterization of genome-wide circadian dynamics at the level of functional groupings of genes across multiple tissues in mouse (liver, lung, adipose, muscle). As with our analysis in rat above, our aim is to identify how individual genes come together to generate orchestrated rhythmic patterns and how these may vary within and across tissues. We further extend this discussion to compare pathway dynamics across mouse and rat, revealing interesting tissue-specific and organism-specific dynamics.

After mapping the transcriptomic data onto mouse-relevant pathways, fractional occupancy analysis, and pathway activity analysis, pathways emerged as significant for each tissue (all p-values ≤ 0.05). We observe structured patterns of activity over the course a 24-hour period in mouse data, as we did in rat. A comprehensive list of the significant pathways that emerged from each tissue from the mouse data is presented in the Appendix (ST 8). In summary, the tissues are characterized as follows:

Each of the tissues were processed using the same Affymetrix platform (MoGene 1.0 ST) which has 33,556 probes. Pre-processing of data with EDGE yielded 4,831 probes that were differentially expressed in liver, 6,322 in adipose, 6,036 in lung, and 818 in muscle. It is unclear why muscle tissue yielded such low relative return given a consistent analysis across all tissues. Liver tissue yielded 49 pathways primarily encompassing carbohydrate and lipid metabolism pathways as well as signaling functions including AMPK, Fox-O, mTOR, and TNF signaling pathways. The lung tissue data yielded 28 significant pathways with comparable representation of pathways related to signaling and metabolic pathways including MAPK, mTOR, PI3K-Akt, TNF, VEGF, and insulin signaling. Adipose tissue yielded 28 significant pathways similarly including signaling pathways such as MAPK, mTOR, GnRH, glucagon, and regulation of lipolysis in adipocytes pathways. Muscle tissue yielded the smallest number of significant pathways (12 pathways) which follows from its relatively small number of differentially expressed genes. Some pathways that did emerge as significant were primarily signaling-related including Jak-STAT, AMPK, and cGMP signaling. A comprehensive list of significant pathways in mouse is included in the Appendix (ST 8) and an overview of the broad categories of pathway representation in mouse tissues is presented in Figure 28.

Pathways resulting from mouse analysis yielded dynamic patterns similar to those observed in rat tissue (Figure 29). Liver tissue exhibits two dominating dynamics across its significant pathway set: cascading circadian expression exemplified by AMPK and fatty acid metabolism pathways, as well as non-cascading circadian dynamics exemplified by the oxidative phosphorylation pathway. Lung tissue cascading circadian activity in effectively all of the pathways that emerge as significant. Adipose yields complexity observed earlier in rat, both cascading circadian dynamics (AMPK signaling) and pathways that exhibit both cascading and non-cascading

circadian expression as exemplified by cAMP, Rap1, and Ras signaling pathways. In the sparse set of significant pathways in muscle, we observe strictly non-cascading circadian expression.

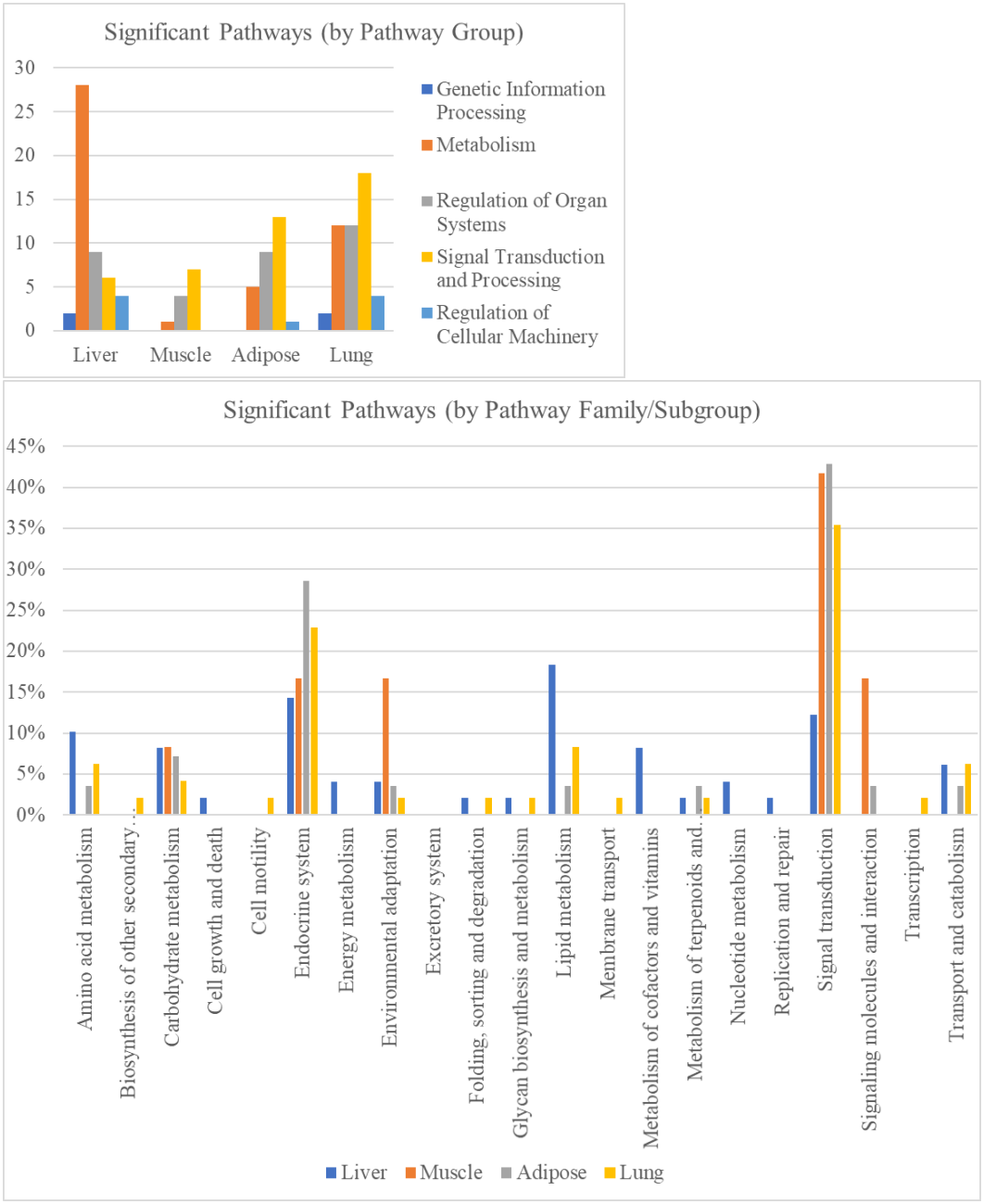

Figure 28 Distribution of pathways with robust circadian activity across tissues in mouse. Pathways are grouped by the (top) group and (bottom) subgroup (family) labels (ST 8). The percentages (bottom) indicate the fraction of total pathways for the corresponding tissue.

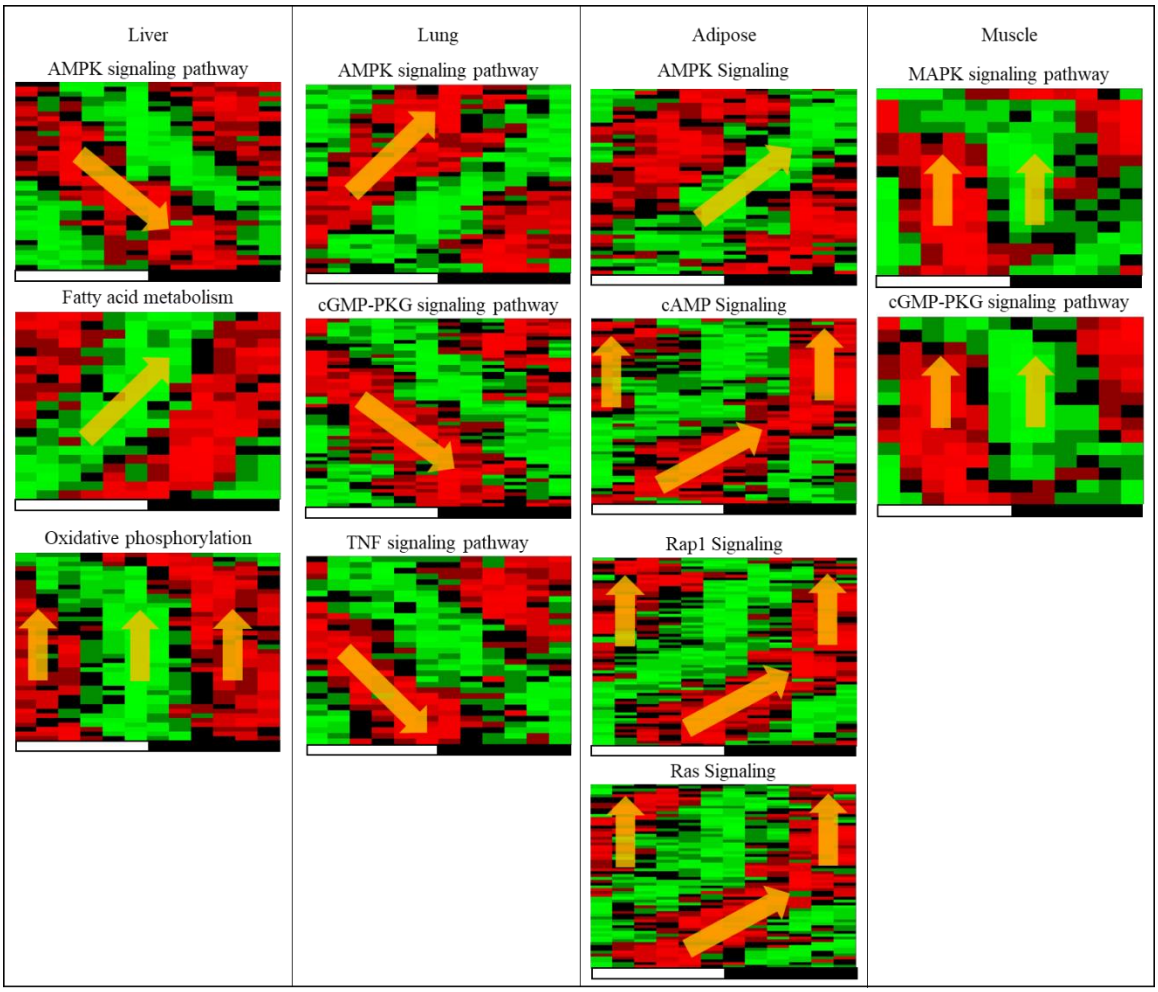

Figure 29 Examples of pathway dynamics that dominate each mouse tissue.

Comparison Across Mouse and Rat Dynamics

Even as we develop our preliminary analysis into the dynamics independently within mouse data, we cannot help but observe similarities and differences in significant pathway content and dynamics between the two model organisms. When considering the distribution of significant pathways categorized by pathway family, we observe that pathways related to signal transduction and endocrine regulation dominate for both mouse and rat tissues (Figure 23 and Figure 28, bottom). Rat tissues exhibit greater proportional representation across certain pathway families including amino acid metabolism, cellular development, and transcriptional events (folding,

sorting, and degradation pathway family). Mouse tissue reports relatively little to no representation for most of these categories. Such observations may speak to a reduced complexity in the physiology of mouse as compared to rat.

Comparison within tissue between organisms reveals that metabolic pathways dominate in liver and signaling pathways dominate in lung for both mouse and rat (Figure 23 and Figure 28, top). Adipose tissues also have comparable representation in both organisms with respect to signaling pathways. However, muscle tissue representation is not consistent for most pathway groups and subgroups between tissues. This is likely due to the low yield from the mouse muscle data. If reliable and not an artifact of experimental error, such observations indicate significant differences in the muscle function between mouse and rat which may inform model organism selection for conditions related to muscle.

We look within distributions of significant pathways across organisms and tissues to analyze circadian pathway dynamics in example pathways. We observe that rat and mouse both expression cascading and non-cascading circadian expression. However, dynamics are not always conserved across organisms or tissues. For example, the mTOR signaling pathway is significant across lung and adipose in mouse and rat but the cascading circadian expression observed in mouse is not observed in rat. Instead, we observe non-cascading circadian expression (Figure 30). The mTOR signaling pathway is a component of various cellular processes (cell metabolism, growth, proliferation and survival) (Laplante and Sabatini 2009). This pathway is observed to be deregulated in humans when certain cancers and type 2 diabetes develops (Sakaguchi, Isono et al. 2006, Laplante and Sabatini 2009). For these and other conditions (solid tumor development and rheumatoid arthritis), mTOR inhibitors, such as rapamycin, are used to stem disease development (Sakaguchi, Isono et al. 2006, Laplante and Sabatini 2009, Li, Brown et al. 2010). Such conditions are multifactorial and thus have consequences across multiple tissues, motivating the

need to characterize this and other relevant pathways across multiple tissues and the model organisms in which these diseases are studied.

The cAMP signaling pathway (Figure 31) is also significant is identical tissues across rat and mouse. This is an example of a pathway in which dynamics are conserved across organisms but not across tissues; cascading circadian expression is observed within liver for mouse and rat, but non-cascading circadian expression is observed within lung for both organisms. The cAMP pathway is an intracellular secondary messenger activated in response to extracellular ligand action and regulated many downstream targets downstream including protein kinases, transcription factors, and repressors which modulate metabolic functions and adaptive immune functions (Raker, Becker et al. 2016). Thus, it is targeted pharmacologically for its immunoregulatory effects within autoimmune and inflammatory conditions including psoriasis, lupus, neurodegenerative disorders, and heart disease (Pierre, Eschenhagen et al. 2009, Raker, Becker et al. 2016). Targeting of the cAMP pathway is not completely characterized and thus merits further investigation into its tissue-specific and organisms-specific effects (Pierre, Eschenhagen et al. 2009). Current scientific understanding has established that therapies which generally enhance cAMP signaling reduce immune response while suppression of cAMP signaling is immunostimulatory (Pierre, Eschenhagen et al. 2009, Raker, Becker et al. 2016).

There also exist examples of pathways who are consistent in their dynamics across organisms and tissues. The AMPK signaling pathway (Figure 32) exhibits cascading circadian expression in both lung and adipose for both rat and mouse. Balancing nutrient supply with energy demand is regulated by the AMPK signaling pathway (Choi, Savage et al. 2007, Nath, Khan et al. 2009, Viollet, Horman et al. 2010). Accordingly, this pathway is responsible for the integration of nutritional and hormonal signals and, when targeted for suppression in muscle and liver tissue, is reported to increase rates of fatty acid oxidation leading to increased energy use and reduced

adipose content (Choi, Savage et al. 2007, Viollet, Horman et al. 2010). Components of this pathway have thus been targeted for activation to treat conditions such as multiple sclerosis (Nath, Khan et al. 2009) and for suppression to treat type II diabetes and obesity (Choi, Savage et al. 2007). As with previously discussed pathways, such pervasive regulatory influence of the AMPK pathways merits additional investigation into the dynamics of this pathway across tissues and within model organisms.

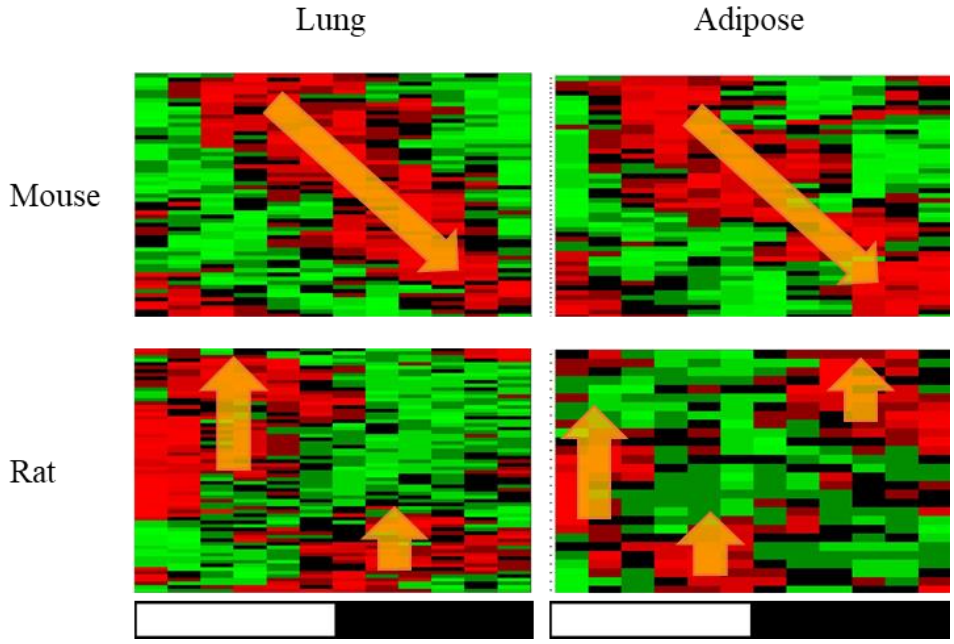

Figure 30 mTOR signaling pathway within adipose and lung in rat and mouse. An example of tissue-specific dynamics that are not conserved across organisms, but which are conserved across tissues.

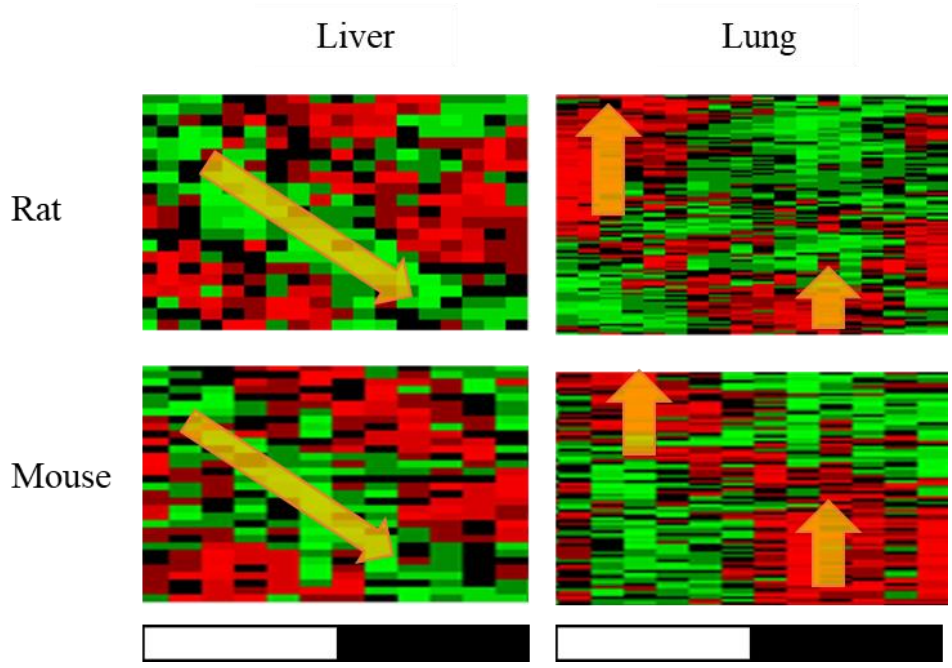

Figure 31 cAMP signaling pathway within liver and lung in rat and mouse. An example of tissue-specific dynamics conserved across organisms.

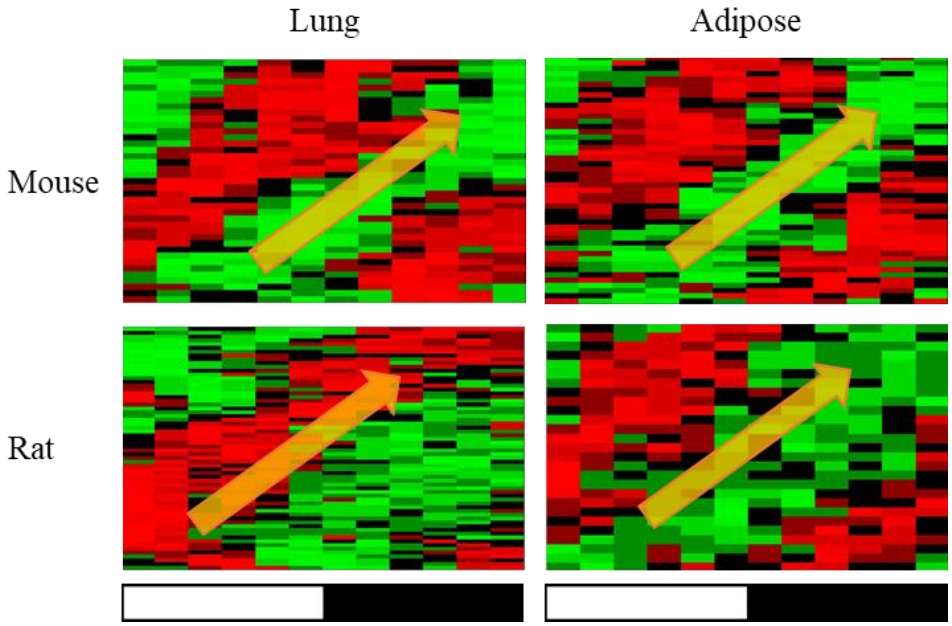

Figure 32 AMPK signaling pathway within adipose and lung in rat and mouse. An example of tissue-specific dynamics conserved across organisms and tissues.

4.5 Concluding Remarks

In the above investigations our pathway-based analysis technique enables the meta-analysis of tissue-specific transcriptomic data by assessing the emergence of coherent dynamic patterns at the level of functionally-related gene groupings (KEGG pathways). We focused on unravelling the circadian dynamic patterns of liver, lung, muscle, and adipose within mouse and rat, two essential pre-clinical research organisms.

One of the defining observations of our analysis of the four tissues is that when considering the coherent or synergistic dynamics of functionally related groupings of genes, the dynamic picture of the circadian patterns becomes more nuanced than the one emerging when considering independent gene expression patterns. We identified the need for appropriate coordination within a pathway, resulting in complex patterns of activity cooperating to perform homeostatic function. The comparison of pathway dynamics within and across organisms point to likely differences in coordination mechanisms and the possible existence of critical mediators whose circadian rhythms are of paramount importance. Further, these results indicate that “rush hour” activity may not necessarily be present at the pathway level, but rather gene activity appears concentrated in a way that optimizes the circadian role of the pathway.

The investigation into mouse endogenous circadian expression and its comparison with dynamics in rat remains ongoing. Presented are preliminary results that reveal evidence of tissue-specific and organism-specific dynamics within signaling and metabolic pathways whose disruption facilitates disease treatment and development. We seek to extend our analysis to fully characterize the differences between the essential model organisms enabling future translational research.

Chapter 5: Conclusion

In the enclosed investigations we present a pathway-based meta-analysis approach integrated with multivariate decomposition techniques (Chapter 2) designed to extract physiological meaning from high-throughput omics data appropriately by analyzing physiological data from a functional and feature-based perspective and with consideration of the multivariate complications of interdependent expression data. We apply this framework to characterize temporal drug effects across multiple tissues and multiple dosing regimens (Chapters 3) and to understand endogenous circadian expression again across multiple tissues as well as across essential pre-clinical animal models: mouse and rat (Chapter 4).

In this dissertation, we seek to highlight how the pathway-based framework enables integration of information across experimental platforms, time scales, dosing regimens, tissues, and organisms. Such comparisons are necessary for the extraction of all possible meaning from the wealth of existing data stored across databases globally and for the development of research that is translatable between organisms.

The framework presented above is a translational research tool, designed modularly to anticipate its use within other omics levels and with use of other pathway databases. We anticipate its use in comparing functional response within additional tissues (Almon, Lai et al.) and organisms, including humans (Wu, Ruben et al.). Characterization of human response is difficult because we cannot sample from humans in the same manner that we can from animal models. However, blood and skin samples are tissues that facilitate longitudinal sampling within humans (Wu, Ruben et al.). (Wu, Ruben et al.) collected skin samples at 4 time points over a 24 h period in their search for potential epidermal biomarkers, focusing their analysis on clock genes. We see additional translational research potential in this data set and have begun to expand on Wu et al.'s analysis by applying our pathway-based framework to this data. Preliminary functional

enrichment already reveals significant metabolic, signaling, and cell regulatory pathway activity in human pathways in KEGG (Table 7). We anticipate expanding on this preliminary investigation and analysis of temporal plasma data (Wu, Ruben et al.) with our pathway-based framework will provide additional translational research merit.

Table 7 Significant pathways that emerged from application of pathway-based analysis framework (Chapter 2) to temporal transcriptomic data capturing endogenous expression in human skin (Wu, Ruben et al. 2018).

Subgroup (Family)	**Pathway Name**
Cell growth and death	Apoptosis
	Cell cycle
	p53 signaling pathway
Cell motility	Regulation of actin cytoskeleton
Transport and catabolism	Endocytosis
	Lysosome
Signal transduction	ErbB signaling pathway
	HIF-1 signaling pathway
	Hippo signaling pathway
	MAPK signaling pathway
	Notch signaling pathway
	Sphingolipid signaling pathway
	TNF signaling pathway
	VEGF signaling pathway
Folding, sorting and degradation	Protein processing in endoplasmic reticulum
Carbohydrate metabolism	Carbon metabolism
Glycan biosynthesis and metabolism	Glycosylphosphatidylinositol (GPI)-anchor biosynthesis
Lipid metabolism	Fatty acid metabolism
Metabolism of terpenoids and polyketides	Terpenoid backbone biosynthesis
Endocrine system	Prolactin signaling pathway
	Thyroid hormone signaling pathway

The pathway-based analysis framework can be further improved with an expansion into topological information. Although we already consider pathway topology within our analysis (Figure 20 and Figure 22), topological information is not incorporated into the pathway scoring

(fractional coverage and pathway activity statistics). However, topological pathway-based analyses enhance functional understanding (Lima-Mendez and van Helden 2009, Yeung and Naef 2018) and future versions of the framework would benefit from incorporating such information. Within our endogenous circadian expression analyses in Chapter 4, we discussing cascading dynamics across pathways, a discussion which would be enhanced if discussion of movement across a pathway was accompanied by a topologically relevant statistic calculated from analysis of data-populated pathway schematics such as presented in Figure 20 and Figure 22.

Acknowledgement of Publications

This dissertation contains significant portions of the following publications:

Acevedo, A., Berthel, A., DuBois, D., Almon, R. R., Jusko, W. J., & Androulakis, I. P. (2019). Pathway-Based Analysis of the Liver Response to Intravenous Methylprednisolone Administration in Rats: Acute Versus Chronic Dosing. Gene regulation and systems biology, 13 (2019): 1177625019840282.

Acevedo A, DuBois DC, Almon RR, Jusko WJ, Androulakis IP. "Pathway-based Analysis of Skeletal Muscle Response to Intravenous Methylprednisolone (MPL) Administration in Rats: Acute versus Chronic Dosing." Physiological Genomics. (submitted)

I, Alison Acevedo, am the original author of this material.

References

Acevedo, A., A. Berthel, D. DuBois, R. R. Almon, W. J. Jusko and I. P. Androulakis (2019). "Pathway-Based Analysis of the Liver Response to Intravenous Methylprednisolone Administration in Rats: Acute Versus Chronic Dosing." Gene Regulation and Systems Biology **13**: 1177625019840282.

Acevedo, A., D. DuBois, R. R. Almon, W. J. Jusko and I. P. Androulakis (2019). "Pathway-Based Analysis of the Muscle Response to Intravenous Methylprednisolone Administration in Rats: Acute Versus Chronic Dosing." Physiological Genomics (submitted).

Albrecht, U. (2012). "Timing to perfection: the biology of central and peripheral circadian clocks." Neuron **74**(2): 246-260.

Almon, R. R., D. C. DuBois, E. H. Brandenburg, W. Shi, S. Zhang, R. M. Straubinger and W. J. Jusko (2002). "Pharmacodynamics and pharmacogenomics of diverse receptor-mediated effects of methylprednisolone in rats using microarray analysis." Journal of pharmacokinetics and pharmacodynamics **29**(2): 103-129.

Almon, R. R., D. C. Dubois, J. Y. Jin and W. J. Jusko (2005). "Pharmacogenomic responses of rat liver to methylprednisolone: an approach to mining a rich microarray time series." The AAPS journal **7**(1): E156-E194.

Almon, R. R., D. C. Dubois, J. Y. Jin and W. J. Jusko (2005). "Temporal profiling of the transcriptional basis for the development of corticosteroid-induced insulin resistance in rat muscle." J Endocrinol **184**(1): 219-232.

Almon, R. R., D. C. DuBois, J. Y. Jin and W. J. Jusko (2005). "Temporal profiling of the transcriptional basis for the development of corticosteroid-induced insulin resistance in rat muscle." Journal of endocrinology **184**(1): 219-232.

Almon, R. R., D. C. DuBois and W. J. Jusko (2007). "A microarray analysis of the temporal response of liver to methylprednisolone: a comparative analysis of two dosing regimens." Endocrinology **148**(5): 2209-2225.

Almon, R. R., D. C. DuBois, W. H. Piel and W. J. Jusko (2004). "The genomic response of skeletal muscle to methylprednisolone using microarrays: tailoring data mining to the structure of the pharmacogenomic time series." Pharmacogenomics **5**(5): 525-552.

Almon, R. R., D. C. DuBois, Z. Yao, E. P. Hoffman, S. Ghimbovschi and W. J. Jusko (2007). "Microarray analysis of the temporal response of skeletal muscle to methylprednisolone: comparative analysis of two dosing regimens." Physiol Genomics **30**(3): 282-299.

Almon, R. R., W. Lai, D. C. DuBois and W. J. Jusko (2005). "Corticosteroid-regulated genes in rat kidney: mining time series array data." American Journal of Physiology-Endocrinology and Metabolism **289**(5): E870-E882.

Almon, R. R., E. Yang, W. Lai, I. P. Androulakis, D. C. DuBois and W. J. Jusko (2008). "Circadian variations in rat liver gene expression: relationships to drug actions." J Pharmacol Exp Ther **326**(3): 700-716.

Almon, R. R., E. Yang, W. Lai, I. P. Androulakis, S. Ghimbovschi, E. P. Hoffman, W. J. Jusko and D. C. DuBois (2008). "Relationships between circadian rhythms and modulation of gene expression by glucocorticoids in skeletal muscle." American Journal of Physiology-Regulatory, Integrative and Comparative Physiology **295**(4): R1031-R1047.

Almon, R. R., E. Yang, W. Lai, I. P. Androulakis, S. Ghimbovschi, E. P. Hoffman, W. J. Jusko and D. C. DuBois (2008). "Relationships between circadian rhythms and modulation of gene expression by glucocorticoids in skeletal muscle." American Journal of Physiology-Regulatory Integrative and Comparative Physiology **295**(4): R1031-R1047.

Alter, O., P. O. Brown and D. Botstein (2000). "Singular value decomposition for genome-wide expression data processing and modeling." Proceedings of the National Academy of Sciences **97**(18): 10101-10106.

Amadoz, A., M. Hidalgo, C. Cubuk, J. Carbonell-Caballero and J. Dopazo (2018). "A comparison of mechanistic signaling pathway activity analysis methods." Brief Bioinform.

Andrews, R. C. and B. R. Walker (1999). "Glucocorticoids and insulin resistance: old hormones, new targets." Clinical science **96**(5): 513-523.

Androulakis, I. P. (2016). "Quantitative systems pharmacology: a framework for context." Current pharmacology reports **2**(3): 152-160.

Androulakis, I. P., E. Yang and R. R. Almon (2007). "Analysis of time-series gene expression data: methods, challenges, and opportunities." Annu Rev Biomed Eng **9**: 205-228.

Aoki, K. F. and M. Kanehisa (2005). "Using the KEGG database resource." Curr Protoc Bioinformatics **Chapter 1**: Unit 1 12.

Ayyar, V. S., R. R. Almon, D. C. DuBois, S. Sukumaran, J. Qu and W. J. Jusko (2017). "Functional proteomic analysis of corticosteroid pharmacodynamics in rat liver: Relationship to hepatic stress, signaling, energy regulation, and drug metabolism." Journal of proteomics **160**: 84-105.

Bader, G. D., M. P. Cary and C. Sander (2006). "Pathguide: a pathway resource list." Nucleic Acids Res **34**(Database issue): D504-506.

Bae, S.-A. and I. P. Androulakis (2018). "Mathematical Analysis of Circadian Disruption and Metabolic Re-entrainment of Hepatic Gluconeogenesis: The intertwining entraining roles of light and feeding." American Journal of Physiology-Endocrinology and Metabolism **314**(6): E531-E542.

Bae, S.-A. and I. P. Androulakis (2019). "Mathematical modeling informs the impact of changes in circadian rhythms and meal patterns on insulin secretion." American Journal of Physiology-Regulatory, Integrative and Comparative Physiology.

Ballard, P. L., J. D. Baxter, S. J. Higgins, G. G. Rousseau and G. M. Tomkins (1974). "General presence of glucocorticoid receptors in mammalian tissues." **94**(4): 998-1002.

Ballard, P. L., J. D. Baxter, S. J. Higgins, G. G. Rousseau and G. M. Tomkins (1974). "General presence of glucocorticoid receptors in mammalian tissues." Endocrinology **94**(4): 998-1002.

Barnes, P. J. (1998). "Anti-inflammatory actions of glucocorticoids: molecular mechanisms." Clinical science **94**(6): 557-572.

Bishehsari, F., F. Levi, F. W. Turek and A. Keshavarzian (2016). "Circadian Rhythms in Gastrointestinal Health and Diseases." Gastroenterology **151**(3): e1-5.

Bodine, S. C. and J. D. Furlow (2015). Glucocorticoids and skeletal muscle. Glucocorticoid Signaling, Springer**:** 145-176.

Boudinot, F. D., R. D'Ambrosio and W. J. Jusko (1986). "Receptor-mediated pharmacodynamics of prednisolone in the rat." **14**(5): 469-493.

Boudinot, F. D., R. D'Ambrosio and W. J. Jusko (1986). "Receptor-mediated pharmacodynamics of prednisolone in the rat." Journal of pharmacokinetics and biopharmaceutics **14**(5): 469-493.

Bryda, E. C. (2013). "The Mighty Mouse: the impact of rodents on advances in biomedical research." Missouri medicine **110**(3): 207.

Buhr, E. D. and J. S. Takahashi (2013). "Molecular components of the Mammalian circadian clock." Handb Exp Pharmacol(217): 3-27.

Buijs, R. M., C. G. van Eden, V. D. Goncharuk and A. Kalsbeek (2003). "The biological clock tunes the organs of the body: timing by hormones and the autonomic nervous system." J Endocrinol **177**(1): 17-26.

Burri, L., G. H. Thoresen and R. K. Berge (2010). "The role of PPAR activation in liver and muscle." PPAR research **2010**.

Campos-Ferraz, P. L., T. Bozza, H. Nicastro and A. H. Lancha Jr (2013). "Distinct effects of leucine or a mixture of the branched-chain amino acids (leucine, isoleucine, and valine) supplementation on resistance to fatigue, and muscle and liver-glycogen degradation, in trained rats." Nutrition **29**(11-12): 1388-1394.

Caporaso, J. G., J. Kuczynski, J. Stombaugh, K. Bittinger, F. D. Bushman, E. K. Costello, N. Fierer, A. G. Pena, J. K. Goodrich and J. I. Gordon (2010). "QIIME allows analysis of high-throughput community sequencing data." Nature methods **7**(5): 335.

Cardone, L., J. Hirayama, F. Giordano, T. Tamaru, J. J. Palvimo and P. Sassone-Corsi (2005). "Circadian clock control by SUMOylation of BMAL1." Science **309**: 1390 - 1394.

Carter, S. L., A. C. Eklund, B. H. Mecham, I. S. Kohane and Z. Szallasi (2005). "Redefinition of Affymetrix probe sets by sequence overlap with cDNA microarray probes reduces cross-platform inconsistencies in cancer-associated gene expression measurements." BMC bioinformatics **6**(1): 107.

Cassone, V. M. (1990). "Effects of melatonin on vertebrate circadian systems." Trends in Neurosciences **13**(11): 457-464.

Castillero, E., N. Alamdari, Z. Aversa, A. Gurav and P.-O. Hasselgren (2013). "PPARβ/δ regulates glucocorticoid-and sepsis-induced FOXO1 activation and muscle wasting." PLoS One **8**(3): e59726.

Choi, C. S., D. B. Savage, L. Abu-Elheiga, Z.-X. Liu, S. Kim, A. Kulkarni, A. Distefano, Y.-J. Hwang, R. M. Reznick and R. Codella (2007). "Continuous fat oxidation in acetyl–CoA carboxylase 2 knockout mice increases total energy expenditure, reduces fat mass, and improves insulin sensitivity." Proceedings of the National Academy of Sciences **104**(42): 16480-16485.

Christiansen, J. J., C. B. Djurhuus, C. H. Gravholt, P. Iversen, J. S. Christiansen, O. Schmitz, J. Weeke, J. O. L. Jørgensen and N. Møller (2007). "Effects of cortisol on carbohydrate, lipid, and protein metabolism: studies of acute cortisol withdrawal in adrenocortical failure." The Journal of Clinical Endocrinology & Metabolism **92**(9): 3553-3559.

Consortium, M. G. S. (2002). "Initial sequencing and comparative analysis of the mouse genome." Nature **420**(6915): 520.

Consortium, R. G. S. P. (2004). "Genome sequence of the Brown Norway rat yields insights into mammalian evolution." Nature **428**(6982): 493.

Consortium, U. (2018). "UniProt: the universal protein knowledgebase." Nucleic acids research **46**(5): 2699.

Cooke, A. A., R. M. Connaughton, C. L. Lyons, A. M. McMorrow and H. M. Roche (2016). "Fatty acids and chronic low grade inflammation associated with obesity and the metabolic syndrome." Eur J Pharmacol **785**: 207-214.

Cunningham, P. S., S. A. Ahern, L. C. Smith, C. S. da Silva Santos, T. T. Wager and D. A. Bechtold (2016). "Targeting of the circadian clock via CK1delta/epsilon to improve glucose homeostasis in obesity." Sci Rep **6**: 29983.

Cutolo, M. and A. T. Masi (2005). "Circadian Rhythms and Arthritis." Rheumatic Disease Clinics of North America **31**(1): 115-129.

Cuzzocrea, S., S. Bruscoli, E. Mazzon, C. Crisafulli, V. Donato, R. Di Paola, E. Velardi, E. Esposito, G. Nocentini and C. Riccardi (2008). "Peroxisome proliferator-activated receptor-α contributes to the anti-inflammatory activity of glucocorticoids." Molecular Pharmacology **73**(2): 323-337.

Da Wei Huang, B. T. S. and R. A. Lempicki (2009). "Bioinformatics enrichment tools: paths toward the comprehensive functional analysis of large gene lists." Nucleic acids research **37**(1): 1.

Denayer, T., T. Stöhr and M. Van Roy (2014). "Animal models in translational medicine: Validation and prediction." New Horizons in Translational Medicine **2**(1): 5-11.

Dibner, C., U. Schibler and U. Albrecht (2010). "The mammalian circadian timing system: organization and coordination of central and peripheral clocks." Annu Rev Physiol **72**: 517-549.

Ding, C. and X. He (2004). K-means clustering via principal component analysis. Proceedings of the twenty-first international conference on Machine learning, ACM.

Doherty, A. (2018). "Circadian rhythms and mental health: wearable sensing at scale." Lancet Psychiatry **5**(6): 457-458.

Doherty, C. J. and S. A. Kay (2010). "Circadian control of global gene expression patterns." Annu Rev Genet **44**: 419-444.

Du, J., W. E. Mitch, X. Wang and S. R. Price (2000). "Glucocorticoids induce proteasome C3 subunit expression in L6 muscle cells by opposing the suppression of its transcription by NF-κB." Journal of Biological Chemistry **275**(26): 19661-19666.

Dvorak, Z. and P. Pavek (2010). "Regulation of drug-metabolizing cytochrome P450 enzymes by glucocorticoids." Drug metabolism reviews **42**(4): 621-635.

Dyar, K. A., D. Lutter, A. Artati, N. J. Ceglia, Y. Liu, D. Armenta, M. Jastroch, S. Schneider, S. de Mateo, M. Cervantes, S. Abbondante, P. Tognini, R. Orozco-Solis, K. Kinouchi, C. Wang, R. Swerdloff, S. Nadeef, S. Masri, P. Magistretti, V. Orlando, E. Borrelli, N. H. Uhlenhaut, P. Baldi, J. Adamski, M. H. Tschöp, K. Eckel-Mahan and P. Sassone-Corsi (2018). "Atlas of Circadian Metabolism Reveals System-wide Coordination and Communication between Clocks." Cell **174**(6): 1571-1585.e1511.

Edery, I. (2000). "Circadian rhythms in a nutshell." Physiol Genomics **3**(2): 59-74.

Eisen, M. B., P. T. Spellman, P. O. Brown and D. Botstein (1998). "Cluster analysis and display of genome-wide expression patterns." Proceedings of the National Academy of Sciences **95**(25): 14863-14868.

Ellenbroek, B. and J. Youn (2016). "Rodent models in neuroscience research: is it a rat race?" Disease models & mechanisms **9**(10): 1079-1087.

Euling, S. Y., C. M. Thompson, W. A. Chiu and R. Benson (2013). "An approach for integrating toxicogenomic data in risk assessment: the dibutyl phthalate case study." Toxicology and applied pharmacology **271**(3): 324-335.

Euling, S. Y., L. White, A. M. Ovacik, S. L. Makris, B. Sen, I. P. Androulakis, S. Hester, K. W. Gaido, A. S. Kim, R. Benson, V. S. Wilson, C. Keshava, N. Keshava, P. M. Foster, L. E. Gray, W. A. Chiu and C. Thompson (2011). "An Approach to Using Toxicogenomic Data in Risk Assessment: Dibutyl Phthalate Case Study." Environmental and Molecular Mutagenesis **52**: S16-S16.

Euling, S. Y., L. D. White, A. S. Kim, B. Sen, V. S. Wilson, C. Keshava, N. Keshava, S. Hester, M. A. Ovacik and M. G. Ierapetritou (2013). "Use of genomic data in risk assessment case study: II. Evaluation of the dibutyl phthalate toxicogenomic data set." Toxicology and applied pharmacology **271**(3): 349-362.

Euling, S. Y., L. D. White, A. S. Kim, B. Sen, V. S. Wilson, C. Keshava, N. Keshava, S. Hester, M. A. Ovacik, M. G. Ierapetritou, I. P. Androulakis and K. W. Gaido (2013). "Use of genomic data in risk assessment case study: II. Evaluation of the dibutyl phthalate toxicogenomic data set." Toxicol Appl Pharmacol **271**(3): 349-362.

Fabregat, A., S. Jupe, L. Matthews, K. Sidiropoulos, M. Gillespie, P. Garapati, R. Haw, B. Jassal, F. Korninger, B. May, M. Milacic, C. D. Roca, K. Rothfels, C. Sevilla, V. Shamovsky, S. Shorser, T. Varusai, G. Viteri, J. Weiser, G. Wu, L. Stein, H. Hermjakob and P. D'Eustachio (2018). "The Reactome Pathway Knowledgebase." Nucleic Acids Res **46**(D1): D649-D655.

Fang, J., S. Sukumaran, D. C. DuBois, R. R. Almon and W. J. Jusko (2013). "Meta-modeling of methylprednisolone effects on glucose regulation in rats." PloS one **8**(12): e81679.

Fang, M., W. R. Guo, Y. Park, H. G. Kang and H. Zarbl (2015). "Enhancement of NAD(+)-dependent SIRT1 deacetylase activity by methylselenocysteine resets the circadian clock in carcinogen-treated mammary epithelial cells." Oncotarget **6**(40): 42879-42891.

Feillet, C. A., U. Albrecht and E. Challet (2006). ""Feeding time" for the brain: a matter of clocks." J Physiol Paris **100**(5-6): 252-260.

García-Campos, M. A., J. Espinal-Enríquez and E. Hernández-Lemus (2015). "Pathway analysis: state of the art." Frontiers in physiology **6**: 383.

Ghosh, D., T. R. Barette, D. Rhodes and A. M. Chinnaiyan (2003). "Statistical issues and methods for meta-analysis of microarray data: a case study in prostate cancer." Functional & Integrative Genomics **3**(4): 180-188.

Gibbs, J. E., S. Beesley, J. Plumb, D. Singh, S. Farrow, D. W. Ray and A. S. Loudon (2009). "Circadian timing in the lung; a specific role for bronchiolar epithelial cells." Endocrinology **150**(1): 268-276.

Ginsburg, G. S. and K. A. Phillips (2018). "Precision medicine: From science to value." Health Affairs **37**(5): 694-701.

Gnocchi, D. and G. Bruscalupi (2017). "Circadian Rhythms and Hormonal Homeostasis: Pathophysiological Implications." Biology (Basel) **6**(1).

Hazra, A., D. C. DuBois, R. R. Almon, G. H. Snyder and W. J. Jusko (2008). "Pharmacodynamic modeling of acute and chronic effects of methylprednisolone on hepatic urea cycle genes in rats." Gene Regul Syst Bio **2**: 1-19.

Hazra, A., N. Pyszczynski, D. C. DuBois, R. R. Almon and W. J. Jusko (2007). "Pharmacokinetics of methylprednisolone after intravenous and intramuscular administration in rats." Biopharm Drug Dispos **28**(6): 263-273.

He, B., K. Nohara, N. Park, Y. S. Park, B. Guillory, Z. Zhao, J. M. Garcia, N. Koike, C. C. Lee, J. S. Takahashi, S. H. Yoo and Z. Chen (2016). "The Small Molecule Nobiletin Targets the Molecular Oscillator to Enhance Circadian Rhythms and Protect against Metabolic Syndrome." Cell Metab **23**(4): 610-621.

Heilbronn, L. K. and L. V. Campbell (2008). "Adipose tissue macrophages, low grade inflammation and insulin resistance in human obesity." Curr Pharm Des **14**(12): 1225-1230.

Holeček, M. (2002). "Relation between glutamine, branched-chain amino acids, and protein metabolism." Nutrition **18**(2): 130-133.

Huang, D. W., B. T. Sherman and R. A. Lempicki (2009). "Systematic and integrative analysis of large gene lists using DAVID bioinformatics resources." Nature protocols **4**(1): 44.

Iyengar, R., S. Zhao, S.-W. Chung, D. E. Mager and J. M. Gallo (2012). "Merging systems biology with pharmacodynamics." Science translational medicine **4**(126): 126ps127-126ps127.

Jiang, H., Y. Deng, H.-S. Chen, L. Tao, Q. Sha, J. Chen, C.-J. Tsai and S. Zhang (2004). "Joint analysis of two microarray gene-expression data sets to select lung adenocarcinoma marker genes." BMC bioinformatics **5**(1): 81.

Jin, J. Y., R. R. Almon, D. C. Dubois and W. J. Jusko (2003). "Modeling of corticosteroid pharmacogenomics in rat liver using gene microarrays." Journal of Pharmacology and Experimental Therapeutics **307**(1): 93-109.

Jin, L., X.-Y. Zuo, W.-Y. Su, X.-L. Zhao, M.-Q. Yuan, L.-Z. Han, X. Zhao, Y.-D. Chen and S.-Q. Rao (2014). "Pathway-based analysis tools for complex diseases: a review." Genomics, proteomics & bioinformatics **12**(5): 210-220.

Jusko, W. J. (2013). "Moving from basic toward systems pharmacodynamic models." Journal of pharmaceutical sciences **102**(9): 2930-2940.

Kaczmarek, J. L., S. V. Thompson and H. D. Holscher (2017). "Complex interactions of circadian rhythms, eating behaviors, and the gastrointestinal microbiota and their potential impact on health." Nutr Rev **75**(9): 673-682.

Kallio, A., N. Vuokko, M. Ojala, N. Haiminen and H. Mannila (2011). "Randomization techniques for assessing the significance of gene periodicity results." BMC bioinformatics **12**(1): 330.

Kamisoglu, K., A. Acevedo, R. R. Almon, S. Coyle, S. Corbett, D. C. Dubois, T. T. Nguyen, W. J. Jusko and I. P. Androulakis (2017). "Understanding physiology in the continuum: integration of information from multiple-omics levels." Frontiers in pharmacology **8**: 91.

Kamisoglu, K., S. E. Calvano, S. M. Coyle, S. A. Corbett and I. P. Androulakis (2014). "Integrated transcriptional and metabolic profiling in human endotoxemia." Shock **42**(6): 499-508.

Kamisoglu, K., S. Sukumaran, E. Nouri-Nigjeh, C. Tu, J. Li, X. Shen, X. Duan, J. Qu, R. R. Almon and D. C. DuBois (2015). "Tandem analysis of transcriptome and proteome changes after a single dose of corticosteroid: a systems approach to liver function in pharmacogenomics." Omics: a journal of integrative biology **19**(2): 80-91.

Kanehisa, M., M. Furumichi, M. Tanabe, Y. Sato and K. Morishima (2016). "KEGG: new perspectives on genomes, pathways, diseases and drugs." Nucleic acids research **45**(D1): D353-D361.

Kanehisa, M. and S. Goto (2000). "KEGG: kyoto encyclopedia of genes and genomes." Nucleic Acids Res **28**(1): 27-30.

Kanehisa, M. and S. Goto (2000). "KEGG: kyoto encyclopedia of genes and genomes." Nucleic acids research **28**(1): 27-30.

Kanehisa, M., Y. Sato, M. Furumichi, K. Morishima and M. Tanabe (2018). "New approach for understanding genome variations in KEGG." Nucleic acids research **47**(D1): D590-D595.

Kanemitsu, T., Y. Tsurudome, N. Kusunose, M. Oda, N. Matsunaga, S. Koyanagi and S. Ohdo (2017). "Periodic variation in bile acids controls circadian changes in uric acid via regulation of xanthine oxidase by the orphan nuclear receptor PPARα." Journal of Biological Chemistry.

KEGG (2019). AMPK Signaling Pathway (Pathway: rno04152). KEGG Online Database, Kyoto Encyclopedia of Genes and Genomes.

KEGG (2019). FoxO signaling pathway (Pathway: rno04068). KEGG Online Database, Kyoto Encyclopedia of Genes and Genomes.

KEGG (2019). PPAR signaling pathway (Pathway: rno03320). KEGG Online Database, Kyoto Encyclopedia of Genes and Genomes.

Khaper, N., C. D. C. Bailey, N. R. Ghugre, C. Reitz, Z. Awosanmi, R. Waines and T. A. Martino (2018). "Implications of disturbances in circadian rhythms for cardiovascular health: A new frontier in free radical biology." Free Radic Biol Med **119**: 85-92.

Kim, K.-Y., D. H. Ki, H. J. Jeong, H.-C. Jeung, H. C. Chung and S. Y. Rha (2007). "Novel and simple transformation algorithm for combining microarray data sets." BMC bioinformatics **8**(1): 218.

Korencic, A., R. Kosir, G. Bordyugov, R. Lehmann, D. Rozman and H. Herzel (2014). "Timing of circadian genes in mammalian tissues." Sci Rep **4**: 5782.

Koves, T. R., J. R. Ussher, R. C. Noland, D. Slentz, M. Mosedale, O. Ilkayeva, J. Bain, R. Stevens, J. R. Dyck and C. B. Newgard (2008). "Mitochondrial overload and incomplete fatty acid oxidation contribute to skeletal muscle insulin resistance." Cell metabolism **7**(1): 45-56.

Krzyszczyk, P., A. Acevedo, E. J. Davidoff, L. M. Timmins, I. Marrero-Berrios, M. Patel, C. White, C. Lowe, J. J. Sherba and C. Hartmanshenn (2018). "The growing role of precision and personalized medicine for cancer treatment." Technology **6**(03n04): 79-100.

Kuo, T., C. A. Harris and J.-C. Wang (2013). "Metabolic functions of glucocorticoid receptor in skeletal muscle." Molecular and cellular endocrinology **380**(1-2): 79-88.

Laplante, M. and D. M. Sabatini (2009). "mTOR signaling at a glance." Journal of cell science **122**(20): 3589-3594.

Lee, J. E. and I. Edery (2008). "Circadian regulation in the ability of Drosophila to combat pathogenic infections." Curr Biol **18**(3): 195-199.
Leek, J. T., E. Monsen, A. R. Dabney and J. D. Storey (2006). "EDGE: extraction and analysis of differential gene expression." Bioinformatics **22**(4): 507-508.
Li, S., M. S. Brown and J. L. Goldstein (2010). "Bifurcation of insulin signaling pathway in rat liver: mTORC1 required for stimulation of lipogenesis, but not inhibition of gluconeogenesis." Proceedings of the National Academy of Sciences **107**(8): 3441-3446.
Lima-Mendez, G. and J. van Helden (2009). "The powerful law of the power law and other myths in network biology." Mol Biosyst **5**(12): 1482-1493.
Liu, A. C., W. G. Lewis and S. A. Kay (2007). "Mammalian circadian signaling networks and therapeutic targets." Nat Chem Biol **3**(10): 630-639.
Liu, J., Y. Peng, X. Wang, Y. Fan, C. Qin, L. Shi, Y. Tang, K. Cao, H. Li and J. Long (2015). "Mitochondrial dysfunction launches dexamethasone-induced skeletal muscle atrophy via AMPK/FOXO3 signaling." Molecular pharmaceutics **13**(1): 73-84.
Liu, Y.-Z., Y.-X. Wang and C.-L. Jiang (2017). "Inflammation: the common pathway of stress-related diseases." Frontiers in Human Neuroscience **11**: 316.
Lu, J., J. C. Lee, M. L. Salit and M. C. Cam (2007). "Transcript-based redefinition of grouped oligonucleotide probe sets using AceView: high-resolution annotation for microarrays." BMC bioinformatics **8**(1): 108.
Macfarlane, D. P., S. Forbes and B. R. Walker (2008). "Glucocorticoids and fatty acid metabolism in humans: fuelling fat redistribution in the metabolic syndrome." Journal of Endocrinology **197**(2): 189-204.
Makris, S. L., S. Y. Euling, L. E. Gray Jr, R. Benson and P. M. Foster (2013). "Use of genomic data in risk assessment case study: I. Evaluation of the dibutyl phthalate male reproductive development toxicity data set." Toxicology and applied pharmacology **271**(3): 336-348.
MATLAB (2016b). "MATLAB and Statistics Toolbox Release 2016a The MathWorks, Inc., Natick, Massachusetts, United States.".
Mavroudis, P., J. Scheff, S. Calvano and I. Androulakis (2013). "Systems biology of circadian-immune interactions." Journal of innate immunity **5**(2): 153-162.
Mavroudis, P. D., D. C. DuBois, R. R. Almon and W. J. Jusko (2018). "Daily variation of gene expression in diverse rat tissues." PLoS One **13**(5): e0197258.
Mavroudis, P. D., D. C. DuBois, R. R. Almon and W. J. Jusko (2018). "Modeling circadian variability of core-clock and clock-controlled genes in four tissues of the rat." PLoS One **13**(6): e0197534.
McEachron, D. L. (2012). "Timing is everything: a chronobiologist's perspective on health, illness, and circadian rhythms. Interview by Gloria F. Donnelly." Holist Nurs Pract **26**(4): 188-193.
McMahon, M., J. Gerich and R. Rizza (1988). "Effects of glucocorticoids on carbohydrate metabolism." Diabetes/metabolism reviews **4**(1): 17-30.
Mecham, B. H., G. T. Klus, J. Strovel, M. Augustus, D. Byrne, P. Bozso, D. Z. Wetmore, T. J. Mariani, I. S. Kohane and Z. Szallasi (2004). "Sequence-matched probes produce increased cross-platform consistency and more reproducible biological results in

microarray-based gene expression measurements." Nucleic Acids Research **32**(9): e74-e74.

Mirsky, H. P., A. C. Liu, D. K. Welsh, S. A. Kay and F. J. Doyle, 3rd (2009). "A model of the cell-autonomous mammalian circadian clock." Proc Natl Acad Sci U S A **106**(27): 11107-11112.

Moore, J. H. and S. M. Williams (2009). "Epistasis and its implications for personal genetics." The American Journal of Human Genetics **85**(3): 309-320.

Morand, E. and M. Leech (1999). "Glucocorticoid regulation of inflammation: the plot thickens." Inflammation Research **48**(11): 557-560.

Morris, J. S., C. Wu, K. R. Coombes, K. A. Baggerly, J. Wang and L. Zhang (2006). "Alternative probeset definitions for combining microarray data across studies using different versions of affymetrix oligonucleotide arrays." Meta-Analysis in Genetics: 1-214.

Mure, L. S., H. D. Le, G. Benegiamo, M. W. Chang, L. Rios, N. Jillani, M. Ngotho, T. Kariuki, O. Dkhissi-Benyahya, H. M. Cooper and S. Panda (2018). "Diurnal transcriptome atlas of a primate across major neural and peripheral tissues." Science **359**(6381).

Nader, N., S. S. M. Ng, Y. Wang, B. S. Abel, G. P. Chrousos and T. Kino (2012). "Liver x receptors regulate the transcriptional activity of the glucocorticoid receptor: implications for the carbohydrate metabolism." PloS one **7**(3): e26751.

Nair, K. S., R. Schwartz and S. Welle (1992). "Leucine as a regulator of whole body and skeletal muscle protein metabolism in humans." American Journal of Physiology-Endocrinology And Metabolism **263**(5): E928-E934.

Nakamura, Y., N. Nakano, K. Ishimaru, N. Ando, R. Katoh, K. Suzuki-Inoue, S. Koyanagki, H. Ogawa, K. Okumura, S. Shibata and A. Nakao (2016). "Inhibition of IgE-mediated allergic reactions by pharmacologically targeting the circadian clock." J Allergy Clin Immunol **137**(4): 1226-1235.

Nath, N., M. Khan, R. Rattan, A. Mangalam, R. S. Makkar, C. de Meester, L. Bertrand, I. Singh, Y. Chen and B. Viollet (2009). "Loss of AMPK exacerbates experimental autoimmune encephalomyelitis disease severity." Biochemical and biophysical research communications **386**(1): 16-20.

Nguyen, T. T., R. R. Almon, D. C. DuBois, W. J. Jusko and I. P. Androulakis (2010). "Comparative analysis of acute and chronic corticosteroid pharmacogenomic effects in rat liver: transcriptional dynamics and regulatory structures." BMC bioinformatics **11**(1): 515.

Nguyen, T. T., R. R. Almon, D. C. DuBois, W. J. Jusko and I. P. Androulakis (2010). "Importance of replication in analyzing time-series gene expression data: corticosteroid dynamics and circadian patterns in rat liver." BMC bioinformatics **11**(1): 279.

Nguyen, T. T., R. R. Almon, D. C. Dubois, S. Sukumaran, W. J. Jusko and I. P. Androulakis (2014). "Tissue-specific gene expression and regulation in liver and muscle following chronic corticosteroid administration." Gene Regul Syst Bio **8**: 75-87.

Nguyen, T. T., R. S. Nowakowski and I. P. Androulakis (2009). "Unsupervised selection of highly coexpressed and noncoexpressed genes using a consensus clustering approach." OMICS A Journal of Integrative Biology **13**(3): 219-237.

Nouri-Nigjeh, E., S. Sukumaran, C. Tu, J. Li, X. Shen, X. Duan, D. C. DuBois, R. R. Almon, W. J. Jusko and J. Qu (2014). "Highly multiplexed and reproducible ion-current-based strategy for large-scale quantitative proteomics and the application to protein expression dynamics induced by methylprednisolone in 60 rats." Analytical chemistry **86**(16): 8149-8157.

Ovacik, M. A., B. Sen, S. Y. Euling, K. W. Gaido, M. G. Ierapetritou and I. P. Androulakis (2013). "Pathway modeling of microarray data: a case study of pathway activity changes in the testis following in utero exposure to dibutyl phthalate (DBP)." Toxicol Appl Pharmacol **271**(3): 386-394.

Ovacik, M. A., B. Sen, S. Y. Euling, K. W. Gaido, M. G. Ierapetritou and I. P. Androulakis (2013). "Pathway modeling of microarray data: A case study of pathway activity changes in the testis following in utero exposure to dibutyl phthalate (DBP)." Toxicology and applied pharmacology **271**(3): 386-394.

Ovacik, M. A., S. Sukumaran, R. R. Almon, D. C. DuBois, W. J. Jusko and I. P. Androulakis (2010). "Circadian signatures in rat liver: from gene expression to pathways." BMC Bioinformatics **11**: 540.

Ovacik, M. A., S. Sukumaran, R. R. Almon, D. C. DuBois, W. J. Jusko and I. P. Androulakis (2010). "Circadian signatures in rat liver: from gene expression to pathways." Bmc Bioinformatics **11**(1): 540.

Paladino, N., M. J. Leone, S. A. Plano and D. A. Golombek (2010). "Paying the circadian toll: the circadian response to LPS injection is dependent on the Toll-like receptor 4." J Neuroimmunol **225**(1-2): 62-67.

Panda, S., M. P. Antoch, B. H. Miller, A. I. Su, A. B. Schook, M. Straume, P. G. Schultz, S. A. Kay, J. S. Takahashi and J. B. Hogenesch (2002). "Coordinated transcription of key pathways in the mouse by the circadian clock." Cell **109**(3): 307-320.

Park, T., S.-G. Yi, Y. K. Shin and S. Lee (2006). "Combining multiple microarrays in the presence of controlling variables." Bioinformatics **22**(14): 1682-1689.

Pascussi, J.-M., L. Drocourt, J.-M. Fabre, P. Maurel and M.-J. Vilarem (2000). "Dexamethasone induces pregnane X receptor and retinoid X receptor-α expression in human hepatocytes: synergistic increase of CYP3A4 induction by pregnane X receptor activators." Molecular Pharmacology **58**(2): 361-372.

Peckett, A. J., D. C. Wright and M. C. Riddell (2011). "The effects of glucocorticoids on adipose tissue lipid metabolism." Metabolism **60**(11): 1500-1510.

Pett, J. P., M. Kondoff, G. Bordyugov, A. Kramer and H. Herzel (2018). "Co-existing feedback loops generate tissue-specific circadian rhythms." Life Science Alliance **1**(3): e201800078.

Pierre, S., T. Eschenhagen, G. Geisslinger and K. Scholich (2009). "Capturing adenylyl cyclases as potential drug targets." Nature reviews Drug discovery **8**(4): 321.

Portaluppi, F., R. Tiseo, M. H. Smolensky, R. C. Hermida, D. E. Ayala and F. Fabbian (2012). "Circadian rhythms and cardiovascular health." Sleep Med Rev **16**(2): 151-166.

Raker, V. K., C. Becker and K. Steinbrink (2016). "The cAMP pathway as therapeutic target in autoimmune and inflammatory diseases." Frontiers in immunology **7**: 123.

Ramakrishnan, R., D. C. DuBois, R. R. Almon, N. A. Pyszczynski and W. J. Jusko (2002). "Fifth-generation model for corticosteroid pharmacodynamics: application to steady-state

receptor down-regulation and enzyme induction patterns during seven-day continuous infusion of methylprednisolone in rats." J Pharmacokinet Pharmacodyn **29**(1): 1-24.
Ramakrishnan, R., D. C. DuBois, R. R. Almon, N. A. Pyszczynski and W. J. Jusko (2002). "Pharmacodynamics and pharmacogenomics of methylprednisolone during 7-day infusions in rats." Journal of Pharmacology and Experimental Therapeutics **300**(1): 245-256.
Ramasamy, A., A. Mondry, C. C. Holmes and D. G. Altman (2008). "Key issues in conducting a meta-analysis of gene expression microarray datasets." PLoS medicine **5**(9): e184.
Rao, R. and I. P. Androulakis (2019). "The physiological significance of the circadian dynamics of the HPA axis: Interplay between circadian rhythms, allostasis and stress resilience." Hormones and behavior **110**: 77-89.
Rao, R. T., M. L. Scherholz and I. P. Androulakis (2018). "Modeling the influence of chronopharmacological administration of synthetic glucocorticoids on the hypothalamic-pituitary-adrenal axis." Chronobiology international **35**(12): 1619-1636.
Ratnam, S., K. N. Maclean, R. L. Jacobs, M. E. Brosnan, J. P. Kraus and J. T. Brosnan (2002). "Hormonal regulation of cystathionine β-synthase expression in liver." Journal of Biological Chemistry **277**(45): 42912-42918.
Rhen, T. and J. A. Cidlowski (2005). "Antiinflammatory action of glucocorticoids—new mechanisms for old drugs." New England Journal of Medicine **353**(16): 1711-1723.
Roussel, D., J.-F. Dumas, G. Simard, Y. MALTHIèRY and R. Patrick (2004). "Kinetics and control of oxidative phosphorylation in rat liver mitochondria after dexamethasone treatment." Biochemical Journal **382**(2): 491-499.
Rui, L. (2011). "Energy metabolism in the liver." Comprehensive physiology **4**(1): 177-197.
Sakaguchi, M., M. Isono, K. Isshiki, T. Sugimoto, D. Koya and A. Kashiwagi (2006). "Inhibition of mTOR signaling with rapamycin attenuates renal hypertrophy in the early diabetic mice." Biochemical and biophysical research communications **340**(1): 296-301.
Schaaf, M. J. and J. A. Cidlowski (2002). "Molecular mechanisms of glucocorticoid action and resistance." The Journal of steroid biochemistry and molecular biology **83**(1-5): 37-48.
Schakman, O., S. Kalista, C. Barbé, A. Loumaye and J.-P. Thissen (2013). "Glucocorticoid-induced skeletal muscle atrophy." The international journal of biochemistry & cell biology **45**(10): 2163-2172.
Scherholz, M. L., N. Schlesinger and I. P. Androulakis (2019). "Chronopharmacology of glucocorticoids." Advanced drug delivery reviews.
Shabalin, A. A., H. Tjelmeland, C. Fan, C. M. Perou and A. B. Nobel (2008). "Merging two gene-expression studies via cross-platform normalization." Bioinformatics **24**(9): 1154-1160.
Short, K. R., J. Nygren, M. L. Bigelow and K. S. Nair (2004). "Effect of short-term prednisone use on blood flow, muscle protein metabolism, and function." The Journal of Clinical Endocrinology & Metabolism **89**(12): 6198-6207.
Silver, A. C., A. Arjona, W. E. Walker and E. Fikrig (2012). "The circadian clock controls toll-like receptor 9-mediated innate and adaptive immunity." Immunity **36**(2): 251-261.
Skarke, C., N. F. Lahens, S. D. Rhoades, A. Campbell, K. Bittinger, A. Bailey, C. Hoffmann, R. S. Olson, L. Chen, G. Yang, T. S. Price, J. H. Moore, F. D. Bushman, C. S. Greene, G. R.

Grant, A. M. Weljie and G. A. FitzGerald (2017). "A Pilot Characterization of the Human Chronobiome." Sci Rep **7**(1): 17141.

Subramanian, A., P. Tamayo, V. K. Mootha, S. Mukherjee, B. L. Ebert, M. A. Gillette, A. Paulovich, S. L. Pomeroy, T. R. Golub and E. S. Lander (2005). "Gene set enrichment analysis: a knowledge-based approach for interpreting genome-wide expression profiles." Proceedings of the National Academy of Sciences **102**(43): 15545-15550.

Sukumaran, S., W. J. Jusko, D. C. Dubois and R. R. Almon (2011). "Light-dark oscillations in the lung transcriptome: implications for lung homeostasis, repair, metabolism, disease, and drug action." J Appl Physiol (1985) **110**(6): 1732-1747.

Sukumaran, S., B. Xue, W. J. Jusko, D. C. Dubois and R. R. Almon (2010). "Circadian variations in gene expression in rat abdominal adipose tissue and relationship to physiology." Physiol Genomics **42A**(2): 141-152.

Sulli, G., E. N. C. Manoogian, P. R. Taub and S. Panda (2018). "Training the Circadian Clock, Clocking the Drugs, and Drugging the Clock to Prevent, Manage, and Treat Chronic Diseases." Trends Pharmacol Sci **39**(9): 812-827.

Sun, Y. N., D. C. DuBois, R. R. Almon and W. J. Jusko (1998). "Fourth-generation model for corticosteroid pharmacodynamics: a model for methylprednisolone effects on receptor/gene-mediated glucocorticoid receptor down-regulation and tyrosine aminotransferase induction in rat liver." J Pharmacokinet Biopharm **26**(3): 289-317.

Sun, Y. N., L. I. McKay, D. C. DuBois, W. J. Jusko and R. R. Almon (1999). "Pharmacokinetic/Pharmacodynamic models for corticosteroid receptor down-regulation and glutamine synthetase induction in rat skeletal muscle by a Receptor/Gene-mediated mechanism." J Pharmacol Exp Ther **288**(2): 720-728.

Swartz, S. L. and R. G. Dluhy (1978). "Corticosteroids: clinical pharmacology and therapeutic use." Drugs **16**(3): 238-255.

Tan, E. and E. M. Scott (2014). "Circadian rhythms, insulin action, and glucose homeostasis." Curr Opin Clin Nutr Metab Care **17**(4): 343-348.

Tomfohr, J., J. Lu and T. B. Kepler (2005). "Pathway level analysis of gene expression using singular value decomposition." BMC bioinformatics **6**(1): 225.

Tseng, G. C., D. Ghosh and E. Feingold (2012). "Comprehensive literature review and statistical considerations for microarray meta-analysis." Nucleic acids research **40**(9): 3785-3799.

Varcoe, T. J. (2018). "Timing is everything: maternal circadian rhythms and the developmental origins of health and disease." J Physiol.

Viollet, B., S. Horman, J. Leclerc, L. Lantier, M. Foretz, M. Billaud, S. Giri and F. Andreelli (2010). "AMPK inhibition in health and disease." Critical reviews in biochemistry and molecular biology **45**(4): 276-295.

Waddell, D. S., L. M. Baehr, J. Van Den Brandt, S. A. Johnsen, H. M. Reichardt, J. D. Furlow and S. C. Bodine (2008). "The glucocorticoid receptor and FOXO1 synergistically activate the skeletal muscle atrophy-associated MuRF1 gene." American Journal of Physiology-Endocrinology and Metabolism **295**(4): E785-E797.

Wallace, A. D. and J. A. Cidlowski (2001). "Proteasome-mediated glucocorticoid receptor degradation restricts transcriptional signaling by glucocorticoids." Journal of Biological Chemistry **276**(46): 42714-42721.

Wilke, R., R. Mareedu and J. Moore (2008). "The pathway less traveled: moving from candidate genes to candidate pathways in the analysis of genome-wide data from large scale pharmacogenetic association studies." Current Pharmacogenomics and Personalized Medicine (Formerly Current Pharmacogenomics) **6**(3): 150-159.

Wong, S. K., K.-Y. Chin, F. H. Suhaimi, A. Fairus and S. Ima-Nirwana (2016). "Animal models of metabolic syndrome: a review." Nutrition & metabolism **13**(1): 65.

Wu, G., M. D. Ruben, R. E. Schmidt, L. J. Francey, D. F. Smith, R. C. Anafi, J. J. Hughey, R. Tasseff, J. D. Sherrill, J. E. Oblong, K. J. Mills and J. B. Hogenesch (2018). "Population-level rhythms in human skin with implications for circadian medicine." Proc Natl Acad Sci U S A.

Xu, H., G. T. Barnes, Q. Yang, G. Tan, D. Yang, C. J. Chou, J. Sole, A. Nichols, J. S. Ross, L. A. Tartaglia and H. Chen (2003). "Chronic inflammation in fat plays a crucial role in the development of obesity-related insulin resistance." J Clin Invest **112**(12): 1821-1830.

Yang, E., R. Almon, D. DuBois, W. Jusko and I. Androulakis (2008). "Extracting global system dynamics of corticosteroid genomic effects in rat liver." Journal of Pharmacology and Experimental Therapeutics **324**(3): 1243-1254.

Yang, E., R. R. Almon, D. C. Dubois, W. J. Jusko and I. P. Androulakis (2008). "Extracting global system dynamics of corticosteroid genomic effects in rat liver." J Pharmacol Exp Ther **324**(3): 1243-1254.

Yang, E. H., R. R. Almon, D. C. DuBois, W. J. Jusko and I. P. Androulakis (2009). "Identification of global transcriptional dynamics." PLoS One **4**(7): e5992.

Yao, Z., E. P. Hoffman, S. Ghimbovschi, D. C. Dubois, R. R. Almon and W. J. Jusko (2008). "Mathematical modeling of corticosteroid pharmacogenomics in rat muscle following acute and chronic methylprednisolone dosing." Mol Pharm **5**(2): 328-339.

Yeung, J., J. Mermet, C. Jouffe, J. Marquis, A. Charpagne, F. Gachon and F. Naef (2018). "Transcription factor activity rhythms and tissue-specific chromatin interactions explain circadian gene expression across organs." Genome Res **28**(2): 182-191.

Yeung, J. and F. Naef (2018). "Rhythms of the Genome: Circadian Dynamics from Chromatin Topology, Tissue-Specific Gene Expression, to Behavior." Trends in Genetics **34**(12): 915-926.

Zaki, N. F. W., D. W. Spence, A. S. BaHammam, S. R. Pandi-Perumal, D. P. Cardinali and G. M. Brown (2018). "Sleep and circadian rhythms in health and disease: a complex interplay." Eur Arch Psychiatry Clin Neurosci.

Zhang, R., N. F. Lahens, H. I. Ballance, M. E. Hughes and J. B. Hogenesch (2014). "A circadian gene expression atlas in mammals: implications for biology and medicine." Proc Natl Acad Sci U S A **111**(45): 16219-16224.

Zhao, W., W. Qin, J. Pan, Y. Wu, W. A. Bauman and C. Cardozo (2009). "Dependence of dexamethasone-induced Akt/FOXO1 signaling, upregulation of MAFbx, and protein catabolism upon the glucocorticoid receptor." Biochemical and biophysical research communications **378**(3): 668-672.

Zhou, D., Y. Wang, L. Chen, L. Jia, J. Yuan, M. Sun, W. Zhang, P. Wang, J. Zuo, Z. Xu and J. Luan (2016). "Evolving roles of circadian rhythms in liver homeostasis and pathology." Oncotarget **7**(8): 8625-8639.

Zvonic, S., Z. E. Floyd, R. L. Mynatt and J. M. Gimble (2007). "Circadian rhythms and the regulation of metabolic tissue function and energy homeostasis." Obesity (Silver Spring) **15**(3): 539-543.

Appendix

ST 1 High-throughput data analyzed for reported investigations

Transcriptional data capturing methylprednisolone influence across liver and muscle in adrenalectomized rats (Sun, DuBois et al. , Jin, Almon et al. , Almon, DuBois et al. , Almon, DuBois et al. , Almon, DuBois et al. , Hazra, Pyszczynski et al. , Hazra, DuBois et al.)

Organ	Acute: Single MPL dose at time zero.	Chronic: Continuous intravenous delivery
Liver	**Transcript:** GEO GDS253 (Sun, DuBois et al. , Jin, Almon et al. , Almon, DuBois et al.) 72 hours, 16 timepoints Affymetrix Probe Set RGU34A (8799 probes)	**Transcript**: GEO GDS972 (Almon, DuBois et al. , Hazra, DuBois et al.) 168 hours, 10 timepoints Affymetrix Probe Set 230A (15967 probe sets)
Skeletal Muscle	**Transcript**: GSE490 (Almon, DuBois et al.) 72 hours, 16 timepoints Affymetrix Probe Set RGU34A (8799 probes)	**Transcript**: GSE5101 (Almon, DuBois et al.) 168 hours, 10 timepoints Affymetrix Probe Set RAE230A (15967 probes)

Transcriptional data capturing drug-free expression in intact rats (Mavroudis, DuBois et al.)

Organ	**Transcriptomic Microarray Studies in Intact Wistar Rats** **24 hours, 22 timepoints, 4 tissues** (Mavroudis, DuBois et al.)
Liver	GEO GSE8988 Affymetrix GeneChips Rat Genome 230A
Lung	GEO GSE25612 Affymetrix GeneChips Rat Genome 230A 2
Adipose	GEO GSE20635 Affymetrix GeneChips Rat Genome 230A 2
Skeletal Muscle	GSE8989 Affymetrix GeneChips Rat Genome 230A

Transcriptional data capturing drug-free expression in intact mice (Zhang, Lahens et al.)

Organ	**Transcriptomic Microarray Studies in Intact Mouse** **48 hours, 24 timepoints, 12 tissues** **(5 used for circadian study)** (Zhang, Lahens et al.)
Liver	GEO GSE54652 Affymetrix MoGene 1.0ST array
Lung	GEO GSE54652 Affymetrix MoGene 1.0ST array
White Adipose	GEO GSE54652 Affymetrix MoGene 1.0ST array
Brown Adipose	GEO GSE54652 Affymetrix MoGene 1.0ST array
Skeletal Muscle	GEO GSE54652 Affymetrix MoGene 1.0ST array

ST 2 Fisher's Exact Test Limitations

The application of the Fisher's Exact Test (FET), in the context of our genomic analysis, compare a pathway's presence in the rat genome compared to the pathway's presence in a data set, making use of contingency tables as depicted in the example in Table 8: Glycolysis/Gluconeogenesis pathway contingency table from the acute muscle data set. Each pathway is analyzed independently within each data set and p-values are generated. These p-values are called f_c p-values, as they report the significance of the fractional coverage calculation. When the f_c and f_c p-values were compared, an interesting peak trend was observed for each data set (Figure 33).

The ratio of data set size to genome size controls the location of this peak. As this ratio grows large (data set size is large relative to genome size), this peak appears and shifts to the right. As the ratio grows small (data set is small relative to genome), the peak shifts left or disappears entirely. Observation of this artifact of the FET motivated us to take a conservative approach in our analysis and disregard pathways with f_c below the location of the peak in the f_c vs. f_c p-value plots, as the meaning and reliability of the f_c p-values for sub-peak pathways are unclear. Thus, pathways below 6% for the acute data and below 18% for the chronic data were removed from this analysis.

Table 8 Example contingency table for Glycolysis/Gluconeogenesis within the acute muscle data set. This data set yields a sufficient number of differentially expressed Affymetrix probes that represent 489 genes. The rat genome consists of the set of unique genes found in all rat-relevant KEGG pathways.

No. of Genes (KEGG Genes)	Within Data Set	Not Within Data Set	Total
Pathway	5	67	72
Not in Pathway	482	8078	8560
Total	489	8145	8634

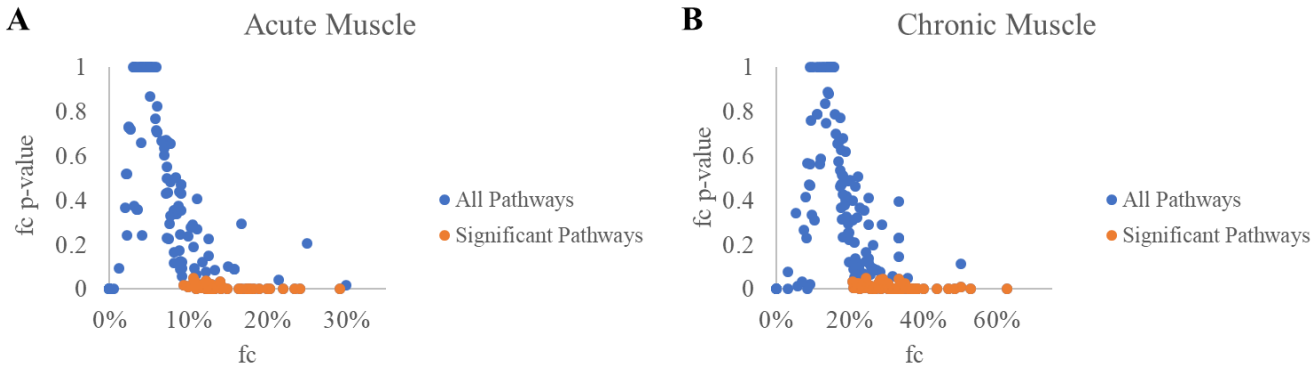

Figure 33 Results of fractional coverage analysis for acute and chronic muscle data sets. Significant pathways refer to the pathways that emerged as significant after entire framework is completed.

ST 3 List of Significant Pathways from Acute Liver Data

KEGG ID	Pathway Name	Pathway Subgroup	Pathway Group
04146	Peroxisome	Transport and catabolism	Cellular Processes
03050	Proteasome	Folding, sorting and degradation	Genetic Information Processing
04141	Protein processing in endoplasmic reticulum	Folding, sorting and degradation	Genetic Information Processing
03010	Ribosome	Translation	Genetic Information Processing
00220	Arginine biosynthesis	Amino acid metabolism	Metabolism
00410	beta-Alanine metabolism	Metabolism of other amino acids	Metabolism
01230	Biosynthesis of amino acids	Amino acid metabolism	Metabolism
00650	Butanoate metabolism	Carbohydrate metabolism	Metabolism
01200	Carbon metabolism	Carbohydrate metabolism	Metabolism
00020	Citrate cycle (TCA cycle)	Carbohydrate metabolism	Metabolism
00270	Cysteine and methionine metabolism	Amino acid metabolism	Metabolism
00982	Drug metabolism - cytochrome P450	Xenobiotics biodegradation and metabolism	Metabolism
00071	Fatty acid degradation	Lipid metabolism	Metabolism
01212	Fatty acid metabolism	Lipid metabolism	Metabolism
00480	Glutathione metabolism	Metabolism of other amino acids	Metabolism
00010	Glycolysis / Gluconeogenesis	Carbohydrate metabolism	Metabolism
00630	Glyoxylate and dicarboxylate metabolism	Carbohydrate metabolism	Metabolism
00980	Metabolism of xenobiotics by cytochrome P450	Xenobiotics biodegradation and metabolism	Metabolism
00190	Oxidative phosphorylation	Energy metabolism	Metabolism
00640	Propanoate metabolism	Carbohydrate metabolism	Metabolism
00620	Pyruvate metabolism	Carbohydrate metabolism	Metabolism
00830	Retinol metabolism	Metabolism of cofactors and vitamins	Metabolism
00140	Steroid hormone biosynthesis	Lipid metabolism	Metabolism
00380	Tryptophan metabolism	Amino acid metabolism	Metabolism
00280	Valine, leucine and isoleucine degradation	Amino acid metabolism	Metabolism
03320	PPAR signaling pathway	Endocrine system	Organismal Systems

ST 4 List of Significant Pathways from Chronic Liver Data

KEGG ID	Pathway Name	Pathway Subgroup	Pathway Group
04140	Autophagy - animal	Transport and catabolism	Cellular Processes
04216	Ferroptosis	Cell growth and death	Cellular Processes
04146	Peroxisome	Transport and catabolism	Cellular Processes
03050	Proteasome	Folding, sorting and degradation	Genetic Information Processing
04141	Protein processing in endoplasmic reticulum	Folding, sorting and degradation	Genetic Information Processing
03010	Ribosome	Translation	Genetic Information Processing
00220	Arginine biosynthesis	Amino acid metabolism	Metabolism
00410	beta-Alanine metabolism	Metabolism of other amino acids	Metabolism
01230	Biosynthesis of amino acids	Amino acid metabolism	Metabolism
01200	Carbon metabolism	Carbohydrate metabolism	Metabolism
00020	Citrate cycle (TCA cycle)	Carbohydrate metabolism	Metabolism
00270	Cysteine and methionine metabolism	Amino acid metabolism	Metabolism
00071	Fatty acid degradation	Lipid metabolism	Metabolism
01212	Fatty acid metabolism	Lipid metabolism	Metabolism
00480	Glutathione metabolism	Metabolism of other amino acids	Metabolism
00010	Glycolysis / Gluconeogenesis	Carbohydrate metabolism	Metabolism
00630	Glyoxylate and dicarboxylate metabolism	Carbohydrate metabolism	Metabolism
00980	Metabolism of xenobiotics by cytochrome P450	Xenobiotics biodegradation and metabolism	Metabolism
00190	Oxidative phosphorylation	Energy metabolism	Metabolism
00640	Propanoate metabolism	Carbohydrate metabolism	Metabolism
00620	Pyruvate metabolism	Carbohydrate metabolism	Metabolism
00830	Retinol metabolism	Metabolism of cofactors and vitamins	Metabolism
00140	Steroid hormone biosynthesis	Lipid metabolism	Metabolism
00380	Tryptophan metabolism	Amino acid metabolism	Metabolism

00280	Valine, leucine and isoleucine degradation	Amino acid metabolism	Metabolism
04910	Insulin signaling pathway	Endocrine system	Organismal Systems
03320	PPAR signaling pathway	Endocrine system	Organismal Systems

ST 5 List of Significant Pathways from Acute Muscle Data

KEGG ID	Pathway Name	Pathway Subgroup	Pathway Group
04210	Apoptosis	Cell growth and death	Cellular Processes
04140	Autophagy - animal	Transport and catabolism	Cellular Processes
04110	Cell cycle	Cell growth and death	Cellular Processes
04218	Cellular senescence	Cell growth and death	Cellular Processes
04216	Ferroptosis	Cell growth and death	Cellular Processes
04115	p53 signaling pathway	Cell growth and death	Cellular Processes
04146	Peroxisome	Transport and catabolism	Cellular Processes
04145	Phagosome	Transport and catabolism	Cellular Processes
04810	Regulation of actin cytoskeleton	Cell motility	Cellular Processes
04152	AMPK signaling pathway	Signal transduction	Environmental Information Processing
04024	cAMP signaling pathway	Signal transduction	Environmental Information Processing
04022	cGMP-PKG signaling pathway	Signal transduction	Environmental Information Processing
04512	ECM-receptor interaction	Signaling molecules and interaction	Environmental Information Processing
04012	ErbB signaling pathway	Signal transduction	Environmental Information Processing
04068	FoxO signaling pathway	Signal transduction	Environmental Information Processing
04340	Hedgehog signaling pathway	Signal transduction	Environmental Information Processing
04066	HIF-1 signaling pathway	Signal transduction	Environmental Information Processing
04390	Hippo signaling pathway	Signal transduction	Environmental Information Processing
04630	JAK-STAT signaling pathway	Signal transduction	Environmental Information Processing
04010	MAPK signaling pathway	Signal transduction	Environmental Information Processing
04072	Phospholipase D signaling pathway	Signal transduction	Environmental Information Processing
04151	PI3K-Akt signaling pathway	Signal transduction	Environmental Information Processing
04015	Rap1 signaling pathway	Signal transduction	Environmental Information Processing
04014	Ras signaling pathway	Signal transduction	Environmental Information Processing

04350	TGF-beta signaling pathway	Signal transduction	Environmental Information Processing
04668	TNF signaling pathway	Signal transduction	Environmental Information Processing
04370	VEGF signaling pathway	Signal transduction	Environmental Information Processing
03050	Proteasome	Folding, sorting and degradation	Genetic Information Processing
00330	Arginine and proline metabolism	Amino acid metabolism	Metabolism
00071	Fatty acid degradation	Lipid metabolism	Metabolism
01212	Fatty acid metabolism	Lipid metabolism	Metabolism
00480	Glutathione metabolism	Metabolism of other amino acids	Metabolism
00561	Glycerolipid metabolism	Lipid metabolism	Metabolism
00564	Glycerophospholipid metabolism	Lipid metabolism	Metabolism
00260	Glycine, serine and threonine metabolism	Amino acid metabolism	Metabolism
00980	Metabolism of xenobiotics by cytochrome P450	Xenobiotics biodegradation and metabolism	Metabolism
00230	Purine metabolism	Nucleotide metabolism	Metabolism
04920	Adipocytokine signaling pathway	Endocrine system	Organismal Systems
04925	Aldosterone synthesis and secretion	Endocrine system	Organismal Systems
04922	Glucagon signaling pathway	Endocrine system	Organismal Systems
04912	GnRH signaling pathway	Endocrine system	Organismal Systems
04910	Insulin signaling pathway	Endocrine system	Organismal Systems
04921	Oxytocin signaling pathway	Endocrine system	Organismal Systems
03320	PPAR signaling pathway	Endocrine system	Organismal Systems
04917	Prolactin signaling pathway	Endocrine system	Organismal Systems
04923	Regulation of lipolysis in adipocytes	Endocrine system	Organismal Systems
04924	Renin secretion	Endocrine system	Organismal Systems
04919	Thyroid hormone signaling pathway	Endocrine system	Organismal Systems
04918	Thyroid hormone synthesis	Endocrine system	Organismal Systems

ST 6 List of Significant Pathways from Chronic Muscle Data

KEGG	Pathway Name	Pathway Subgroup	Pathway Group
04210	Apoptosis	Cell growth and death	Cellular Processes
04218	Cellular senescence	Cell growth and death	Cellular Processes
04216	Ferroptosis	Cell growth and death	Cellular Processes
04810	Regulation of actin cytoskeleton	Cell motility	Cellular Processes
04140	Autophagy - animal	Transport and catabolism	Cellular Processes
04136	Autophagy - other	Transport and catabolism	Cellular Processes
04144	Endocytosis	Transport and catabolism	Cellular Processes
04142	Lysosome	Transport and catabolism	Cellular Processes
04137	Mitophagy - animal	Transport and catabolism	Cellular Processes
04146	Peroxisome	Transport and catabolism	Cellular Processes
04152	AMPK signaling pathway	Signal transduction	Environmental Information Processing
04371	Apelin signaling pathway	Signal transduction	Environmental Information Processing
04022	cGMP-PKG signaling pathway	Signal transduction	Environmental Information Processing
04012	ErbB signaling pathway	Signal transduction	Environmental Information Processing
04068	FoxO signaling pathway	Signal transduction	Environmental Information Processing
04066	HIF-1 signaling pathway	Signal transduction	Environmental Information Processing
04010	MAPK signaling pathway	Signal transduction	Environmental Information Processing
04150	mTOR signaling pathway	Signal transduction	Environmental Information Processing
04070	Phosphatidylinositol signaling system	Signal transduction	Environmental Information Processing
04151	PI3K-Akt signaling pathway	Signal transduction	Environmental Information Processing
04015	Rap1 signaling pathway	Signal transduction	Environmental Information Processing
04071	Sphingolipid signaling pathway	Signal transduction	Environmental Information Processing
04350	TGF-beta signaling pathway	Signal transduction	Environmental Information Processing
04370	VEGF signaling pathway	Signal transduction	Environmental Information Processing

04310	Wnt signaling pathway	Signal transduction	Environmental Information Processing
03050	Proteasome	Folding, sorting and degradation	Genetic Information Processing
03060	Protein export	Folding, sorting and degradation	Genetic Information Processing
04141	Protein processing in endoplasmic reticulum	Folding, sorting and degradation	Genetic Information Processing
04120	Ubiquitin mediated proteolysis	Folding, sorting and degradation	Genetic Information Processing
03040	Spliceosome	Transcription	Genetic Information Processing
03013	RNA transport	Translation	Genetic Information Processing
00330	Arginine and proline metabolism	Amino acid metabolism	Metabolism
00220	Arginine biosynthesis	Amino acid metabolism	Metabolism
01230	Biosynthesis of amino acids	Amino acid metabolism	Metabolism
00270	Cysteine and methionine metabolism	Amino acid metabolism	Metabolism
00380	Tryptophan metabolism	Amino acid metabolism	Metabolism
00280	Valine, leucine and isoleucine degradation	Amino acid metabolism	Metabolism
01210	2-Oxocarboxylic acid metabolism	Carbohydrate metabolism	Metabolism
01200	Carbon metabolism	Carbohydrate metabolism	Metabolism
00020	Citrate cycle (TCA cycle)	Carbohydrate metabolism	Metabolism
00051	Fructose and mannose metabolism	Carbohydrate metabolism	Metabolism
00010	Glycolysis / Gluconeogenesis	Carbohydrate metabolism	Metabolism
00630	Glyoxylate and dicarboxylate metabolism	Carbohydrate metabolism	Metabolism
00030	Pentose phosphate pathway	Carbohydrate metabolism	Metabolism
00640	Propanoate metabolism	Carbohydrate metabolism	Metabolism
00620	Pyruvate metabolism	Carbohydrate metabolism	Metabolism
00190	Oxidative phosphorylation	Energy metabolism	Metabolism
00920	Sulfur metabolism	Energy metabolism	Metabolism
00071	Fatty acid degradation	Lipid metabolism	Metabolism
01212	Fatty acid metabolism	Lipid metabolism	Metabolism
00670	One carbon pool by folate	Metabolism of cofactors and vitamins	Metabolism
00480	Glutathione metabolism	Metabolism of other amino acids	Metabolism

04920	Adipocytokine signaling pathway	Endocrine system	Organismal Systems
04922	Glucagon signaling pathway	Endocrine system	Organismal Systems
04912	GnRH signaling pathway	Endocrine system	Organismal Systems
04910	Insulin signaling pathway	Endocrine system	Organismal Systems
04921	Oxytocin signaling pathway	Endocrine system	Organismal Systems
03320	PPAR signaling pathway	Endocrine system	Organismal Systems
04917	Prolactin signaling pathway	Endocrine system	Organismal Systems
04919	Thyroid hormone signaling pathway	Endocrine system	Organismal Systems
04710	Circadian rhythm	Environmental adaptation	Organismal Systems

ST 7 Significant Pathways in Rat Expression Data

Pathway Group	Pathway Subgroup (Family)	Pathway Name	Liver	Muscle	Adipose	Lung
Regulation of Cellular Machinery and Cellular Processes	Cell growth and death	Apoptosis	0	0	0	1
		Cell cycle	1	0	1	1
		Cellular senescence	0	0	1	1
		Ferroptosis	1	1	1	1
		Necroptosis	0	0	1	0
		p53 signaling pathway	0	0	1	1
	Cell motility	Regulation of actin cytoskeleton	0	0	1	1
	Transport and catabolism	Autophagy - animal	1	1	1	1
		Endocytosis	0	1	1	1
		Lysosome	1	1	1	1
		Mitophagy - animal	0	1	1	1
		Peroxisome	1	1	0	0
		Phagosome	1	0	1	0
Signal Transduction and Processing	Signal transduction	AMPK signaling pathway	1	1	1	1
		Apelin signaling pathway	0	1	1	1
		cAMP signaling pathway	0	1	0	0
		cGMP-PKG signaling pathway	0	1	1	1
		ErbB signaling pathway	0	1	1	0
		FoxO signaling pathway	1	1	1	1
		HIF-1 signaling pathway	0	1	0	1
		Hippo signaling pathway	0	0	1	1
		Hippo signaling pathway - multiple species	0	0	0	1
		MAPK signaling pathway	0	1	0	1
		mTOR signaling pathway	1	0	1	1
		NF-kappa B signaling pathway	0	0	0	1
		Notch signaling pathway	0	0	1	0
		Phosphatidylinositol signaling system	0	0	0	1
		Phospholipase D signaling pathway	0	0	0	1
		PI3K-Akt signaling pathway	0	0	1	1
		Rap1 signaling pathway	0	0	0	1

		Ras signaling pathway	0	0	0	1
		Sphingolipid signaling pathway	0	0	1	1
		TGF-beta signaling pathway	0	0	1	1
		TNF signaling pathway	0	0	1	1
		VEGF signaling pathway	0	1	0	1
		Wnt signaling pathway	0	0	1	1
	Signaling molecules and interaction	ECM-receptor interaction	0	0	1	1
Genetic Information Processing	Folding, sorting and degradation	Proteasome	1	1	0	1
		Protein export	1	1	1	1
		Protein processing in endoplasmic reticulum	1	1	1	1
		RNA degradation	0	1	1	1
		SNARE interactions in vesicular transport	0	0	0	1
		Ubiquitin mediated proteolysis	0	1	1	1
	Replication and repair	DNA replication	1	0	1	0
		Homologous recombination	0	0	1	0
		Mismatch repair	1	0	0	0
		Nucleotide excision repair	1	0	1	1
	Transcription	RNA polymerase	1	0	0	1
		Spliceosome	1	1	1	1
	Translation	mRNA surveillance pathway	1	0	1	0
		Ribosome	1	1	0	0
		Ribosome biogenesis in eukaryotes	0	1	1	1
		RNA transport	1	1	1	1
Metabolism	Amino acid metabolism	Alanine, aspartate and glutamate metabolism	1	0	0	0
		Arginine and proline metabolism	1	1	0	0
		Arginine biosynthesis	1	0	0	0
		Biosynthesis of amino acids	1	1	0	0
		Cysteine and methionine metabolism	1	1	0	0

		D-Glutamine and D-glutamate metabolism	0	0	0	1
		Glutathione metabolism	1	0	0	0
		Glycine, serine and threonine metabolism	1	0	0	0
		Lysine degradation	1	0	0	1
		Tryptophan metabolism	1	0	0	0
		Valine, leucine and isoleucine degradation	1	0	0	0
	Biosynthesis of other secondary metabolites	Caffeine metabolism	1	0	0	0
	Carbohydrate metabolism	2-Oxocarboxylic acid metabolism	1	1	0	0
		Amino sugar and nucleotide sugar metabolism	0	0	0	1
		Carbon metabolism	1	1	0	0
		Citrate cycle (TCA cycle)	1	1	0	0
		Glycolysis / Gluconeogenesis	1	1	0	0
		Glyoxylate and dicarboxylate metabolism	1	1	0	0
		Inositol phosphate metabolism	0	0	0	1
		Pentose phosphate pathway	1	0	0	0
		Propanoate metabolism	1	0	0	0
		Pyruvate metabolism	1	1	0	0
	Energy metabolism	Nitrogen metabolism	1	1	0	0
		Oxidative phosphorylation	1	1	0	0
		Sulfur metabolism	1	0	0	0
	Glycan biosynthesis and metabolism	Glycosaminoglycan degradation	0	0	1	0
		Glycosphingolipid biosynthesis - ganglio series	0	0	1	0
		N-Glycan biosynthesis	1	0	0	1
		Other types of O-glycan biosynthesis	0	0	0	1
	Lipid metabolism	Biosynthesis of unsaturated fatty acids	1	0	0	0
		Fatty acid biosynthesis	0	1	0	0

		Fatty acid degradation	1	1	0	0
		Fatty acid metabolism	1	0	0	0
		Glycerolipid metabolism	1	0	0	0
		Glycerophospholipid metabolism	0	0	0	1
		Primary bile acid biosynthesis	1	0	0	0
		Steroid biosynthesis	1	0	0	0
		Synthesis and degradation of ketone bodies	1	0	0	0
	Metabolism of cofactors and vitamins	Biotin metabolism	0	0	0	1
		One carbon pool by folate	1	0	1	0
	Metabolism of terpenoids and polyketides	Terpenoid backbone biosynthesis	1	0	0	1
	Nucleotide metabolism	Purine metabolism	1	0	0	0
Regulation of Organ Systems	Endocrine system	Adipocytokine signaling pathway	0	0	0	1
		Aldosterone synthesis and secretion	0	1	0	0
		Glucagon signaling pathway	0	1	1	0
		GnRH signaling pathway	0	1	0	0
		Insulin signaling pathway	1	1	1	1
		Oxytocin signaling pathway	0	1	1	0
		Parathyroid hormone synthesis, secretion and action	0	1	1	1
		PPAR signaling pathway	1	0	0	0
		Progesterone-mediated oocyte maturation	0	0	1	1
		Prolactin signaling pathway	1	0	0	1
		Regulation of lipolysis in adipocytes	0	0	1	0
		Relaxin signaling pathway	0	1	1	1
		Thyroid hormone signaling pathway	0	1	1	1
		Thyroid hormone synthesis	0	0	1	0
		Circadian rhythm	0	1	1	1

	Environmental adaptation	Thermogenesis	1	1	0	1

ST 8 Significant Pathways in Mouse Expression Data

Pathway Group	Pathway Subgroup	Pathway	Adipose	Liver	Muscle	Lung
Regulation of Cellular Machinery and Cellular Processes	Cell growth and death	Ferroptosis	0	1	0	0
	Cell motility	Regulation of actin cytoskeleton	0	0	0	1
	Transport and catabolism	Autophagy - animal	0	1	0	1
		Endocytosis	0	0	0	1
		Lysosome	0	1	0	1
		Peroxisome	1	1	0	0
Signal Transduction and Processing	Membrane transport	ABC transporters	0	0	0	1
	Signal transduction	AMPK signaling pathway	1	1	1	1
		Apelin signaling pathway	1	1	0	1
		Calcium signaling pathway	0	0	0	1
		cAMP signaling pathway	1	0	0	0
		cGMP-PKG signaling pathway	1	0	1	1
		FoxO signaling pathway	0	1	0	1
		HIF-1 signaling pathway	1	0	0	1
		Hippo signaling pathway	0	0	0	1
		Jak-STAT signaling pathway	0	0	1	0
		MAPK signaling pathway	1	0	1	1
		mTOR signaling pathway	1	1	0	1
		Notch signaling pathway	0	0	0	1
		Phosphatidylinositol signaling system	1	0	1	1
		Phospholipase D signaling pathway	1	0	0	1
		PI3K-Akt signaling pathway	1	0	0	1
		Rap1 signaling pathway	1	0	0	1
		Ras signaling pathway	1	0	0	1

		Sphingolipid signaling pathway	0	1	0	0
		TNF signaling pathway	0	1	0	1
		VEGF signaling pathway	0	0	0	1
	Signaling molecules and interaction	Cell adhesion molecules (CAMs)	0	0	1	0
		Cytokine-cytokine receptor interaction	0	0	1	0
		ECM-receptor interaction	1	0	0	0
Genetic Information Processing	Folding, sorting and degradation	Proteasome	0	0	0	1
		Protein processing in endoplasmic reticulum	0	1	0	0
	Replication and repair	Fanconi anemia pathway	0	1	0	0
	Transcription	RNA polymerase	0	0	0	1
Metabolism	Amino acid metabolism	Alanine, aspartate and glutamate metabolism	1	0	0	0
		beta-Alanine metabolism	0	0	0	1
		Cysteine and methionine metabolism	0	1	0	0
		Glutathione metabolism	0	1	0	1
		Glycine, serine and threonine metabolism	0	1	0	0
		Tryptophan metabolism	0	1	0	0
		Valine, leucine and isoleucine degradation	0	1	0	1
	Biosynthesis of other secondary metabolites	Neomycin, kanamycin and gentamicin biosynthesis	0	0	0	1
	Carbohydrate metabolism	Amino sugar and nucleotide sugar metabolism	0	0	0	1
		Carbon metabolism	0	1	0	0
		Glyoxylate and dicarboxylate metabolism	0	1	0	0
		Inositol phosphate metabolism	0	0	1	0
		Propanoate metabolism	1	0	0	1
		Pyruvate metabolism	1	1	0	0
		Starch and sucrose metabolism	0	1	0	0
	Energy metabolism	Oxidative phosphorylation	0	1	0	0

		Sulfur metabolism	0	1	0	0
	Glycan biosynthesis and metabolism	N-Glycan biosynthesis	0	1	0	0
		Other glycan degradation	0	0	0	1
	Lipid metabolism	Biosynthesis of unsaturated fatty acids	0	1	0	1
		Ether lipid metabolism	0	1	0	0
		Fatty acid biosynthesis	0	1	0	0
		Fatty acid elongation	0	1	0	0
		Fatty acid metabolism	0	1	0	1
		Glycerolipid metabolism	1	1	0	0
		Glycerophospholipid metabolism	0	1	0	1
		Primary bile acid biosynthesis	0	1	0	0
		Sphingolipid metabolism	0	0	0	1
		Steroid biosynthesis	0	1	0	0
	Metabolism of cofactors and vitamins	Folate biosynthesis	0	1	0	0
		Nicotinate and nicotinamide metabolism	0	1	0	0
		One carbon pool by folate	0	1	0	0
		Riboflavin metabolism	0	1	0	0
	Metabolism of terpenoids and polyketides	Terpenoid backbone biosynthesis	1	1	0	1
	Nucleotide metabolism	Purine metabolism	0	1	0	0
		Pyrimidine metabolism	0	1	0	0
Regulation of Organ Systems	Endocrine system	Adipocytokine signaling pathway	0	1	0	0
		Aldosterone synthesis and secretion	1	0	0	1
		Estrogen signaling pathway	0	0	0	1
		Glucagon signaling pathway	1	1	0	0
		GnRH signaling pathway	1	0	0	1
		Insulin secretion	0	0	0	1
		Insulin signaling pathway	0	1	0	1
		Melanogenesis	0	0	0	1
		Oxytocin signaling pathway	0	0	1	0

		Parathyroid hormone synthesis, secretion and action	1	1	1	1
		PPAR signaling pathway	0	1	0	0
		Progesterone-mediated oocyte maturation	1	0	0	0
		Prolactin signaling pathway	0	1	0	0
		Regulation of lipolysis in adipocytes	1	1	0	1
		Relaxin signaling pathway	1	0	0	1
		Thyroid hormone signaling pathway	1	0	0	1
		Thyroid hormone synthesis	0	0	0	1
	Environmental adaptation	Circadian entrainment	0	0	1	0
		Circadian rhythm	1	1	1	1
		Thermogenesis	0	1	0	0